Journal of High Energy Physics

Exploring improved holographic theories for QCD: part II

Published by Institute of Physics Publishing for SISSA

Received: *October 17, 2007*
Accepted: *January 25, 2008*
Published: *February 7, 2008*

Exploring improved holographic theories for QCD: part II

U. Gürsoy,[ab] **E. Kiritsis**[ac] **and F. Nitti**[a]

[a] *CPHT, Ecole Polytechnique, CNRS, 91128, Palaiseau, France*
[b] *Laboratoire de Physique Théorique, Ecole Normale Supérieure, 24, Rue Lhomond, Paris 75005, France*
[c] *Department of Physics, University of Crete, 71003 Heraklion, Greece*
E-mail: gursoy@cpht.polytechnique.fr, kiritsis@cpht.polytechnique.fr, nitti@cpht.polytechnique.fr

Abstract: This paper is a continuation Arxiv:0707.1324 where improved holographic theories for QCD were set up and explored. Here, the IR confining geometries are classified and analyzed. They all end in a "good" (repulsive) singularity in the IR. The glueball spectra are gapped and discrete, and they favorably compare to the lattice data. Quite generally, confinement and discrete spectra imply each other. Asymptotically linear glueball masses can also be achieved. Asymptotic mass ratios of various glueballs with different spin also turn out to be universal. Meson dynamics is implemented via space filling $D_4-\bar{D}_4$ brane pairs. The associated tachyon dynamics is analyzed and chiral symmetry breaking is shown. The dynamics of the RR axion is analyzed, and the non-perturbative running of the QCD θ-angle is obtained. It is shown to always vanish in the IR.

Keywords: Confinement, AdS-CFT Correspondence, Lattice QCD, Gauge-gravity correspondence.

JHEP02(2008)019

Contents

1. Introduction and summary

This paper is a direct sequel of [1], and the reader is guided there for a comprehensive introduction and summary of results of both papers. In the first part of this work, two of the authors establish and motivate a general 5D holographic setup to describe 4D gauge theories with a large number of colors (large N_c). The setup described there constitutes a bottom-up approach, motivated in part from known features of 5D non-critical string theory and in part by what we expect from QCD.

The pure gauge dynamics is encoded holographically in the solution of a two-derivative action for the expected 5D fields: the 5D metric (dual to the YM stress tensor), a scalar (the dilaton, dual to $Tr[F^2]$), and a pseudoscalar (the axion, dual to $Tr[F \wedge F]$). The dilaton potential is expected to be non-trivial and is expected to obtain non-trivial contributions from the non-propagating four-form. In practice, the potential (and the associated superpotential) is in one-to-one correspondence with the QCD β-function and is chosen in such a way as to reproduce known features (e.g. UV asymptotic freedom and IR confinement) of the gauge theory. This is what makes our approach phenomenological.

The resulting backgrounds present an improvement over pre-existing models of "phenomenological holography", e.g. [2, 3]: among other advantages, the backgrounds we present incorporate the running of the coupling and asymptotic freedom; establish a one-to-one correspondence between the 5D geometry and the gauge theory parameters, namely the β-function $\beta(\lambda)$, and the dynamically generated IR scale $\Lambda_{\rm QCD}$ and do not require specifying the boundary conditions in the IR. Moreover, they provide a natural environment to study non-perturbative dynamical phenomena such as confinement, generation of the mass gap and chiral-symmetry breaking.

Part I is devoted to establish and motivate the setup, and to analyze the perturbative UV regime of the correspondence. The present work, on the other hand, focuses on the analysis of the non-perturbative regime. As one of our main results, we establish a relation between color confinement (i.e. an area law for the Wilson loop) and the properties of the geometry in the IR, and we show that confining backgrounds always exhibit a mass gap and generically a discrete spectrum. This is a nontrivial statement, as in our models there is no IR boundary (which would automatically guarantee both confinement *and* a mass gap). In most of this work we focus on the pure Yang-Mills sector, which we describe holographically by a 5D Einstein-Dilaton system. We discuss the addition of N_f matter flavors in the quenched approximation $N_f \ll N_c$, so that we can neglect the backreaction of the 5D fields dual to the operators containing quarks.

The structure of the present paper is as follows. In section 2 we give an overview of the setup discussed in [1]. We recall how asymptotic freedom demands the UV geometry to be asymptotically AdS_5 with logarithmic corrections. We then review the holographic dictionary, mapping field theory quantities to their geometrical counterparts. In particular, there is a one-to-one correspondence between the superpotential associated to the geometry and the exact field theory β-function. In the last subsection we analyze the IR behavior of space-times that have AdS_5 UV asymptotics, showing that backgrounds that are not conformal in the IR necessarily exhibit an IR singularity.

In section 3 we provide a complete characterization of 5D asymptotically AdS_5 backgrounds that exhibit confinement in the IR. Here, as a definition of confinement, we require that the Wilson loop exhibits an area law behavior. We compute the Wilson loop holographically, using the prescription of [4], as the action of a classical string world-sheet with fixed UV boundary conditions. We show that confinement requires the scale factor to vanish sufficiently fast in the IR. We formulate this requirement in terms of the superpotential and the 4D β-function. We then discuss the holographic computation of the 't Hooft loop, relevant for the potential between two color-magnetic charges, in order to investigate whether screening behavior is present.

In section 4 we perform a holographic computation of the (regularized) QCD vacuum energy.

In section 5 we discuss the dynamics of the 5D axion. This field does not backreact on the geometry in the large N_c limit, however its normal modes give the spectrum of 4D pseudoscalar glueballs. In addition, its UV source is associated to the *theta*-angle of YM and its IR properties are relevant for the discussion of the effective QCD θ-parameter. We argue that this field must vanish in the IR. In this way a pseudo-scalar glueball condensate is dynamically generated. This suggests that the effects of the θ-parameter are screened in the IR.

In section 6 we discuss the general features of the low-energy particle spectrum in our model, obtained from the fluctuations of the bulk fields around the background. For scalar and tensor glueballs, in all confining potentials the spectrum is gapped and discrete. With the exception of a certain class of "pathological" geometries in which the singularity is not screened, the particle spectrum can be computed unambiguously imposing normalizability of the eigenfunctions. We find potentials where the glueballs have a linear asymptotic spectrum, i.e. $m_n^2 \sim n$. We discuss the addition of flavor branes along the lines of [5], where it was proposed that chiral symmetry breaking is correctly described by open string tachyon condensation. We show that this idea can be naturally implemented in our setup. We discuss the asymptotics of the tachyon background and the qualitative features of the spectrum of mesons.

In section 7 we discuss the parameters of the gravity backgrounds and their relations with the gauge theory parameters. We show that, once confining asymptotics in the IR are imposed, the 5D backgrounds are completely specified by the dilaton potential plus the arbitrary choice of a single integration constant, that only affects the overall energy scale. It is in one-to-one correspondence to a choice of $\Lambda_{\rm QCD}$ in the dual field theory.

In section 8 we give some concrete examples, in which we specify the exact β-function, solve numerically for the corresponding geometry and compute, again numerically, the glueball spectrum. We compare our results with the available lattice data, and with similar computations in other models. In particular, we show that the "linear confinement" background fits particularly well the lattice data. On the other hand, in hard-wall models like [2, 3], or generically in models with a "quadratic" mass spectrum, the agreement is not as good.

Some of the technical details can be found in the appendices. In particular, the reader interested in the details of the characterization of confining backgrounds, including their various geometric properties, is referred to appendix A.

2. Building blocks of holographic QCD

In this section we review some properties of the 5d backgrounds and their holographic interpretation. Some of these points where extensively discussed in [1].

2.1 The 5D backgrounds

As detailed in [1], we take a "minimal" non-critical approach to holographic large N_c QCD type theories, in which the 5D string theory dual has, as low energy excitations, the duals of the lowest-dimension gauge invariant operators. In the pure glue sector these are: the five-dimensional metric $g_{\mu\nu}$ (dual to the YM stress tensor); a scalar field ϕ which we call the dilaton (dual to the YM operator $\mathrm{Tr}F^2$) and an axion, dual to $\mathrm{Tr}F\tilde{F}$. We may ignore the axion when searching for the QCD vacuum solution as its contribution is subleading in $1/N_c$ [23]. It can be included in the sequel (this is discussed in section 5) as it does affect some important physics, in particular that of flavor singlet mesons. The scalar ϕ encodes the running of the YM coupling, and it is naturally identified with the 5D string dilaton.

We should emphasize that we think of the 5D bulk theory as a (non-critical) string theory, not just gravity. However, we restrict ourselves to the two-derivative effective action, including a general dilaton potential, that contains also a subclass of higher α' terms as argued in [1].

Therefore, the string-frame action describing the low-lying excitations is:

$$S_S = M^3 N_c^2 \int d^5x\sqrt{-g_S}\,\frac{1}{\lambda^2}\left[R + 4g_S^{\mu\nu}\frac{\partial_\mu\lambda}{\lambda}\frac{\partial_\nu\lambda}{\lambda} + V_S(\lambda)\right] \tag{2.1}$$

where we have introduced the 't Hooft coupling

$$\lambda \equiv N_c e^{\phi}\ . \tag{2.2}$$

It is related to the 't Hooft coupling of the gauge theory, up to a multiplicative constant. $V_S(\lambda)$ is an "effective potential" originating from integrating-out the non-dynamical 4-form, [1] and other higher curvature corrections. We do not attempt here to derive $V_S(\lambda)$ from first principles. We determine certain of its properties by requiring that the geometry that follows from V_S reproduces some known features of the Yang-Mills dynamics. In particular, requiring UV asymptotic freedom constraints the asymptotics of the potential for small values of λ. Requiring an area law for the Wilson loop on the other hand constrains the asymptotics of the potential for large λ. From now on we also define for convenience a renormalized dilaton Φ as

$$\lambda = e^{\Phi}\ . \tag{2.3}$$

We mostly work with the Einstein frame metric,

$$g_{\mu\nu} = e^{-\frac{4}{3}\Phi}(g_S)_{\mu\nu}, \tag{2.4}$$

for which the action reads:

$$S = M^3 N_c^2 \int d^5x\sqrt{-g}\left[R - \frac{4}{3}g^{\mu\nu}\partial_\mu\Phi\partial_\nu\Phi + V(\Phi)\right] \quad , \quad V(\Phi) = e^{4\Phi/3}V_S(\Phi)\,. \tag{2.5}$$

In the large N_c limit we assume, $g_{\mu\nu}$ and Φ are independent of N_c.

We search backgrounds of the form:

$$g_{\mu\nu} = du^2 + e^{2A(u)}\eta_{ij}dx^i dx^j = e^{2A(r)}\left(dr^2 + \eta_{ij}dx^i dx^j\right), \quad \Phi = \Phi(u), \tag{2.6}$$

where x^i are the 4D space-time coordinates, and $\eta_{ij} = diag(-,+,+,+)$. We write the metric in two different coordinate systems, related by:

$$\frac{dr}{du} = e^{-A(u)}. \tag{2.7}$$

We name the first set of coordinate system the *domain-wall coordinates*. The second set involving r will be called the *conformal coordinates* as the metric is explicitly conformally flat in this coordinate system. Throughout the paper, we will use a prime for d/du and a dot for d/dr.

The independent Einstein's equations take the following form (in domain-wall coordinates):

$$\Phi'^2(u) = -\frac{9}{4}A''(u), \quad V(\Phi) = 3A''(u) + 12A'^2(u). \tag{2.8}$$

These equations can be written in first-order form in terms of a superpotential $W(\Phi)$ [6]:

$$\Phi' = \frac{dW}{d\Phi}, \qquad A' = -\frac{4}{9}W, \tag{2.9}$$

$$V(\Phi) = -\frac{4}{3}\left(\frac{dW}{d\Phi}\right)^2 + \frac{64}{27}W^2. \tag{2.10}$$

Given any scale factor $A(u)$ such that $A''(u) \leq 0$, one can invert the relation between Φ and u using the first equation (2.8) and find a superpotential $W(\Phi) = -4/9\, A'(u(\Phi))$. This determines a potential, such that the given $A(u)$ is a solution. This useful property allows to investigate the backgrounds under consideration starting directly from a parametrization of the metric, rather than the dilaton potential.

In conformal coordinates, Einstein's equations (2.8) read:

$$\dot{\Phi}^2(r) = -\frac{9}{4}\left(\ddot{A}(r) - \dot{A}^2(r)\right), \quad V(\Phi) = e^{-2A(r)}\left(3\ddot{A}(r) + 9\dot{A}^2(r)\right), \tag{2.11}$$

or, in terms of the superpotential:

$$\dot{\Phi} = \frac{dW}{d\Phi}e^A, \quad \dot{A} = -\frac{4}{9}We^A. \tag{2.12}$$

As shown in [1], asymptotic freedom in the gauge theory translates into an asymptotic AdS_5 region,[1] where the dilaton asymptotes to $-\infty$, and $W \to W_0 > 0$:

$$A(u) \sim -u/\ell + O(\log u), \quad \Phi(u) \sim -\log\left[-\frac{u}{\ell} - \log(\ell\Lambda)\right] + O(1), \qquad u \to -\infty, \tag{2.13}$$

or, in conformal coordinates:

$$A(r) \sim -\log r/\ell + O\left(\frac{1}{\log r}\right), \quad \Phi \sim -\log(-\log(r\Lambda)) + O(1), \qquad r \sim \ell e^{u/\ell} \to 0. \tag{2.14}$$

[1]We should note that "asymptotically AdS_5" here has a different meaning that the similar term in the mathematics literature (see for example [7] and the references therein). Here the corrections to the AdS_5 metric are also logarithmic, while there they are powers of the conformal coordinate r.

The AdS scale ℓ is fixed by the value of $W(\lambda)$ for $\lambda = 0$: $\ell = (9/4)W_0^{-1}$; Λ is an integration constant whose meaning will be clarified in section 7. The subleading terms are also fixed, order by order by matching the β-function coefficients. This corresponds to a dilaton potential of the form $V(\Phi) \sim V_0 + V_1 e^{\Phi} + V_2 e^{2\Phi} + O(e^{3\Phi})$. Since $\lambda \sim e^{\Phi}$ is small in this region, we expect this potential to be generated by the full resummation of the α' expansion, and is to be interpreted as an "effective potential." The information of its weak coupling expansion maps on the field theory side, to the perturbative β-function.

In this paper we are mostly concerned with the opposite regime, i.e. the large λ IR region. One of our goals is to find which solutions to (2.8), satisfying the UV asymptotics (2.13), provide an area-law for the Wilson loop, and what kind of potentials are necessary to realize those solutions. Before addressing this problem, we give some preliminary discussion about the holographic dictionary and the infra-red properties of 5D geometries.

2.2 Holographic dictionary

In order to exploit the gauge-gravity duality, we must first establish a dictionary between the 5D and 4D quantities. In particular we must identify the Yang Mills coupling and energy scale on the gravity side. For this we use the dictionary established in [1].

At a given position in the fifth dimension, the four-dimensional energy scale is set by the scale factor $e^A(u)$, as seen from eq (2.6). This, we argue, leads to the identification:

$$\log E \leftrightarrow A(u). \tag{2.15}$$

Close to the AdS_5 boundary, this reduces to the familiar identification $E = 1/r$. The correspondence (2.15) does not fix the absolute units of the 4D energy scale with respect to the scale factor. This is consistent with the observation that a constant shift in $A(u)$ leaves Einstein's equations (2.8) invariant, and can be used to change the unit energy in a given background.

Notice that the overall scale factor in (2.15) is in the *Einstein frame*. In pure AdS_5 with a constant dilaton this distinction does not matter, but in our backgrounds the dilaton does not asymptote to a constant in the UV, therefore this clarification is needed. In particular, the Einstein frame scale factor has the important property of being monotonically decreasing with u (see section 2.3). This property is not shared by the string frame metric. Monotonicity is crucial if we want our geometry to be dual to a single RG flow from the UV to the IR (and not, e.g, to two different UV theories that flow to the same IR). For a discussion on the string corrections to (2.15), see [1].

The β-function. We identify[2] the 4D 't Hooft coupling $\lambda = g^2_{\rm YM} N_c$ as[3]

$$\lambda = e^{\Phi}. \tag{2.16}$$

[2]There are some ambiguities in this identification that are discussed in [1].

[3]As stated in 2.2, the string dilaton, $\phi \equiv \log g_s$, is related to Φ by $\phi \equiv \Phi - \log N_c$. Φ is the appropriate variable to use in the large N_c limit.

With the identification (2.15), it follows that the β-function of the 't Hooft coupling is related to 5D fields as:

$$\beta(\lambda) \equiv \frac{d\lambda}{d\log E} = \lambda\frac{d\Phi}{dA}, \tag{2.17}$$

or, in terms of the phase-space variable X, introduced in [1],

$$X \equiv \frac{\Phi'}{3A'} \quad , \quad \beta = 3\lambda X \tag{2.18}$$

The above definition is independent of reparametrizations of the radial coordinate, and can be expressed either in the r, u coordinates, or by using Φ as a radial coordinate.

Einstein's equations can be rewritten in terms of $X(\Phi)$ as:

$$\Phi' = -\frac{4}{3}W_0 X e^{-\frac{4}{3}\int_{-\infty}^{\Phi} X d\Phi}, \tag{2.19}$$

$$A' = -\frac{4}{9}W_0 e^{-\frac{4}{3}\int_{-\infty}^{\Phi} X d\Phi}, \tag{2.20}$$

Here, $W_0 > 0$ is the asymptotic value of the superpotential as $\Phi \to -\infty$. It is related to the asymptotic AdS_5 scale ℓ by

$$W_0 = \frac{9}{4\ell}. \tag{2.21}$$

From these equations, the superpotential is related to X as:

$$X(\Phi) = -\frac{3}{4}\frac{d\log W(\Phi)}{d\Phi}\,. \tag{2.22}$$

We deduce that fixing the function $X(\lambda)$ (hence the β-function) specifies the superpotential (up to an overall multiplicative constant). Then, the equations of motion (2.19) and (2.20) determine the geometry up to two integration constants and an overall length scale ℓ. As we show in section 7, only one of the two integration constants is physical, the second one being an artifact of reparametrization invariance.

2.3 Infrared properties of asymptotically AdS_5 backgrounds

In the holographic approach to strongly coupled gauge theories, confinement at low energies is typically related to the termination of space-time at a certain point in the radial coordinate. In five-dimensional holography, with asymptotic AdS_5 in the UV, this often implies the presence of a singularity in the bulk. We show here that, unless the IR is conformal, a curvature singularity is always present when we restrict ourselves to a two-derivative effective action. Specifically, we prove the following statement:

Proposition 1. *Consider any solution of (2.8) such that* $\exp A(r) \sim \ell/r$ *as* $r \to 0$ *(with* $r > 0$*). Then,*

- *The scale factor* $e^{A(r)}$ *is monotonically decreasing*
- *There are only three possible, mutually exclusive IR behaviors:*
  1. *there is another asymptotic* AdS_5 *region, at* $r \to \infty$*, where* $\exp A(r) \sim \ell'/r$*, and* $\ell' \leq \ell$ *(equality holds if and only if the space is exactly* AdS_5 *everywhere);*

2. *there is a curvature singularity at some finite value of the radial coordinate,* $r = r_0$*;*

3. *there is a curvature singularity at* $r \to \infty$*, where the scale factor vanishes and the space-time shrinks to zero size.*

That the scale factor must be monotonic in this context is well known, and it is most clear in the u coordinates: the first equation in (2.8) implies that $A''(u) < 0$, therefore $A'(u)$ must be monotonically decreasing. In the UV, $A(u) \sim -u/\ell$ so for any u we must have

$$A'(u) \leq -1/\ell < 0, \quad \forall u. \tag{2.23}$$

As a consequence, $A(u)$ itself must be monotonically decreasing from the UV to the IR. This is a version of the holographic c-theorem [9].

We now investigate possible IR behaviors. In conformal coordinates, the bound (2.23) translates to:

$$\frac{d}{dr} e^{-A(r)} \geq \frac{1}{\ell}. \tag{2.24}$$

Suppose that the r coordinate extends to $+\infty$. Then, either the l.h.s. of (2.24) asymptotes to constant $\ell'^{-1} > \ell^{-1}$, or it asymptotes to infinity. In the former case, we obtain:

$$e^{A(r)} \sim \frac{\ell'}{r}, \quad r \to \infty. \tag{2.25}$$

This implies that the space-time is asymptotically AdS_5 in the IR, with a smaller AdS_5 radius ℓ'. The gauge theory flows to an IR conformal fixed point, and is therefore not confining.[4]

If instead $\frac{d}{dr}\, e^{-A(r)} \to +\infty$ as $r \to +\infty$, then the curvature scalar diverges, as can be seen from its expression:

$$R(r) = -e^{-2A}\left(12\dot{A}^2 + 8\ddot{A}\right). \tag{2.26}$$

In this case, $e^{-2A(r)}$ diverges faster than r^2, and $\dot{A}^2$ and $\ddot{A}$ do not vanish faster than r^{-2}, forcing eq. (2.26) to diverge as $r \to \infty$. Moreover, the scale factor $e^{A(r)}$ vanishes for large r, as claimed.

There is another possibility, i.e. that the space-time ends at a finite value r_0. This can happen because the scale factor e^A shrinks to zero, or some of its derivatives diverge[5] at r_0. In either case eq. (2.26) indicates that we are in the presence of a curvature singularity at r_0.

These considerations were derived in the context of 5D Einstein-Dilaton gravity, but they are more general, because they follow only from the condition $A''(u) < 0$. This can be shown to be equivalent to the Null Energy Condition (NEC) (see e.g. [11]). Therefore the arguments of this subsection can be extended to any bulk field content, provided its stress tensor satisfies the NEC.

[4]Five-dimensional holographic duals of the Bank-Zaks fixed points are in this class, [10].

[5]We are always assuming that the space-time terminates due to some non-trivial dynamics, rather than because of some boundary at some otherwise regular point $r = r_0$. This is in contrast with the original AdS/QCD approach which advocates an AdS space with an IR boundary.

JHEP02(2008)019

3. Confining backgrounds

Here we would like to characterize the backgrounds that exhibit confinement. By "confinement" we understand an area law behavior for the Wilson loop. Our analysis allows a simple classification of confining background in terms of the metric, superpotential, or β-function IR asymptotics.

3.1 The Wilson loop test

In this subsection we review the holographic computation of the Wilson Loop, [4, 12]. The potential energy $E(L)$ of an external quark-antiquark pair separated by a distance L and evolved in time T, can be computed holographically by the action of a classical string embedded in the 5D space-time, with a single boundary which is a rectangular loop with sides L and T on the AdS_5 boundary. We have,

$$TE(L) = S_{\rm NG}\left[X^\mu_{\rm min}(\sigma,\tau)\right] . \tag{3.1}$$

Here $S_{\rm NG}$ is the Nambu-Goto action evaluated on the world-sheet embedding $X^\mu_{\rm min}(\sigma,\tau)$ with minimum area:

$$S_{\rm NG} = T_f\int d\tau d\sigma\sqrt{-\det g_S}, \qquad (g_S)_{\alpha\beta} = (g_S)_{\mu\nu}\partial_\alpha X^\mu\partial_\beta X^\nu, \quad \alpha,\beta = 1,2 \tag{3.2}$$

with $T_f = \frac{1}{2\pi\ell_s^2}$ the fundamental string tension and $(g_S)_{\mu\nu}$ the bulk *string frame* metric. For a generic 5D metric of the form:

$$(g_S)_{\mu\nu}dx^\mu dx^\nu = g_{\rm ss}(s)ds^2 - g_{00}(s)dt^2 + g_{\|}(s)d\vec{x}^2, \tag{3.3}$$

[12] showed that, for differentiable world-sheets, one can write:

$$E(L) = T_f f(s_F)L - 2T_f\int_{s_B}^{s_F} ds\frac{g(s)}{f(s)}\sqrt{f^2(s) - f^2(s_F)} \tag{3.4}$$

where the functions $f(s), g(s)$ are defined as:

$$f^2(s) = g_{00}(s)g_{\|}(s), \quad g^2(s) = g_{00}(s)g_{\rm ss}(s) \tag{3.5}$$

and s_F is the turning point of the world-sheet in the bulk. Implicitly, s_F depends on L through the relation:

$$L = 2\int_{s_B}^{s_F} ds\frac{g(s)}{f(s)}\frac{1}{\sqrt{f^2(s)/f^2(s_F) - 1}}, \tag{3.6}$$

where s_B denotes the boundary. For large L, the second term in eq. (3.4) is subleading.

Expressions (3.4) and (3.6) drastically simplify if we use conformal coordinates, $s = r$,

$$(g_S)_{\mu\nu}(r) = e^{2A_S(r)}\eta_{\mu\nu}, \quad A_S(r) = A(r) + \frac{2}{3}\Phi(r), \quad f(r) = g(r) = e^{2A_S(r)}, \tag{3.7}$$

to obtain:

$$L = 2\int_0^{r_F} dr\frac{1}{\sqrt{e^{4A_S(r)-4A_S(r_F)} - 1}}. \tag{3.8}$$

In the neighborhood of $r = 0$ the integral is finite, because the integrand behaves as $e^{-2A_S(r)} \sim r^2$, and $r_F \sim L^3$ for small L. Around r_F we may expand the denominator as:

$$\frac{1}{\sqrt{e^{4A_S(r)-4A_S(r_F)}-1}} \simeq \frac{1}{\sqrt{4A_S'(r_F)(r_F-r)+8A_S''(r_F)(r_F-r)^2+\cdots}}. \tag{3.9}$$

The integral is finite for generic r_F and grows indefinitely as r_F approaches a stationary point r_* of $A_S(r)$, where $A_S'(r_*) = 0$. This must correspond to a minimum since A_S starts decreasing at $r = 0$. In other words, if there exists such a stationary point r_*, then

$$r_F \to r_* \quad as \quad L \to \infty. \tag{3.10}$$

The large L behavior of the quark-antiquark potential energy is thus (from (3.4)

$$E(L) \sim T_f e^{2A_S(r_*)} L \tag{3.11}$$

which exhibits an area law if and only if A_S is finite at the minimum. From eq. (3.11) we read off the confining string tension as,

$$T_s = T_f e^{2A_S(r_*)} \tag{3.12}$$

Notice that the finiteness of the string tension is not directly related to the value of the metric at the end of space, as sometimes assumed. Even if the space-time shrinks to zero-size at the singularity, which is the generic behavior of the *Einstein's frame* metric, this does not impede an area law: the string frame scale factor has a global minimum at a regular point in the bulk, and classical string world-sheets *never probe* the region of space beyond that point and never reach the singularity.

Equation (3.11) captures the leading behavior of the quark-antiquark potential. In QCD the first subleading correction is the Lüscher term, $\sim 1/L$. As shown in [14], this term arises in some confining backgrounds (e.g. [13]) from the first quantum corrections to the classical Wilson loop in [12]. It would be interesting to see if this is also the case in the models we are considering.

3.2 Confining IR asymptotics

We are now ready to answer the question: *which IR asymptotics give rise to confinement.*

Here we discuss a special class of metrics, that demonstrate particularly interesting features: namely the space-times with infinite range of the conformal coordinate, $r \in (0, \infty)$. In appendix A we give a complete discussion including other types of backgrounds. There, we also present the asymptotic values of some of the interesting quantities. The reader can find a summary of the classification in table 1 at the end of this section.

Consider a class of space-times whose Einstein frame metric has the form (2.6), with the asymptotics:

$$A(r) \to -Cr^\alpha + \cdots, \qquad r \to \infty, \quad \alpha, C > 0 \tag{3.13}$$

up to *generic* subleading terms. Here, $C^{-1/\alpha} \equiv R$ is a length scale controlling the IR dynamics.

The singularity is at $r \to \infty$, and the space-time shrinks to zero-size there.[6] To check whether the fundamental string is confining we need the string-frame scale factor,

$$A_S(r) = A(r) + \frac{2}{3}\Phi(r). \tag{3.14}$$

As we have discussed in the previous subsection, confinement is equivalent to the existence of a minimum of the expression (3.14), where e^{A_S} is non-zero. Due to the AdS UV asymptotics, $A_S \to +\infty$ as $r \to 0$. Therefore a necessary and sufficient condition for confinement is that A_S *does not asymptote to* $-\infty$ at the IR singularity, $r \to +\infty$.[7]

The asymptotics of the dilaton can be obtained using the first equation in (2.11):

$$\Phi(r) \sim -\frac{3}{2}A(r) + \frac{3}{4}\log|\dot{A}(r)| + \Phi_0. \tag{3.15}$$

Indeed, (3.15) solves eq. (2.11) up to a term proportional to $(\ddot{A}/\dot{A})^2 \sim r^{-2}$, regardless of the subleading behavior in (3.13).

Using (3.15) we obtain the asymptotic form of the string frame scale factor (3.14):

$$A_S \sim \frac{1}{2}\log|\dot{A}(r)| \sim \frac{(\alpha-1)}{2}\log r/R, \qquad ds_S^2 \sim \left(\frac{r}{R}\right)^{\alpha-1}\left(dr^2 + \eta_{ij}dx^i dx^j\right) \tag{3.16}$$

Notice that the leading power-law term has canceled! Moreover the first surviving term is completely determined only by the leading power divergence of the Einstein frame scale factor.

With the simple result (3.16), we can immediately determine which backgrounds lead to confinement:

- $\alpha \geq 1 \Longrightarrow$ confinement:
  the string frame scale factor approaches $+\infty$ in the IR, thus it has a minimum at finite r. The special case $\alpha = 1$ also leads to confinement. The minimum is reached as $r \to \infty$, and the confining string tension is $T_f \lim_{r\to\infty} \exp[2A_S(r)]$.[8] Notice that when $\alpha = 1$ the asymptotic geometry (in the string frame) is 5D Minkowski space-time with linear dilaton.

- $\alpha < 1 \Longrightarrow$ no confinement:
  A_S asymptotes to $-\infty$ for large r, hence the confining string tension vanishes. It is easy to show that the same result applies if $\alpha = 0$, and the scale factor $A(r)$ goes to $-\infty$ slower than any power-law (e.g. logarithmically).[9]

[6]The singularity is at a *finite* value $u_{\rm IR}$ of the u coordinate. See appendix A.

[7]Since we are assuming that the singularity is at $r \to \infty$, and Φ is monotonically increasing from $\Phi = -\infty$ at $r = 0$, A_S cannot diverge to $-\infty$ at some finite r. Therefore, if there is a minimum for A_S, the string tension is certainly finite.

[8]One could think of a situation where the string frame scale factor has multiple minima at r_i, with nonzero values for $\exp[A(r_i)]$ (otherwise there would be a singularity at finite r.) In this case, the classical analysis implies that the string world-sheet has to stop at the minimum closest to the AdS boundary, and never knows about the existence of the others. However, quantum corrections may plausibly trigger the decay into other minima with lower tension. We don't consider this possibility any further, and we will always treat backgrounds with a single minimum of A_S.

[9]As discussed in section 2.3 $A(r)$ cannot asymptote to a finite constant.

We can relate the asymptotics (3.13) to the β-function and to the superpotential, as follows: first we compute the X-variable, defined in eq (2.18), as a function of r, then, using eq. (3.15) we can invert asymptotically the relation between Φ and r and substitute it in the expression above. This gives:

$$X(\lambda) = -\frac{1}{2}\left[1 + \frac{3}{4}\frac{\alpha - 1}{\alpha}\frac{1}{\log\lambda} + \cdots\right], \qquad \lambda \to \infty. \tag{3.17}$$

We note that, generically, the point r_* where $A'_S = 0$ corresponds to $X = -1/2$. In (3.17), the point $X = -1/2$ is first reached at r_*, and then at the singularity $r = +\infty$ where λ diverges.

The asymptotic form of the superpotential is, from eq. (2.22):

$$W(\Phi) \sim \Phi^{\frac{\alpha-1}{2\alpha}} e^{2\Phi/3}, \qquad \Phi \to +\infty. \tag{3.18}$$

Notice that in the leading asymptotics of the superpotential or of $X(\lambda)$ there is no trace of the dimensionfull constant C that controls the "steepness" of the warp factor in eq. (3.13). The appearance of the parameter $R = C^{-1/\alpha}$ in the metric is the manifestation, in conformal coordinates, of the dynamical generation of the IR scale, as we will show explicitly in section 7. It is fixed by the integration constants of Einstein's eqs, rather than by fundamental parameters appearing in $W(\lambda)$.

The idea that some aspect of the geometry, which determines the IR scale, can be related to the integration constants rather than some *a priori* chosen parameter, was already present in the "braneless approach" to AdS/QCD of [15]. As we will discuss in section 6.6.1 however, the spectral properties of the background analyzed in [15] suffer from some pathologies, that make it conceptually equivalent to models with a hard IR cutoff, in which some additional, arbitrary boundary conditions in the IR must be supplied.

We can also relax the requirement that $A(r)$ grows as a simple power-law, since from eq. (3.16) we see that all that is needed for confinement is the condition $\log|\dot{A}| > 0$ asymptotically. This is true for any function $A(r)$ whose asymptotics is bounded above and below as:

$$C_1 r^{\alpha_1} < -A(r) < C_2 r^{\alpha_2}, \qquad \alpha_{1,2} \geq 1, \qquad C_{1,2} \geq 0 \tag{3.19}$$

3.3 General confinement criteria

In appendix A we analyze also the backgrounds where the singularity is at finite $r = r_0$. They always exhibit area law. The analysis in the previous section, together with appendix A, allows us to formulate a general criterion for confinement in 5D holographic models:

General criterion for confinement (geometric version). *A geometry that shrinks to zero size in the IR is dual to a confining 4D theory if and only if the Einstein metric in conformal coordinates vanishes as (or faster than) e^{-Cr} as $r \to \infty$, for some $C > 0$.*

(It is understood here that a metric vanishing at finite $r = r_0$ also satisfies the above condition).

Comparing the superpotentials found in all the examples studied in appendix A, eqs. (A.21), (A.36), (A.50), and (A.65), we see that one can treat simultaneously all cases by using the following parametrization for large λ:

$$W(\lambda) \sim (\log\lambda)^{P/2}\lambda^{Q}, \quad \beta(\lambda) = 3\lambda X(\lambda) \sim -\frac{9}{4}\lambda\left(Q + \frac{P}{2}\frac{1}{\log\lambda}\right), \tag{3.20}$$

where P and Q are real numbers. This implies for the Einstein and string frame dilaton potentials:

$$V(\Phi) \sim (\log\lambda)^{P}\lambda^{2Q}, \qquad V_S(\Phi) \sim (\log\lambda)^{P}\lambda^{(2Q-4/3)} \tag{3.21}$$

An equivalent characterization of the confining backgrounds is:

General criterion for confinement (superpotential). *A 5D background is dual to a confining theory if the superpotential grows as (or faster than)* $(\log\lambda)^{P/2}\lambda^{2/3}$ *as* $\lambda \to \infty$ *for some* $P \geq 0$.

The relation between parameters P and α (appearing in (3.13), is given in table 1.

One can also relate the IR properties directly to the large λ asymptotics of the β-function. Computing $X(\lambda) = \beta(\lambda)/(3\lambda)$ from the superpotential via eq. (2.22), one obtains the following form of the same criterion:

General criterion for confinement (β-function). *A 5D background is dual to a confining theory if and only if*

$$\lim_{\lambda\to\infty}\left(X(\lambda) + \frac{1}{2}\right)\log\lambda = K, \qquad -\infty \leq K \leq 0 \tag{3.22}$$

In the above form[10] the condition for confinement does not make any explicit reference to any coordinate system. Yet, we can determine the geometry if we specify K. In particular:

1. $K = -\infty$: the scale factor vanishes at some finite r_0, not faster than a power-law.
2. $-\infty < K < -3/8$: the scale factor vanishes at some finite r_0 faster than any power-law.
3. $-3/8 < K < 0$: the scale factor vanishes as $r \to \infty$ faster than $e^{-Cr^{1+\epsilon}}$ for some $\epsilon > 0$.
4. $K = 0$: the scale factor vanishes as $r \to \infty$ as e^{-Cr} (or faster), but slower than $e^{-Cr^{1+\epsilon}}$ for any $\epsilon > 0$.

The borderline case, $K = 3/8$, is certainly confining (by continuity), but whether or not the singularity is at finite r depends on the subleading terms. When K is finite, we can relate it to the parameters Q and P appearing in the superpotential: if $K < \infty$, then $Q = 2/3$ and $P = -8K/3$. The classification of the various possible IR asymptotics in terms of their confining properties is summarized in table 1.

[10] We are assuming that the limit exists, and that the β-function does not oscillate infinitely many times across $-3/(2\lambda)$ as $\lambda \to \infty$. This possibility seems remote from a physical point of view.

	$r \in (0, \infty)$			$r \in (0, r_0)$	
$A(r) \sim$	$-\gamma \log r$	$-Cr^{\alpha}$		$-C(r_0 - r)^{-\tilde{\alpha}}$	$\delta \log(r_0 - r)$
		$0 < \alpha < 1$	$\alpha \geq 1$		
Confining	**No**	**No**	**Yes**	**Yes**	**Yes**
Q	$\frac{2}{3}\sqrt{1 - \frac{1}{\gamma}} < \frac{2}{3}$	$\frac{2}{3}$	$\frac{2}{3}$	$\frac{2}{3}$	$\frac{2}{3}\sqrt{1 + \frac{1}{\delta}} > \frac{2}{3}$
P	arbitrary	$\frac{\alpha-1}{\alpha} < 0$	$\frac{\alpha-1}{\alpha} \in [0, 1)$	$\frac{\tilde{\alpha}+1}{\tilde{\alpha}} > 1$	arbitrary
K	> 0	> 0	$-\frac{3}{8}P \in \left(-\frac{3}{8}, 0\ \right]$	$-\frac{3}{8}P \in \left(-\infty, \frac{3}{8}\right)$	$-\infty$

Table 1: Summary of confining asymptotics. As required by the NEC, the parameters $\alpha, \tilde{\alpha}, \gamma, \delta, C$ are all assumed positive, and $\gamma \geq 1$

We note that, if we classify the backgrounds in terms of P and Q, our analysis covers the entire range of these parameters. As a result, our classification is not limited to superpotentials that behave asymptotically as (3.20), but it also applies to any superpotential that for large λ is bounded between two functions of the form (3.20), for two appropriate pairs (Q_1, P_1) and (Q_2, P_2).

For most of the confining backgrounds, although the space-time is singular in the Einstein frame, the string frame geometry is regular for large r (see appendix A). In fact, in these situations, all curvature invariants vanish for large r. The dilaton however diverges. Therefore, in the string frame the singularity manifests itself as a strong coupling region in a weakly curved space-time.

Interestingly, as discussed in the previous subsection, string world-sheets do not probe the strong coupling region, at least classically. This is because the geodesic surfaces ending on the AdS boundary do not stretch beyond the minimum of the scale factor. At that point, the t'Hooft coupling may be of order one, but the *string* coupling $g_s = \lambda/N_c$ is still small. This can be intuitively attributed to the fact that the string tries to stay away from the region where the metric becomes large, since this would generate a larger world-sheet area.

Therefore, singular confining backgrounds have generically the property that the singularity is *repulsive*, i.e. only highly excited states can probe it. This will also be reflected in the analysis of the particle spectrum, in the next subsection. This consideration makes our conclusions more robust, since they are insensitive to the region near the singularity, where quantum effects may become important. As the classical string world-sheet never probes the strong curvature region, a semiclassical analysis is reliable.

One could also worry that a direct coupling of the dilaton to the world-sheet curvature scalar could spoil this analysis. This is not so, as shown in appendix C.

JHEP02(2008)019

3.4 Magnetic charge screening

In confining theories, one expects the dual magnetic gauge group to be Higgsed, leading to a screening of the magnetic charges. In our setup, magnetic monopoles can be described as the endpoints of D1-branes. Therefore the calculation of the monopole-antimonopole potential proceeds exactly like the one for the quark-antiquark potential, with a D-string replacing the fundamental string. In this section we discuss the case of infinite range backgrounds, leaving the finite case to appendix B.

The D-string action is[11]

$$S_D = T_{D_1} \int d^2\xi e^{-\Phi} \sqrt{-det\, g_{\alpha\beta}}, \tag{3.23}$$

where $g_{\alpha\beta}$ is the induced metric on the world-sheet and the target space metric is in the string frame. We work in the conformal coordinates,

$$ds^2 = e^{2A_S} \left(dr^2 + \eta_{ij} dx^i dx^j\right), \tag{3.24}$$

and reabsorb the factor of the dilaton in the conformal factor of the target space metric, reducing the problem to a string with Nambu-Goto action propagating in a target space with an effective metric:

$$ds^2 = e^{2A_D(r)} \left(dr^2 + \eta_{ij} dx^i dx^j\right), \quad A_D = A_S - \frac{\Phi}{2} = A + \frac{\Phi}{6}. \tag{3.25}$$

The properties of the string embedding can then be deduced using the same techniques as in the previous subsections.

For large L the energy of this a configuration is simply given by

$$E = e^{2A_D(r_F(L))} L + \cdots, \tag{3.26}$$

where $r_F(L)$ is the bulk position of turning point of the worldsheed with length L on the boundary. The relation between r_F and L is given by a formula similar to eq. (3.8), with the substitution $A_S \to A_D$.

To avoid the magnetic charge confinement, it must be that the scale factor e^{A_D} of the "D-string frame" metric, eq. (3.25), vanishes at the IR singularity.

In the confining backgrounds of section 3.2, with large r asymptotics (3.13)–(3.15) and $\alpha \geq 1$, the scale factor e^{A_D} in eq. (3.25) does indeed vanish as $r \to \infty$; the magnetic string tension is zero and the magnetic charges are not confined. The question remains, whether they feel an inverse power-law potential or they are truly screened in which case the potential falls-off exponentially or faster. Below, we show that the latter holds for the backgrounds under consideration.

[11]One might expect that the magnetic and electric quark potentials are related by $\lambda \to 1/\lambda$ duality, in the Einstein frame. This is the case for gauge theories that are deformations of $\mathcal{N} = 4$ sYM and others that descend from ten dimensions but not in general. In the Einstein frame the electric string action is proportional to $\lambda^{\frac{4}{D-2}}$ while the magnetic one to $\lambda^{\frac{6-D}{D-2}}$. For $D = 10$, these factors are inverses of each other, but not for $D = 5$ relevant here.

In order to answer this question, one has to study the potential energy (3.26) for large L: to do this, one has to invert asymptotically the relation between r_F and L from the D-string analog of eq. (3.8), and insert it into eq. (3.26).

The asymptotic form of the D-string metric is

$$A_D^{(\alpha)}(r) \sim -\frac{3C}{4} r^\alpha + \cdots \qquad \alpha \geq 1, \tag{3.27}$$

where we are restrict to the confining case. We must evaluate

$$L^{(\alpha)}(r_F) = \int_0^{r_F} \frac{dr}{\left[e^{4\left(A_D^{(\alpha)}(r) - A_D^{(\alpha)}(r_F)\right)} - 1\right]^{1/2}}. \tag{3.28}$$

By assumption, there are no other singularities of $\exp[A_D]$ for any finite r, and we assume that there are no other local extrema. Thus, the only region in which $L(r_F)$ could diverge is $r_F \to \infty$.

We show below that, for $\alpha \geq 1$, $L^{(\alpha)}(r_F)$ is finite in this limit. We first divide the integration range in two regions, $0 < r < r_1$, $r_1 < r < r_F$, such that in the second region the asymptotic form of the scale factor (3.27) holds. Consider the integral in the first region:

$$\begin{aligned}
\int_0^{r_1} \frac{dr}{\left[e^{4(A_D(r_F) - A_D(r))} - 1\right]^{1/2}} &= \int_0^{r_1} dr \frac{e^{4(A_D(r_F) - A_D(r_1))}}{\left[e^{4(A_D(r) - A_D(r_1))} - e^{4(A_D(r_F) - A_D(r_1))}\right]^{1/2}} \\
&< \frac{e^{4A_D(r_F)}}{e^{4A_D(r_1)}} \int_0^{r_1} \frac{dr}{\left[e^{4(A_D(r) - A_D(r_1))} - 1\right]^{1/2}} \\
&= \frac{e^{4A_D(r_F)}}{e^{4A_D(r_1)}} \, L(r_1).
\end{aligned} \tag{3.29}$$

The inequality follows from our assumption that A_D is monotonically decreasing. Since $L(r_1)$ is finite for finite r_1, and $\exp[4A_D(r_F)] \to 0$ as $r_F \to \infty$, the r.h.s vanishes in this limit. Therefore, for large r_F the dominant contribution to $L(r_F)$ comes from the region $r > r_1$.

To analyze the behavior of the integral over the asymptotic region, consider first the case $\alpha = 1$. We have:

$$L^{(1)}(r_F) \sim \int_{r_1}^{r_F} \frac{dr}{\left[e^{3C(r_F - r)} - 1\right]^{1/2}} = \frac{1}{3C} \int_0^{3C(r_F - r_1)} \frac{dy}{\sqrt{e^y - 1}}, \tag{3.30}$$

and

$$\lim_{r_F \to +\infty} L^{(1)}(r_F) = \frac{1}{3C} \int_0^{+\infty} \frac{dy}{\sqrt{e^y - 1}} = L_{\max} < +\infty. \tag{3.31}$$

Next consider $\alpha > 1$. For large $r < r_F$, the following inequality holds:

$$r_F^\alpha - r^\alpha > r_F^{\alpha - 1}(r_F - r). \tag{3.32}$$

It follows that

$$L^{(\alpha)}(r_F) \sim \int_{r_1}^{r_F} \frac{dr}{\left[e^{3C(r_F^\alpha - r^\alpha)} - 1\right]^{1/2}} < \int_{r_1}^{r_F} \frac{dr}{\left[e^{3C r_F^{\alpha-1}(r_F - r)} - 1\right]^{1/2}} \sim \frac{1}{r_F^{\alpha-1}} L^{(1)}(r_F), \tag{3.33}$$

which implies that for $\alpha > 1$

$$\lim_{r_F \to +\infty} L^{(\alpha)}(r_F) = 0. \tag{3.34}$$

We showed that $L^{(\alpha)}(r_F)$ cannot be larger than a maximum value $L^{(\alpha)}_{\max}$, which is reached at $+\infty$ if $\alpha = 1$, and at some finite $r_{\max}$ if $\alpha > 1$. Therefore two monopoles at a distance larger than $L_{\max}$ cannot be connected by a smooth world-sheet. In this case, the configuration that minimizes the action consists of two straight lines separated by a distance L and joined by a line at constant $r = \infty$. This configuration has the same energy as the one with two straight lines only as the contribution from the piece at the singularity vanishes.[12] Therefore for $L > L_{\max}$ the monopoles are non-interacting. This shows that in the backgrounds with an infinite range of r, the magnetic charges are screened.

The finite r_0 case is discussed in appendix B, where we show that the monopole charges are screened, except in backgrounds with power-law decay $\exp A \sim (r_0 - r)^\delta$ with $\delta < 1/15$. This case falls into the range $0 < \delta < 1$, which turns out to be problematic also for other reasons as we show in the discussion of the particle spectrum in section 6.

3.4.1 Absence of screening in hard-wall models

In the simplest models proposed as a holographic description of chiral dynamics of QCD [2, 3], the space-time ends at an IR boundary before any singularity. According to our discussion in this section, one finds linear confinement both for the electric *and* the magnetic charges. This is contrary to the expectations from the gauge theory dynamics. In fact, the computation of the magnetic string Wilson loop is exactly the same as that of the electric one, since the wall has the same effect on both objects. This was computed for the cut-off AdS_5 background in e.g. [16], where the expected area law was found.

4. The QCD vacuum energy

An interesting question in YM theory concerns the value of the vacuum energy, and this is closely related to the so called gluon condensate, $\langle Tr[F^2]\rangle$. Typically they are UV divergent. Of course one would try to renormalize them by subtracting the divergences. We do not know of an unambiguous way to define them beyond perturbation theory.[13] Indeed, once the divergences are subtracted one might as well subtract also the finite piece. We also stress that the gluon condensate is also defined in a semi-phenomenological fashion via the SVZ sum rules. Therefore, without quarks, it is not obvious how to define it.[14]

Because of this we will calculate the divergent (holographic) full vacuum energy to leading order in $1/N_c$. To do this, we will introduce the usual UV cutoff near the AdS_5 boundary

[12] One should take this argument with a grain of salt. This is because, unlike the configuration that stretches only up to r_F, this configuration falls into the singularity, hence one should worry about various string and quantum corrections to the classical solution. At any rate, our final statement about the magnetic screening is valid as existence of an $L_{\max}$ is sufficient for that.

[13] See however [20] for another discussion.

[14] This is unlike the CP-odd condensate $\langle Tr[F \wedge F]\rangle$ that we will calculate in section 5. The reason is that the operator $Tr[F \wedge F]$ does not need a holographic renormalization.

and will compute the Euclidean action of the vacuum QCD solution. The Gibbons-Hawking boundary term is important in this calculation.

$$S_5 = S_E + S_{\rm GH} \tag{4.1}$$

$$S_E = -M^3 N_c^2 \int d^5x\sqrt{g}\left[R - \frac{4}{3}(\partial\Phi)^2 + V(\Phi)\right] \tag{4.2}$$

$$S_{\rm GH} = 2M^3 N_c^2 \int_{\partial M} d^4x\sqrt{h}\; K \tag{4.3}$$

Evaluated on a solution the Einstein action is

$$S_E = \frac{2}{3}M^3 N_c^2 \int d^5x\sqrt{g}\;\; V(\Phi) = \frac{2}{3}M^3 N_c^2 V_4 \int_\epsilon^{r_0} dr\; e^{5A}\;\; V(\Phi) \tag{4.4}$$

$$= 2M^3 N_c^2 V_4 \int_\epsilon^{r_0} dr\; \frac{d}{dr}(e^{3A}\dot{A}) = 2M^3 N_c^2 V_4 \left[e^{3A}\dot{A}\right]_\epsilon^{r_0} \tag{4.5}$$

where V_4 is the space-time volume and we introduced a IR cutoff ϵ in the bulk. For all our confining backgrounds, the contribution from the singularity vanishes automatically. This is a good consistency check of the procedure as only the contribution from the UV boundary should survive. We therefore obtain

$$\mathcal{S}_E = -2M^3 N_c^2 V_4\; e^{3A(\epsilon)} \dot{A(\epsilon)} \tag{4.6}$$

For the GH term, the trace of the extrinsic curvature is $K = 4e^{-A}\dot{A}$ and therefore

$$\mathcal{S}_{\rm GH}^\epsilon = 8M^3 N_c^2 V_4\; e^{3A(\epsilon)} \dot{A}(\epsilon) \tag{4.7}$$

Putting everything together we obtain for the vacuum energy density (Euclidean action divided by the space-time volume)

$$\mathcal{E}_{\rm QCD} = 6M^3 N_c^2\; e^{3A(\epsilon)} \dot{A}(\epsilon) \tag{4.8}$$

Note that this is negative as $\dot{A} < 0$. We can re-express the result in terms of the cutoff energy scale, $\Lambda_{\rm UV}$

$$A(\epsilon) = \log \Lambda_{\rm UV}$$

Then the bare vacuum energy density satisfies

$$\frac{\partial \log \mathcal{E}_{\rm QCD}}{\partial \log \Lambda_{\rm UV}} = 4 - \frac{4}{9}\Phi'^2 = 4 - \frac{4\beta^2(\lambda)}{9\lambda^2} \simeq 4 - \frac{4b_0^2\lambda^2}{9} + \mathcal{O}(\lambda^3) \tag{4.9}$$

Another (related) equation determines the coupling dependence

$$\frac{\partial \log \mathcal{E}_{\rm QCD}}{\partial \lambda(\Lambda_{\rm UV})} = \frac{4}{\beta(\lambda)} - \frac{\beta(\lambda)}{4\lambda^2} \tag{4.10}$$

5. The axion background

The axion a is dual to the instanton density $Tr[F \wedge F]$. In particular its UV boundary value is the UV value of the QCD θ-angle. Moreover, its profile $a(r)$ in the vacuum solution may be interpreted as the "running" θ-angle in analogy with the dilaton, that we interpret as the running coupling constant . Such an interpretation should be qualified, as it may suggest the false impression that UV divergences renormalize the θ angle in QCD. We will return to this later.

The question of the θ dependence of large N_c QCD and the associated η' problem has led to several advances that culminated with the Witten-Veneziano solution, [21, 22]. It states that although naively the θ dependence is expected to be non-perturbative, at large N_c this is not so. It enters at order $1/N_c^2$ in YM theory. It generates a θ-depended vacuum energy that scales as $\frac{\theta^2}{N_c^2}$ and provides the correct mass (of order $1/N_c$) to the η'. Such expectations have been verified in the holographic realization of a four-dimensional confining gauge theory based on D_4 branes, [23].

Here we analyze the structure of the background solution for the axion in five dimensions relevant for pure YM theory. The action in the Einstein frame and the corresponding equation of motion are:

$$S_a = \frac{M^3}{2} \int d^5x \sqrt{-g}\; Z(\lambda)\;\; (\partial_\mu a)^2 \,, \qquad \frac{1}{\sqrt{g}} \partial_\mu \left[Z(\lambda) \sqrt{g} g^{\mu\nu} \partial_\nu \right] a = 0 \tag{5.1}$$

where $Z(\lambda)$ captures a part of the α' corrections. It was shown in appendix B.1 of [1] that $Z(\lambda)$ depends in general on the 't Hooft coupling λ. In perturbative string theory and to leading order in α', $Z(\lambda) = \lambda^2$. However, as was the case for the potential, we expect a constant leading term also here,

$$Z(\lambda) = Z_a + \mathcal{O}(\lambda^2) \quad , \quad \lambda \to 0 \tag{5.2}$$

The axion field equation is to be solved on a given metric and dilaton background, i.e. we neglect the backreaction of the axion [1].

For a radially dependent axion the equation becomes

$$\ddot{a} + \left(3\dot{A} + (\partial_\lambda \log Z) \dot{\lambda} \right) \dot{a} = 0 \tag{5.3}$$

This equation can be integrated once as

$$\dot{a} = \frac{C\; e^{-3A}}{\ell\; Z(\lambda)} \tag{5.4}$$

The equation (5.3) has two independent solutions. One is a constant, $f_0(r) = constant$. The other $f_1(r)$ can be obtained by integrating (5.4) and choosing the initial conditions so that it vanishes at the boundary $r = 0$:

$$f_1 = \int_0^r \frac{dr}{\ell} \frac{e^{-3A}}{Z(\lambda)} \tag{5.5}$$

where we divided by the AdS length so that the function is dimensionless. A first observation is that the function $f_1(r)$ is strictly increasing.

Since near the boundary, $Z = Z_a + \cdots$, $e^{\Phi} = -\frac{1}{b_0 \log(r\Lambda)} + \cdots$ and $e^A = \frac{\ell}{r} + \cdots$ we obtain

$$\lim_{r \to 0} f_1(r) = \frac{r^4}{4Z_a \ell^4}\left[1 + \mathcal{O}\left(\frac{1}{\log(r\Lambda)}\right)\right] \tag{5.6}$$

where we chose an arbitrary normalization for this solution. This solution is the one normalizable in the UV.

The constant solution should be related to the UV value of the θ-angle as

$$f_0 = \theta_{\rm UV} + 2\pi k \quad , \quad k \in Z \tag{5.7}$$

The different values of the integer k correspond to an infinite number of vacua, [23]. Such vacua exhibit in general oblique confinement and they are degenerate to leading order in the $1/N_c$ expansion. As it is known and we will also see it explicitly below, their degeneracy is lifted to the next order. They can be separated by domain walls that are the D_2 branes. The full background solution therefore reads

$$a(r) = \theta_{\rm UV} + 2\pi k + C\ f_1(r) \tag{5.8}$$

where we take by convention $\theta_{\rm UV} \in [0, 2\pi)$. The coefficient C is proportional to the expectation value of the QCD instanton density operator in the QCD vacuum. Using the precise holographic formula and (5.6) we obtain

$$C = \frac{4Z_a\ell^4}{(2\Delta - 4)}\frac{\langle F \wedge F \rangle}{32\pi^2} = Z_a \ell^4 \frac{\langle F \wedge F \rangle}{32\pi^2} \tag{5.9}$$

Substituting the solution in the effective action we obtain, for the (θ-dependent) energy per unit three-volume, the following boundary terms

$$\mathcal{E}(\theta_{\rm UV}) = \frac{M^3}{2}\int dr \sqrt{g} Z(\Phi)(\partial a)^2 = \frac{M^3}{2} e^{3A} Z(\lambda) a\dot{a}\Big|_{r=0}^{r=r_0} = \frac{M^3}{2\ell} C\ a(r)\Big|_{r=0}^{r=r_0} \tag{5.10}$$

where we have used the equations of motion to write the on-shell action as a boundary term. r_0 is the position of the singularity in the IR. It may be finite or infinite, as discussed in the previous sections.

We expect that the only contribution to the θ dependent vacuum energy should come from the UV boundary. The reason is that there should be only one boundary in the theory. The presence of a second boundary would imply that the holographic dynamics of the theory is incomplete. Therefore, we should not expect a contribution from $r = r_0$. In order for this to be true, the axion should vanish at the singularity.[15] We must therefore have,

$$E(\theta_{\rm UV}) = \frac{M^3}{2\ell} C(\theta_{\rm UV} + 2\pi k) \quad , \quad a(r_0) = \theta_{\rm UV} + 2\pi k + C f_1(r_0) = 0 \tag{5.11}$$

[15] Allowing any other value at the singularity, $a(r_0) \equiv a_0$ we obtain for the vacuum energy density, $\mathcal{E} \sim (\theta_{\rm UV} - a_0)^2$ in contradiction with all large-N_c expectations, [21, 22].

Solving the IR equation assuming $f_1(r_0) \neq 0$ we obtain

$$E(\theta_{\rm UV}) = -\frac{M^3}{2\ell}\ {\rm Min}_k\ \frac{(\theta_{\rm UV}+2\pi k)^2}{f_1(r_0)} \quad , \quad \frac{a(r)}{\theta_{\rm UV}+2\pi k} = \left[1-\frac{f_1(r)}{f_1(r_0)}\right] = \frac{\int_r^{r_0}\frac{dr}{e^{3A}Z(\lambda)}}{\int_0^{r_0}\frac{dr}{e^{3A}Z(\lambda)}} \tag{5.12}$$

where the minimum on k (that we denote by k_0) is obtained in order to choose the k-vacuum that minimizes the energy. From (5.12) we can extract the topological susceptibility as

$$\chi = \frac{M^3}{\int_0^{r_0}\frac{dr}{e^{3A}Z(\lambda)}} \tag{5.13}$$

We have obtained the expected quadratic and non-analytic behavior for $E(\theta)$. We have also determined that the instanton vacuum condensate is non-zero

$$\frac{\langle F\wedge F\rangle}{32\pi^2} = -\frac{\theta_{\rm UV}+2\pi k_0}{Z_a\ell^4 f_1(r_0)} = -\frac{\theta_{\rm UV}+2\pi k_0}{\ell^3\int_0^{r_0}dr\frac{Z(0)}{e^{3A}Z(\lambda)}} \tag{5.14}$$

Notice, that the constant $Z(0)$ drops out of all quantities of interest associated with the axion, except the topological susceptibility. Moreover, the condensate is finite without a renormalization of the $F\wedge F$ operator. This is in accordance with lattice results [25].

We also observe a very interesting corollary: *If we view $a(r)$ as an effective θ-angle (in analogy with the t' Hooft coupling) it vanishes in the IR!* .

We now study the dimensionless constant $f_1(r_0)$ that is proportional to the inverse of the topological vacuum susceptibility

$$f_1(r_0) = \int_0^{r_0}\frac{dr}{\ell}\frac{e^{-3A}}{Z(\lambda)} \tag{5.15}$$

The integrand is a positive function as $Z(\lambda)$ is multiplying the axion kinetic energy and is therefore expected to be non-negative. Moreover we do not expect the integrand to diverge at a point before the singularity r_0, as e^A vanishes only at r_0, and $Z(\lambda)$ is also not expected to vanish. Therefore, the only potential pathological behavior is a divergence at r_0.

To study the region around the singularity we will have to study the two cases (r_0 finite or infinite) separately.

- We first consider the IR asymptotics in the infinite range case, namely the singularity at $r=\infty$. From section 3.2, for large r and in the Einstein frame:

$$\log\lambda = \frac{3}{2}Cr^\alpha+\cdots \quad , \quad A=-Cr^\alpha+\cdots \tag{5.16}$$

We also assume that for large λ,

$$Z(\lambda)\sim\lambda^d+\cdots \quad , \quad \lambda\to\infty \tag{5.17}$$

Then:

1. if $d \neq 2$

$$f_1(r_0 = \infty) = \int^{\infty} \frac{dr}{\ell} \ \exp[\frac{3C}{2}(2-d)r^{\alpha} + \cdots] \tag{5.18}$$

In order for this not to diverge, we ask $d > 2$. In this case the low energy asymptotics of the axion are

$$\begin{aligned} \frac{a(r)}{\theta_{\rm UV} + 2\pi k_0} &\simeq \frac{1}{f_1(\infty)} \int_r^{\infty} dr \exp\left[-\frac{3}{2}(d-2)Cr^{\alpha}\right] = \\ &= \frac{1}{\alpha f_1(\infty)} \left(\frac{3(d-2)C}{2}\right)^{\frac{1}{\alpha}} \Gamma\left[\frac{1}{\alpha}, \frac{3}{2}(d-2)Cr^{\alpha}\right] \\ &\simeq \frac{1}{\alpha f_1(\infty)} \left(\frac{3(d-2)C}{2}\right)^{\frac{2}{\alpha}-1} r^{\alpha-1} \exp\left[-\frac{3}{2}(d-2)Cr^{\alpha}\right] \\ &\sim E^{\frac{3}{2}(d-2)} \left(\log E\right)^{\frac{\alpha-1}{\alpha}} \end{aligned} \tag{5.19}$$

where in the last expression we have replaced the radial variable with the holographic energy using (2.15).

2. For $d = 2$,

$$f_1(r_0 = \infty) = \int^{\infty} dr \ r^{-\frac{3}{2}(\alpha-1)} + \cdots \tag{5.20}$$

In order to obtain a finite result, $\alpha > 5/3$. This is stronger than the confinement condition $\alpha \geq 1$. The low energy asymptotics of the axion are

$$\begin{aligned} \frac{a(r)}{\theta_{\rm UV} + 2\pi k_0} &\simeq \frac{1}{f_1(\infty)} \int_r^{\infty} dr \ r^{-\frac{3}{2}(\alpha-1)} \\ &= \frac{2\theta_{\rm UV}}{(3\alpha-5) f_1(\infty)} r^{-\frac{(3\alpha-5)}{2}} \sim (-\log E)^{-\frac{(3\alpha-5)}{2\alpha}} \end{aligned} \tag{5.21}$$

and the effective θ-angle grows slowly in the IR. However, as it is shown in section 6.5.3, in order for the 0^{+-} glueballs to have a discrete spectrum, we must demand $d > 2$ and therefore this case seems not relevant for QCD.

- Similar remarks apply to confining backgrounds with r_0 finite. In particular $f_1(r_0)$ is finite if $d \geq 2$. When $d > 2$ then at low energy

$$\theta(E) \sim E^{\frac{3}{2}(d-2)} \tag{5.22}$$

while for $d = 2$, the low energy running is by the inverse power of the logarithm of the energy.

A comment is in order here concerning the relevance of higher-derivative corrections to the IR asymptotics of the solution. Such corrections can be obtained by substituting $Z(\lambda) \to Z(R, (\partial\lambda)^2, \lambda)$. This is indeed the most general form as higher powers of $(\partial a)^2$ are suppressed by extra powers of $1/N_c$. All arguments made above go through with this more general kinetic function.

The oblique confinement vacua, labeled by k, long-lived in the large-N_c limit, [23] with lifetimes that scale as $\mathcal{O}(N_c)$. The D_2 brane, discussed in [1] is a domain wall separating two such consecutive vacua, as k jumps by ± 1 when crossing the D_2 domain walls.

5.1 Screening of CP violation in the IR

The essence of the strong CP problem lies in the fact that a non-zero θ-parameter in QCD breaks CP (except at $\theta = \pi$) and provides a non-trivial contribution to the neutron dipole moment. The stringent experimental limits on this quantity constrain θ to be very small, ($\preceq 10^{-9}$) [24]. This is known as the strong CP problem: why is θ so small in nature?

In pure YM, the case that we are studying here, the nature of the strong CP problem changes, as there are no quarks, and no baryons. However, the issue is how strong are the CP violating effects of a nontrivial $\theta_{\rm UV}$ in observable data. For a pure gauge theory, a CP-violating effect can be the decay of an (excited) 0^{+-} glueball to 0^{++} glueballs. How important such effects are at low energy depends on the way the axion solution behaves at all radial distances. The behavior of the radial axion profile is shown in figures 1 and 2.

It is tempting to think of the radial axion solution as a "running θ-angle" in analogy with the similar intuition concerning the dilaton that has been justified quantitatively in numerous holographic setups. Here however, such an interpretation needs to be qualified, as there are strong indications from lattice [25], that θ as a coupling in the bare Lagrangian does not receive UV-singular corrections, that would force it to renormalize. That being said, it is direct on the other hand in the holographic context to see that parity violations at low energy although proportional to $\theta_{\rm UV}$, have numerical coefficients that are due to this radial change of the axion and such coefficients can be small.

It is well known that in theories where non-perturbative corrections can be controlled, that $\theta_{\rm eff}$ at low energy receives finite corrections and is different from $\theta_{\rm UV}$. A simple example of this are $\mathcal{N} = 2$ gauge theories in four-dimensions. There, the effective field theory in the Coulomb branch can be exactly solved, [26], and exact effective superpotential calculated. Its real part is the effective θ-angle, which does receive instanton corrections. Although here the effective theory is abelian the effective θ-angle can affect low energy physics as some monopoles and dyons can be light. In large-N_c YM, instantons are apparently suppressed exponentially, but as was argued in early works, [21, 22], such non-perturbative effects can affect θ-related physics at leading orders in $1/N_c$. We therefore advocate that the radial change of the axion can be interpreted as a finite renormalization of the θ-angle in QCD. Of course the quantitatively precise statement is that the axion solution must be used in accordance with the standard rules of the gauge theory/gravity correspondence to calculate physical quantities.

The discussion above as well as figures 1 and 2 suggest that the CP-violating effects of $\theta_{\rm UV}$ are screened at sufficiently low energy, whatever the UV value of the θ-parameter. Moreover, the IR vanishing of the axion is power-like as we have shown above. As we argue in section 6.5.3, the expected value of the exponent d in (5.17) is $d = 4$ from parity independence of asymptotic glueball spectra.

There have been attempts to calculate QCD data at small values of $\theta_{\rm UV}$, on the lattice. Results in particular exist on the topological susceptibility as well as the θ-dependence of the glueball spectrum, [27]. Such calculations can in principle be confronted with similar calculations using the present framework, but we will not do this here.

The relevance of this discussion in the case where quarks are present is more complex

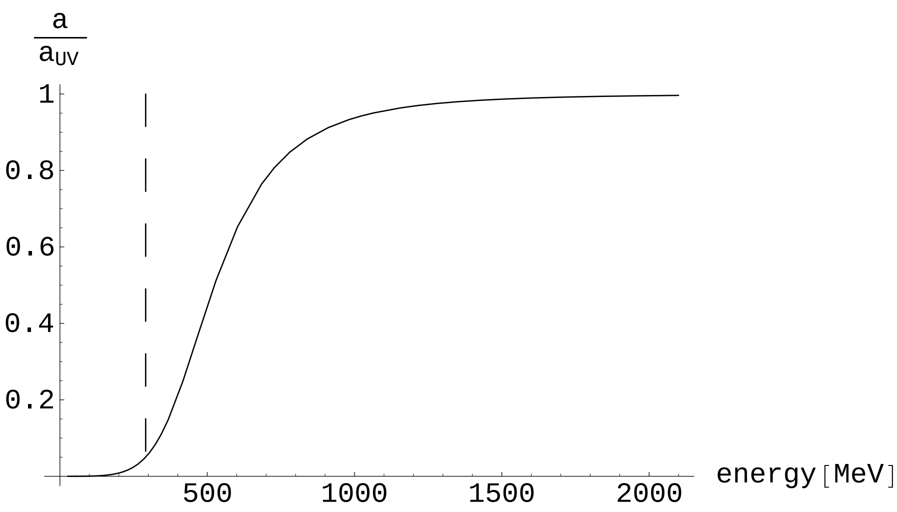

Figure 1: An example of the axion profile (normalized to one in the UV) as a function of energy, in one of the explicit cases we treat numerically in section 8. The energy scale is in MeV, and it is normalized to match the mass of the lowest scalar glueball from lattice data, $m_0 = 1475\,MeV$. The axion kinetic function is taken as $Z(\lambda) = Z_a(1 + c_a\lambda^4)$, with $c_a = 100$ while it does not depend on the value of Z_a. The vertical dashed line corresponds to $\Lambda_{\rm QCD}$ as defined in eq. (7.10). In this particular case $\Lambda = 290\,MeV$.

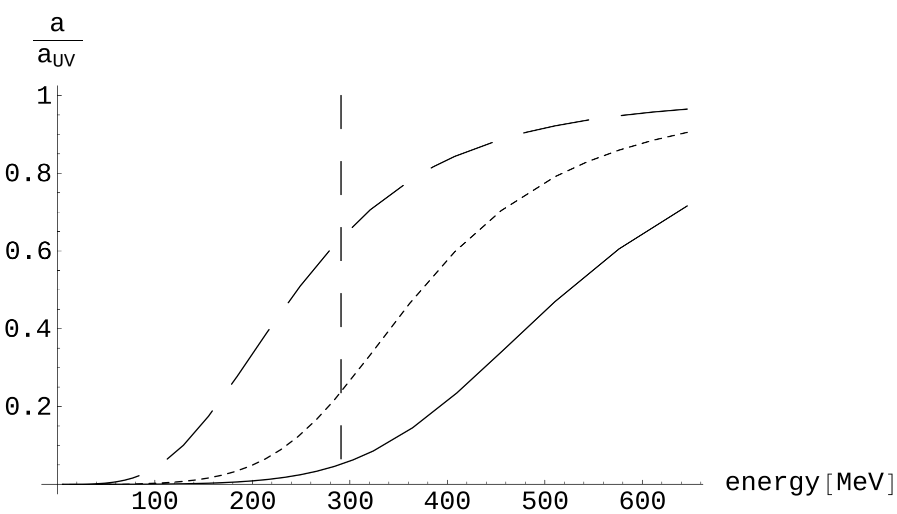

Figure 2: A detail showing the different axion profiles for different values of c_a. The values are $c_a = 0.1$ (dashed line), $c_a = 10$ (dotted line) and $c_a = 100$ (solid line).

and we will not attempt it here although we will show several of the relevant ramifications in section 6.7.

6. The particle spectrum

In gauge-gravity dualities, the particle spectrum of the 4D theory is obtained from the spectrum of fluctuations of the bulk fields around the background. Reviews of glueball spectra calculations in the holographic context can be found in [28]. In this section we first give a general overview of the spectra of various particle species (glueballs and mesons). Then, in section 8, we compute numerically the glueball spectrum of some concrete backgrounds that exhibit asymptotic freedom in the UV and confinement in the IR. The main results of this analysis can be summarized as follows:

1. In the previous section we showed that in order for the theory to confine, the Einstein frame scale factor must vanish at least as fast as $\exp[-Cr^{\alpha}]$ with $\alpha \geq 1$, $C \geq 0$. Remarkably, this is the *same condition* one obtains from the requirement of mass-gap in the spectrum. Therefore, using holography, we can directly relate the existence of a confining string with the existence of a mass gap.

2. Among the class of confining backgrounds we have considered, we find examples that exhibit an asymptotic "linear" mass spectrum, $m_n^2 \sim n$.

In this section we are mostly interested in confining backgrounds in which the scale factor exhibits exponential decay at $r \to \infty$; in the last subsection we briefly discuss the backgrounds with a singularity at finite r.

6.1 General properties of the spectra

Here we discuss the spectrum from a general point of view and leave the details and comparison with the lattice results to section 8. We mostly work in the conformal frame, where the properties of the spectrum are more transparent. The spectrum of particles up to spin 2 is determined by the fluctuation equations of the various bulk fields in the solution. Typically, one can identify fluctuations $\xi(r, x^i)$ with a diagonal kinetic term and a quadratic action of the form

$$S[\xi] \sim \int dr d^4x\, e^{2B(r)} \left[(\partial_r\xi)^2 + (\partial_i\xi)^2 + M^2(r)\xi^2\right], \tag{6.1}$$

where $B(r)$ and $M^2(r)$ are functions depending on the background and on the type of fluctuation in question.

The linearized field equation reads:

$$\ddot{\xi} + 2\dot{B}\dot{\xi} + \Box_4\xi - M^2(r)\xi = 0. \tag{6.2}$$

To look for 4D mass eigenstates, the standard procedure is to write:

$$\xi(r,x) = \xi(r)\xi^{(4)}(x), \qquad \Box\xi^{(4)}(x) = m^2\xi^{(4)}(x). \tag{6.3}$$

Then, eq. (6.2) can be put into a Schrödinger form by defining a wave-function associated to the fluctuation ξ,

$$\xi(r) = e^{-B(r)}\psi(r)\,. \tag{6.4}$$

Eq. (6.2) becomes

$$-\frac{d^2}{dr^2}\psi + V(r)\psi = m^2\psi, \tag{6.5}$$

with the potential given by,

$$V(r) = \frac{d^2B}{dr^2} + \left(\frac{dB}{dr}\right)^2 + M^2(r). \tag{6.6}$$

The Schrödinger equation (6.5) is to be solved on the space of square-integrable functions $\psi(r)$, as can be seen inserting (6.4) into the quadratic action: the kinetic term of a given 4D mode $\xi^{(4)}(x)$ reads:

$$\left(\int dr e^{2B(r)}|\xi(r)|^2\right)\int d^4x\left(\partial_\mu\xi^{(4)}(x)\right)^2 = \left(\int dr|\psi(r)|^2\right)\int d^4x\left(\partial_\mu\xi^{(4)}(x)\right)^2. \tag{6.7}$$

Requiring finiteness of the kinetic term leads to

$$\int dr|\psi(r)|^2 < \infty. \tag{6.8}$$

Therefore, in these coordinates, the problem of finding the spectrum translates into a standard quantum mechanical problem. The general features of the spectrum can be inferred from the properties of the effective Schrödinger potential (6.6). Given the functions $B(r)$ and $M(r)$ we can obtain useful information without finding explicit solutions.

In the case we are mostly interested in, i.e. the infinite-range case, a number of interesting properties of the spectrum can be derived in full generality.

6.2 Existence of a mass gap

Consider first the effective potential in the asymptotically AdS_5 region, $r \sim 0$. There, the potential behaves universally, since $B(r) \sim 3/2A(r)$ in the UV for all kinds of fluctuations:

$$V(r) \sim \frac{15}{4}\frac{1}{r^2} \to +\infty, \qquad r \to 0 \tag{6.9}$$

Next, notice that the equation (6.5) can be written as:

$$\left(P^\dagger P + M^2(r)\right)\psi = m^2\psi, \qquad P = (-\partial_r + \dot{B}(r)) \tag{6.10}$$

Taking into account also the behavior near $r = 0$, the following statements hold:

1. *if $M^2(r) \geq 0$ the spectrum is non-negative*

2. *If the space-time extends to $r = +\infty$, and if moreover $V(r)$ does not vanish as $r \to \infty$, then there is a mass gap.*

The second statement follows from the fact that, if the singularity is at $r \to +\infty$, there can be no normalizable zero-mode solutions to eq. (6.5) with $M^2(r) = 0$. Indeed, the $m = 0$ solutions can be found exactly:

$$\psi_0^{(1)}(r) = e^{B(r)}, \qquad \psi_0^{(2)} = e^{B(r)}\int_0^r dr' e^{-2B(r')} \tag{6.11}$$

It is easy to see that $\psi_0^{(1)}$ is not normalizable in the UV, since there $B \sim -3/2 \log r$. On the other hand, $\psi_0^{(2)}$ is not normalizable in the IR, no matter what is the behavior of $B(r)$ as $r \to \infty$. See [11] for a detailed discussion. Since there are no normalizable zero-modes, the only obstacle to having a mass gap would be a continuous spectrum starting at zero. This cannot be the case if $V(r)$ does not vanish as $r \to \infty$.

If the singularity is at a finite $r = r_0$, this argument still holds if the scale factor vanishes at least as $(r_0 - r)^\delta$, with $\delta > 1$. Then, again one can show that there are no zero-modes. For $0 < \delta < 1$ things are more subtle, and we will leave this case for separate discussion in section 6.6.1.

For the various particle types we analyze (vector mesons, and glueballs of spins up to 2) we will see that property 1 always holds, in fact $M^2 = 0$. Moreover, for all particles we consider, it turns out that the function $B(r)$ has the same IR asymptotics as $A(r)$. In the backgrounds with infinite r range, as $r \to \infty$:

$$A(r) \sim -\left(\frac{r}{R}\right)^\alpha, \tag{6.12}$$

therefore

$$V(r) = \dot{B}^2(r) + \ddot{B}(r) \sim R^{-2}\left(\frac{r}{R}\right)^{2(\alpha-1)}. \tag{6.13}$$

We see that the mass gap condition is $\alpha \geq 1$. *This is the same condition we found independently for quark confinement.* If we require $\alpha > 1$ strictly, we moreover obtain a purely discrete spectrum, since then $V(r) \to +\infty$ for large r. If $\alpha = 1$ the spectrum becomes continuous for $m^2 \geq V(r \to \infty)$.

6.3 Large n mass asymptotics and linear confinement

In the confining backgrounds, where the potential behaves as in eq. (6.13) for large r and as (6.9) for small r, the large eigenvalue asymptotics of eq. (6.5) may be obtained through the WKB approximation: the quantization condition is approximately given by the quantization of the action integral:

$$n\pi = \int_{r_1}^{r_2} \sqrt{m^2 - V(r)}dr \tag{6.14}$$

where r_1 and r_2 are the turning points. For large m^2, $r_1 \sim 0$, and $(r_2/R)^{2(\alpha-1)} \simeq R^2 m^2$, so we can write:

$$n\pi = m\int_0^{R(mR)^{1/(\alpha-1)}} \sqrt{1 - \frac{V(r)}{m^2}}dr \tag{6.15}$$

Assuming $m^2 \gg V(r)$ in the intermediate region, the second term under the square root becomes relevant only when $V(r)$ takes its asymptotic form. We can therefore write

$$n\pi \simeq m\int_0^{R(mR)^{1/(\alpha-1)}} \sqrt{1 - \left[\left(\frac{r}{R}\right)^{\alpha-1}\frac{1}{mR}\right]^2}dr = \left(\frac{m}{\Lambda}\right)^{\frac{\alpha}{\alpha-1}} \int_0^1 dx\sqrt{1 - x^{2(\alpha-1)}} \tag{6.16}$$

where $\Lambda = R^{-1}$. For large n:

$$m \sim \Lambda\, n^{\frac{\alpha-1}{\alpha}}. \tag{6.17}$$

In particular we have "linear confinement" ($m^2 \sim n$) if $\alpha = 2$.[16] For $\alpha \to \infty$ the spectrum looks similar to the one of a "particle in a box" potential, $m^2 \sim n^2$, characteristic of "hard wall" models and more generically of any background with finite r_0 (see section 6.6).

6.4 Universal asymptotic mass ratios

Here we derive some general properties of the glueball spectrum that are independent of the specific potential chosen. In this section, we consider the backgrounds where $X \to -1/2$ at the singularity. As we have seen, this is generic in confining backgrounds with singularity at $r = +\infty$. The function B in (6.2) generally asymptotes to

$$B \to B_f \log(\lambda), \quad as \quad \lambda \to \infty, \tag{6.18}$$

where the coefficient B_f depends on the type of particle. It is essentially determined by the normalization of the kinetic term in the effective action of the specific type of background fluctuation that correspond to the particle in question.

One can also write down the effective Schrödinger potential (6.6) using λ as a coordinate,

$$V_s(\lambda) = \frac{3V_0}{4} X^2 e^{\frac{2}{3}\int^\lambda \frac{d\lambda'}{\lambda'}\left(\frac{1}{X}-4X\right)} \left(\lambda^2 \frac{d^2B}{d\lambda^2} + \lambda \frac{dB}{d\lambda}\left(\frac{1}{3X} + 1 - \frac{4X}{3} + \lambda \frac{d\log|X|}{d\lambda}\right) + \left(\lambda \frac{dB}{d\lambda}\right)^2\right). \tag{6.19}$$

From (6.19) we observe that V_s in the IR asymptotes to,

$$V_s \to \frac{9}{4l^2} e^{2A_0 + \frac{2}{3}\int^\infty \frac{d\lambda'}{\lambda'}\left(\frac{1}{X}-4X\right)} B_f^2 > 0. \tag{6.20}$$

The exponential depends on the specified β-function of the gauge theory. However the constant B_f is universal for a given type of particle, i.e. it is independent of the specified running of the gauge coupling. For example B_f is 1 both for the 0^{++} glueballs and the 2^{++} glueballs, i.e.

$$\frac{V_s(0^{++})(r)}{V_s(2^{++})(r)} \to 1, \qquad r \to +\infty. \tag{6.21}$$

This means that the glueballs have a spectrum whose slope is independent of their spin for large mass:

$$\frac{m^2_{n\to\infty}(0^{++})}{m^2_{n\to\infty}(2^{++})} = 1 \tag{6.22}$$

[16] A dilaton and/or a warp factor $A(r)$ behaving as r^2 for large r, were advocated in [29], in order to obtain a linear spectrum for mesons. In that work, the authors suggest an AdS_5 space-time together with a dilaton with r^2 asymptotics. Such a background is sometimes referred to as a "soft wall" model, and has been used to compute meson-related quantities (see e.g. [31] for recent work). A similar approach was adopted in [30] to treat both baryons and mesons. In that work it is the scale factor, rather than the dilaton, that drives the IR asymptotics.

We should stress that those backgrounds, unlike the ones we study here, are not obtained as solutions of any set of field equations. For example, from our previous discussion it is apparent that, if the dilaton grows as r^2 in the IR, its backreaction is such that the space-time cannot be close to AdS_5 for large r, independently of the form of the dilaton potential. Moreover, as we discuss in section 5.4, the dynamics of mesons could be described by a different mechanism [5] which does not necessarily require $\alpha = 2$ for a linear meson spectrum.

This fits nicely with the semi-classical string models (see e.g. [32]) for the glueballs that predict

$$\frac{m^2}{2\pi\sigma_a} = 2n + J + c, \tag{6.23}$$

where σ_a is the adjoint string tension, J is the angular momentum and c is some number of order 1. Our finding (6.22) is in accord with the general prediction of such models that the adjoint string tension is universal for glueballs with different spin.

Next, we move to specific analysis of the spectra of different species of glueballs.

6.5 Glueball spectra

At the lowest mass level the bulk theory contains the dilaton Φ, the metric $g_{\mu\nu}$, and the axion a. The spectrum of physical fluctuations of these fields is dual to the spectrum of glueballs in the gauge theory, as these fields come from the closed sting sector. The physical massive fluctuations of the minimal metric+dilaton system consists of one spin-2 mode (5 degrees of freedom), and one spin-0 mode.[17] The fluctuations of the axion field correspond to pseudoscalar glueballs. They do not mix with those in the scalar sector of the metric-dilaton system, since we neglect the backreaction of the axion on the geometry.[18]

Throughout this section we consider only the IR asymptotics of the type (3.13),

$$A(r) \sim -\left(\frac{r}{R}\right)^{\alpha} + \cdots, \qquad \alpha \geq 1 \tag{6.24}$$

with no further assumptions on the subleading behavior. We will consider the case with singularity at finite r in section 6.6

6.5.1 Scalar glueballs

In 5D Einstein-Dilaton gravity there exists a single gauge invariant spin-0 mode,[19] $\zeta(r,x)$, satisfying the equation (6.2) with

$$B_0(r) = \frac{3}{2}A(r) + \frac{1}{2}\log X^2, \qquad M(r) = 0, \tag{6.26}$$

The effective Schrödinger potential is given by eq. (6.6). Notice that, both for large and small r, the second term in B_0 (6.26) is negligible. Therefore the leading asymptotics are,

$$V_0(r) \sim \begin{cases} \frac{9}{4}R^{-2}\left(\frac{r}{R}\right)^{2(\alpha-1)}, & r \to \infty, \\ \sim \frac{15}{4}\frac{1}{r^2}, & r \to 0. \end{cases} \tag{6.27}$$

[17] See e.g. [11] for a complete discussion of the identification of the physical fluctuations and the corresponding field equations. In the massless sector there are a massless spin-2 (2 polarization), one massless spin-1 (2 polarizations) and 2 massless spin-0 modes. However we will not have massless modes in our spectra, so we will not consider this case further. In [11] it was shown that in general the presence of a massless spin-2 mode is only possible if an IR singularity appears and if special non-local boundary conditions are put at the singularity. This is compatible with the Weinberg-Witten theorem [33].

[18] However, they are expected to mix with η' if we introduce flavor branes.

[19] Here "gauge invariace" refers to the linearized 5D diffeomorphisms. The precise definition of this field is

$$\zeta = \psi - \frac{1}{3X(r)}\delta\phi = \psi - \frac{\lambda}{\beta(\lambda)}\delta\phi, \tag{6.25}$$

where $\delta\phi$ and ψ are the fluctuations in the dilaton and in the scalar part of the g_{ij} metric component. See e.g. [11].

We have a mass gap and discrete spectrum if and only if $\alpha > 1$.

In the UV, the gauge invariance of ζ indicates that it is dual to the renormalization group invariant operator $\beta(\lambda)Tr[F^2]$ [34].

6.5.2 Tensor glueballs

The massive spin-2 glueballs are described by transverse traceless tensor fluctuations h_{ij} of the 4D part of the metric:

$$ds^2 = e^{2A(r)}\left(dr^2 + (\eta_{ij} + h_{ij})dx^i dx^j\right) \tag{6.28}$$

These fluctuations satisfy the equation (6.2) with

$$B_2(r) = \frac{3}{2}A(r), \qquad M(r) = 0 \tag{6.29}$$

The effective Schrödinger potential has the same asymptotics as (6.27):

$$V_2(r) \sim \begin{cases} \frac{9}{4}R^{-2}\left(\frac{r}{R}\right)^{2(\alpha-1)}, & r \to \infty, \\ \frac{15}{4}\frac{1}{r^2}, & r \to 0. \end{cases} \tag{6.30}$$

Together with (6.27) this confirms (6.22). However, due to the difference between (6.26) and (6.29), the spin-0 and spin-2 glueball spectra are not degenerate. This is unlike the AdS/QCD models with exact AdS metric and constant dilaton: there the scalar and tensor modes are exactly degenerate. We will see in an explicit background that the lowest-lying spin-0 glueball is lighter than the lowest spin-2 glueball. We expect this fact to be generic, although we can not provide a proof in our set-up.

6.5.3 Pseudo-scalar glueballs

The Einstein frame axion action in the conformal coordinates reads:

$$S_a = -\frac{M^3}{2}\int d^5x Z(\lambda)e^{3A}(\partial a)^2. \tag{6.31}$$

Since the axion appears quadratically, this is also the action for the fluctuations. We thus have:

$$B_a(r) = \frac{3}{2}A(r) + \frac{1}{2}\log Z(\lambda). \tag{6.32}$$

To leading order in string perturbation theory, $Z(\lambda) = \lambda^2$. However, this in general is expected to receive corrections from the 5-form, similar to the dilaton potential. Indeed, if this were not the case one would find a puzzling result: one would obtain a continuous spectrum for the pseudo-scalar glueballs starting at $m = 0$. To see this, assume as in section 5 that $Z(\lambda) = \lambda^d$ for large λ. Then, using eq. (3.15) in (6.32) we obtain:

$$\begin{aligned} B_a(r) &= \frac{3}{2}\left(1 - \frac{d}{2}\right)A(r) + \frac{d}{2}\frac{3}{4}(\alpha-1)\log r/R \\ &\sim \begin{cases} \frac{3}{4}(d-2)\,(r/R)^{\alpha} & d \neq 2 \\ \frac{3}{4}(\alpha-1)\log r/R & d = 2, \end{cases} \end{aligned} \tag{6.33}$$

where we used (6.24). The IR asymptotics of the Schrödinger potential are (using (6.6)),

$$V_a(r) \sim \begin{cases} \frac{9}{16}\left[(d-2)^2/R^2\right](r/R)^{2(\alpha-1)} & d \neq 2 \\ \left[\frac{9}{16}(\alpha-1)^2 - \frac{3}{4}(\alpha-1)\right]\frac{1}{r^2} & d = 2. \end{cases} \tag{6.34}$$

Thus the potential and the spectrum have the same features as the other glueballs, *unless* the perturbative result $d = 2$ is unmodified.

The asymptotic mass ratio for large n of the 0^{-+} to 0^{++} glueball states can be read-off comparing the large r asymptotics of (6.34) for $d \neq 2$ and (6.27):

$$\frac{V(0^{-+})}{V(0^{++})} \to \frac{1}{4}(d-2)^2 \tag{6.35}$$

Using the expected asymptotic glueball universality argument (as in (6.22))

$$\frac{m^2_{n\to\infty}(0^{-+})}{m^2_{n\to\infty}(0^{++})} = \frac{m^2_{n\to\infty}(0^{++})}{m^2_{n\to\infty}(2^{++})} = 1, \tag{6.36}$$

we can determine

$$d = 4. \tag{6.37}$$

This result predicts an interesting renormalization of the bare axion kinetic term, (6.31).

It is appropriate to point out that the effective Schrödinger potential for the 0^{-+} trajectory of glueballs can be written in terms of the background axion solution (5.12) as

$$V_a(r) = \frac{1}{4}\frac{\dddot{a}}{\dot{a}} \tag{6.38}$$

An interesting corollary of this relation is that the potential is independent of the UV θ-angle of QCD, $\theta_{\rm UV}$.

When $\theta \neq 0$ glueballs of different parities mix as well as their energies become θ-dependent to next order in $1/N_c$. The θ-dependence of the glueball spectrum can be calculated by considering the first order ($\mathcal{O}(1/N_c^2)$) backreaction of the axion solution to the QCD vacuum. This can be an interesting test as lattice data on this exist, [27]. We will not attempt however the calculation in this paper.

6.6 Singularity at finite r_0

In the previous subsections we considered backgrounds with infinite range in r. Here we discuss the case in which the IR singularity is at some finite $r = r_0$. As discussed in appendix A and summarized in table 1, these backgrounds generically lead to a confining string potential. To analyze the mass spectrum, consider the case when the IR singularity has the following form:

$$A(r) \sim \delta \log(r_0 - r), \quad r \to r_0. \tag{6.39}$$

The effective Schrödinger potential (6.6) has the same asymptotic form in the IR both for the scalar and the tensor glueballs. This is because the functions (6.26) and (6.29), differ only by a function of $X(r)$ which, as shown in appendix A, asymptotes to a (δ-dependent) constant as $r \to r_0$. Then, both for the spin-0 and the spin-2 glueballs, the effective Schrödinger potential has the following asymptotic form:

$$V(r) \sim \frac{15}{4}\frac{1}{r^2} \quad (r \to 0), \qquad V(r) \sim \frac{9}{4}\frac{\delta(\delta - 2/3)}{(r - r_0)^2}, \quad (r \to \infty). \tag{6.40}$$

For $\delta > 2/3$, $V \to +\infty$ in the IR, and by the same general argument we used in subsection 4.1 we obtain a mass gap and a discrete spectrum. The treatment of the case $0 < \delta < 2/3$ (in fact $0 < \delta < 1$) requires extra care, as we discuss in the next subsection.

The large mass asymptotics of both the scalar and the tensor glueballs in the backgrounds (6.39) are universal. They depend neither on δ nor the details of the metric in the bulk: due to (6.40), the Schrödinger equation for large eigenvalues is effectively the one for a particle in a box of size r_0, so for large mass eigenstates we obtain

$$m_n^2 \sim \frac{n^2}{r_0^2}. \tag{6.41}$$

This does not *a priori* prevent the mesons to have a linear mass spectrum, since this is driven by the tachyon dynamics,[20] as in the infinite range case.

In the case of power-law behavior for $A(r)$,

$$A(r) \sim -\frac{C}{(r_0 - r)^{\tilde{\alpha}}}, \qquad \tilde{\alpha}, C > 0 \tag{6.42}$$

the potential in the IR always asymptotes to $+\infty$, and it is steeper than $(r_0 - r)^{-2}$ in the IR:

$$V(r) \sim \frac{9}{4}\frac{C^2}{(r_0 - r)^{2\tilde{\alpha}+2}} \tag{6.43}$$

6.6.1 The pathologies for $0 < \delta < 1$

As discussed in [11] in a different context (see also [36] for a related discussion), this range of parameters is somewhat pathological, since it requires additional boundary conditions at the singularity, and the spectrum is not determined by the normalization condition alone.

The Schrödinger equation for a generic mass eigenstate close to r_0 is:

$$-\ddot{\psi} + V(r) \sim -\ddot{\psi} + \frac{9}{4}\frac{\delta(\delta - 2/3)}{(r - r_0)^2}\psi = m^2\psi. \tag{6.44}$$

For $r \sim r_0$ we can neglect the mass term on the r.h.s, and find the asymptotic solution close to r_0:

$$\psi(r) \sim c_1(r_0 - r)^{3\delta/2} + c_2(r_0 - r)^{1-3\delta/2}. \tag{6.45}$$

For $\delta < 1$ both solutions are square-integrable, and they both vanish at r_0 if in addition $\delta < 2/3$. Therefore, for $0 < \delta < 1$, normalizability alone is not enough to fix the spectrum uniquely. One has to specify some extra boundary conditions at the singularity, which may

[20]This observation avoids the arguments put forward in [35] regarding the meson spectra in gravity duals.

be given by fixing the ratio c_1/c_2.[21] In contrast, for $\delta \geq 1$ normalizability in the IR *forces* the choice $c_2 = 0$, and there is no ambiguity.

Ultimately it is this extra input at the singularity that determines the spectrum in a background with $\delta < 1$, and not the dynamics of the theory at any finite energy. This situation is not so different from the hard-wall models [2, 3], where one also has to specify IR boundary conditions for the fluctuations to compute the spectrum.

We note here that the background studied of Csaki and Reece in [15] falls in this class of examples: one can easily check that its metric in conformal frame behaves as in eq. (6.39) with $\delta = 1/3$. In computing the spectrum, IR Neumann boundary conditions are chosen in [15], but according to the present discussion this is as good a choice as any other.

6.7 Adding flavor

A small number $N_f \ll N_c$ of quark flavors can be included in our setup by adding space-time filling "flavor-branes". In this case they are pairs of space-filling $D4 - \bar{D}4$ branes. It was proposed in [5] that the proper treatment of the flavor sector (including chiral symmetry breaking) involves the dynamics of the open string tachyon of the $D4 - \bar{D}4$ system. According to this, the meson sector of the 4D gauge theory is captured holographically by the open string DBI+WZ action, which schematically reads, in the string frame,

$$S[T, A^L, A^R] = S_{\rm DBI} + S_{\rm WZ} \tag{6.46}$$

where the DBI action for the pair is

$$S_{\rm DBI} = \int drd^4x \, \frac{N_c}{\lambda} \, \mathbf{Str} \left[V(T) \left(\sqrt{-\det \left(g_{\mu\nu} + D_{\{\mu} T^\dagger D_{\nu\}} T + F^L_{\mu\nu} \right)} + \right. \right. \tag{6.47}$$
$$\left. \left. + \sqrt{-\det \left(g_{\mu\nu} + D_{\{\mu} T^\dagger D_{\nu\}} T + F^R_{\mu\nu} \right)} \right) \right]$$

Here T is the tachyon, a complex $N_f \times N_f$ matrix. $A^{L,R}_\mu$ are the world-volume gauge fields of the $\mathrm{U}(N_f)_L \times \mathrm{U}(N_f)_R$ flavor symmetry, under which the tachyon is transforming as the $(N_f, \bar{N}_f)$, a fact reflected in the presence of the covariant derivatives[22]

$$D_\mu T \equiv \partial_\mu T - iTA^L_\mu + iA^R_\mu T \quad , \quad D_\mu T^\dagger \equiv \partial_\mu T^\dagger - iA^L_\mu T^\dagger + iT^\dagger A^R_\mu \tag{6.48}$$

transforming covariantly under

$$T \to V_R T V_L^\dagger \quad , \quad A^L \to V_L (A^L - iV_L^\dagger dV_L) V_L^\dagger \quad , \quad A^R \to V_R (A^R - iV_R^\dagger dV_R) V_R^\dagger \tag{6.49}$$

as well as the field strengths $F^{L,R} = dA_{L,R} - iA_{L,R} \wedge A_{L,R}$ of the $A^{L,R}$ gauge fields. $\lambda \equiv e^\Phi = N_c e^\phi$ is as usual the 't Hooft coupling. We have also used the symmetric trace ($\equiv Str$) prescription although higher order terms of the non-abelian DBI action are not

[21] In operator language, the Hamiltonian of this problem is symmetric but not essentially self-adjoint, and it admits an infinite number of self-adjoint extensions, each with a different spectrum, parametrized by the choice of c_1/c_2.

[22] We are using the conventions of [5].

known. It turns out that such a prescription is not relevant for the vacuum structure in the meson sector (as determined by the classical solution of the tachyon) neither for the mass spectrum. The reason is that we may treat the light quark masses as equal to the first approximation and then in the vacuum, $T = \tau \mathbf{1}$ with τ real, and this is insensitive to non-abelian ramifications. Expanding around this solution, the non-abelian ambiguities in the higher order terms do not enter at quadratic order. Therefore, for the spectrum we might as well replace $Str \to Tr$.

The WZ action on the other hand is given by:[23]

$$S_{\rm WZ} = T_4 \int_{M_5} C \wedge {\rm Str}\ \exp\left[i2\pi\alpha' \mathcal{F}\right] \tag{6.50}$$

where M_5 is the world-volume of the D4-$\overline{\rm D4}$ branes that coincides with the full space-time. Here, C is a formal sum of the RR potentials $C = \sum_n (-i)^{\frac{5-n}{2}} C_n$, and $\mathcal{F}$ is the curvature of a superconnection $\mathcal{A}$. In terms of the tachyon field matrix T and the gauge fields A^L and A^R living respectively on the branes and antibranes, they are (We will set $2\pi\alpha' = 1$ and use the notation of [18]):

$$i\mathcal{A} = \begin{pmatrix} iA_L & T^\dagger \\ T & iA_R \end{pmatrix}, \qquad i\mathcal{F} = \begin{pmatrix} iF_L - T^\dagger T & DT^\dagger \\ DT & iF_R - TT^\dagger \end{pmatrix} \tag{6.51}$$

The curvature of the superconnection is defined as:

$$\mathcal{F} = d\mathcal{A} - i\mathcal{A}\wedge\mathcal{A} \quad , \quad d\mathcal{F} - i\mathcal{A}\wedge\mathcal{F} + i\mathcal{F}\wedge\mathcal{A} = 0 \tag{6.52}$$

Note that under (flavor) gauge transformation it transforms homogeneously

$$\mathcal{F} \to \begin{pmatrix} V_L & 0 \\ 0 & V_R \end{pmatrix} \mathcal{F} \begin{pmatrix} V_L^\dagger & 0 \\ 0 & V_R^\dagger \end{pmatrix} \tag{6.53}$$

In [5] the relevant definitions and properties of this *supermatrix* formalism can be found.

By expanding we obtain

$$S_{\rm WZ} = T_4 \int C_5 \wedge Z_0 + C_3 \wedge Z_2 + C_1 \wedge Z_4 + C_{-1} \wedge Z_6 \tag{6.54}$$

where Z_{2n} are appropriate forms coming from the expansion of the exponential of the superconnection. In particular, $Z_0 = 0$, signaling the global cancellation of 4-brane charge, which is equivalent to the cancelation of the gauge anomaly in QCD. Further, as was shown in [5]

$$Z_2 = d\Omega_1 \quad , \quad \Omega_1 = iSTr(V(T^\dagger T))Tr(A_L - A_R) - \log\det(T) d(StrV(T^\dagger T)) \tag{6.55}$$

This terms provides the Stuckelberg mixing between $Tr[A^L_\mu - A^R_\mu]$ and the QCD axion that is dual to C_3. Dualizing the full action we obtain

$$\begin{aligned} S_{CP-odd} &= \frac{M^3}{2N_c^2}\int d^5x\sqrt{g}Z(\lambda)\left(\partial a + i\Omega_1\right)^2 \\ &= \frac{M^3}{2}\int d^5x\sqrt{g}Z(\lambda)\left(\partial_\mu a + \zeta\partial_\mu V(\tau) - \sqrt{\frac{N_f}{2}}V(\tau)A^A_\mu\right)^2 \end{aligned} \tag{6.56}$$

[23]This expression was proposed in [17] and proved in [18, 19] using boundary string field theory

with

$$\zeta = \Im \log \det T \quad , \quad A_L - A_R \equiv \frac{1}{2N_f} A^A \mathbb{I} + (A_L^a - A_R^a)\lambda^a \tag{6.57}$$

and where we have set the tachyon to it vev $T = \tau \mathbf{1}$. This term is invariant under the $\mathrm{U}(1)_A$ transformations

$$\zeta \to \zeta + \epsilon \quad , \quad A_\mu^A \to A_\mu^A - \sqrt{\frac{2}{N_f}} \partial_\mu \epsilon \quad , \quad a \to a - N_f \epsilon V(\tau) \tag{6.58}$$

reflecting the QCD $\mathrm{U}(1)_A$ anomaly. It is this Stuckelberg term together with the kinetic term of the tachyon field that is responsible for the mixing between the QCD axion and the η'. In terms of degrees of freedom, we have two scalars a, ζ and an (axial) vector, A_μ^A. We can use gauge invariance to remove the longitudinal components of A^A. Then an appropriate linear combination of the two scalars will become the 0^{-+} glueball field while the other will be the η'. The transverse (5d) vector will provide the tower of $\mathrm{U}(1)_A$ vector mesons.

The next term in the WZ expansion couples the baryon density to a one-form RR field C_1. There is no known operator expected to be dual to this bulk form. However its presence and coupling to baryon density can be understood as follows. Before decoupling the N_c D_3 branes, its dual form C_2 couples to the $\mathrm{U}(1)_B$ on the D_3 branes via the standard $C_2 \wedge F_B$ WZ coupling. This is dual to a free field, the doubleton, living only at the boundary of the bulk. Once we add the probe $D_4 + \bar{D}_4$ branes the free field is now a linear combination of A^B and an N_f/N_c admixture of A^V originating on the flavor branes. The orthogonal combination is the baryon number current on the flavor branes and it naturally couples to C_1. Therefore the C_1 field is expected to be dual to the topological baryon current at the boundary.

Finally the form of the last term requires some explanation. By writing $Z_6 = d\Omega_5$ we may rewrite this term as

$$\int F_0 \wedge \Omega_5 \quad , \quad F_0 = dC_{-1} \tag{6.59}$$

$F_0 \sim N_c$ is nothing else but the dual of the five-form field strength. This term then provides the correct Chern-Simons form that reproduces the flavor anomalies of QCD. Its explicit form in terms of the gauge fields $A_{L,R}$ and the tachyon was given in equation (3.13) in [5].

To proceed further and analyze the vacuum solution we set $T = \tau \, \mathbf{1}$ and set the vectors to zero. Then the action (6.46) collapses to

$$S[\tau, A_M] = N_c N_f \int dr d^4x \; e^{-\Phi} V(\tau) \sqrt{-\det\left(g_{\mu\nu} + \partial_\mu \tau \partial_\nu \tau\right)} \tag{6.60}$$

Following [5] we assume the following tachyon potential, motivated/calculated in studies of tachyon condensation:

$$V(\tau) = V_0 e^{-\frac{\mu^2}{2}\tau^2} \tag{6.61}$$

where μ has dimension of mass. It is fixed by the requirement that τ has the correct bulk mass to couple to the quark bilinear operator on the boundary.

In our minimal setup, the brane-antibrane system fills the whole bulk. Therefore these fields are bulk fields. We will eventually expand the action at most to quadratic order in the gauge fields.

Chiral symmetry breaking in the IR is described by a non-trivial tachyon profile. For small N_f we can neglect the backreaction of the tachyon on the metric-dilaton system, and solve the equation for the tachyon profile on a given background, e.g. one of the confining backgrounds we discussed. Once a solution for the tachyon is found, the spectrum of mesons is given by the spectrum of fluctuations around this background. For example, vector mesons are described by the fluctuations of the components A_i around the $A_i = 0$ configuration, in a given background for the metric, dilaton and tachyon.

6.7.1 Tachyon dynamics

In the conformal frame, the action (6.60) becomes:

$$S[\tau] = N_c N_f \int dr d^4x e^{4A_s(r)-\Phi(r)} V(\tau)\sqrt{e^{2A_s(r)} + \dot{\tau}(r)^2}, \tag{6.62}$$

from which we obtain the nonlinear field equation:

$$\ddot{\tau} + \left(3\dot{A}_S - \dot{\Phi}\right)\dot{\tau} + e^{2A_S}\mu^2\tau + e^{-2A_S}\left[4\dot{A}_S - \dot{\Phi}\right](\dot{\tau})^3 + \mu^2\tau(\dot{\tau})^2 = 0. \tag{6.63}$$

The tachyon is dual to the dimension 3 quark bilinear operator. Near the boundary, $r \to 0$, we expect $\tau = mr + \sigma r^3 + \cdots$.[24] Thus, in the UV We may ignore the non-linear terms in eq. (6.63), which then reduces to the equation for a free scalar field with mass μ on an asymptotically AdS_5 background. In order for this to be dual to the quark bilinear operator, with naive dimension 3 (to leading order), we need $3 = 2 + \sqrt{4 - \mu^2\ell^2}$, hence $\mu^2\ell^2 = 3$.

It is argued in [5] that consistency of the bulk gauge theory (i.e. absence of extra gauge anomalies in the IR) requires the tachyon to diverge before or at the singularity. In appendix D we analyze the possible singularities of the solutions of eq. (6.63), in backgrounds with IR asymptotics (6.24). We show that the only consistent solution for $r \to \infty$, is such that the tachyon diverges exponentially:

$$\tau(r) \sim \tau_0 \exp\left[\frac{2}{\alpha}\frac{R}{\ell^2} r\right], \qquad r \to \infty, \tag{6.64}$$

where τ_0 is an integration constant determined by UV initial conditions.

We also analyze possible singularities of the solutions at finite r. We find that generically, the tachyon cannot diverge at any finite r, where both A_S and Φ are regular, except special points where $4\dot{A}_s - \dot{\Phi} = 0$. This does not happen in our backgrounds. Instead, the generic solution of (6.63) has a singularity at finite r_*, where $\tau(r_*)$ stays finite but its derivatives diverges:

$$\tau \sim \tau_* + \gamma\sqrt{r_* - r}. \tag{6.65}$$

Such solutions are unphysical, since around r_* the backreaction on the metric is no longer negligible: the tachyon stress tensor diverges as $1/(r_* - r)$, and our assumption that the tachyon does not perturb the background is invalid. On the other hand this is not physically

[24] For simplicity, here we take all quark masses to be equal. The tachyon is therefore proportional to the identity matrix in flavor space.

reasonable, since adding a small number of flavors should not change dramatically the pure gauge dynamics in the large N_c limit.[25]

Discarding all but the exponentially divergent solution singles out special initial conditions in the UV, which correspond to fixing the chiral condensate as a function of the quark mass [5], i.e. the coefficients of the subleading and leading terms in the UV expansion of $\tau(r)$.

6.7.2 Vector mesons

Once the correct tachyon profile is found from eq. (6.63), this enters the action for the tachyon and the bulk gauge fields fluctuations, and determines their spectrum. The resulting 4D mass eigenstates correspond to the various mesons in the dual theory. Here, we only consider the vector mesons, that correspond to the transverse vector components of the 5D gauge fields, $A_i = A_i^L + A_i^R$.

The quadratic action for the gauge fields is, from eq. (6.46):

$$S \sim -\frac{1}{4}\int dr d^4x\, e^{-\Phi} V(\tau)\sqrt{-\hat{g}}\hat{g}^{\mu\nu}\hat{g}^{\rho\sigma}F_{\mu\rho}F_{\nu\sigma}, \tag{6.66}$$

where $\hat{g}$ is the effective (open string) metric felt by the gauge fields in the presence of the tachyon:

$$d\hat{s}^2 = \left(e^{2A_S} + (\dot{\tau})^2\right) dr^2 + e^{2A_S}\eta_{ij}dx^i dx^j. \tag{6.67}$$

This metric is still asymptotically AdS, since e^{2A_S} dominates in the UV, however, although still conformally flat, it is not in the conformal frame. It differs considerably from the bulk background metric in the IR.

The large r behavior of $A_S(r)$ and $\tau(r)$ are, from eq. (3.16) and (6.64):

$$A_S(r) \sim \frac{\alpha-1}{2}\log r/R, \qquad \tau(r) \sim \tau_0 \exp\left[\frac{2}{\alpha}\frac{R}{\ell^2}r\right], \qquad \alpha \geq 1. \tag{6.68}$$

The second term dominates $\hat{g}_{rr}$ in the infrared. To recast the action in the form (6.1), and read-off the effective Schrödinger potential for the mesons, we change variables from r to τ. Using (6.68) to express A_S as a function of τ in the IR, the effective metric becomes for large τ:

$$d\hat{s}^2 \sim d\tau^2 + \left(\frac{\alpha\ell^2}{2R^2}\log\tau/\tau_0\right)^{\alpha-1}\eta_{ij}dx^i dx^j, \tag{6.69}$$

where we have neglected the first term in $\hat{g}_{rr}$. We now pass to a new conformal frame, by changing variables from τ to $\hat{r}$, defined by

$$d\tau = \left(\frac{\alpha\ell^2}{2R^2}\log\tau/\tau_0\right)^{(\alpha-1)/2} d\hat{r} + \cdots, \tag{6.70}$$

[25] Notice that the backreaction is not problematic if the tachyon itself, and not just its derivative, diverge: the stress tensor is multiplied by the tachyon potential, that vanishes exponentially fast as $\tau \to \infty$, resulting in the recombination of the branes-antibrane pairs in the IR, which leaves the unperturbed metric and dilaton background.

which is solved asymptotically for large τ by:

$$\hat{r} = \left(\frac{2R^2}{\alpha\ell^2}\right)^{(\alpha-1)/2} \frac{\tau}{(\log\tau/\tau_0)^{(\alpha-1)/2}} + \cdots. \tag{6.71}$$

To leading order we can also replace $\log\tau/\tau_0$ by $\log r/\tau_0$ in the above relation and the metric reads:

$$d\hat{s}^2 = e^{2\hat{A}(\hat{r})}\left(d\hat{r}^2 + \eta_{ij}dx^i dx^j\right) \sim \left[\frac{\alpha\ell^2}{2R^2}\log\hat{r}/\tau_0\right]^{\alpha-1}\left(d\hat{r}^2 + \eta_{ij}dx^i dx^j\right). \tag{6.72}$$

The action for the transverse vector fluctuations becomes:

$$S = -\frac{1}{2}\int d\hat{r}d^4x e^{-\Phi}V(\hat{r})e^{\hat{A}(\hat{r})}\left[(\partial_{\hat{r}}A_i)^2 + (\partial_j A_i)^2\right], \tag{6.73}$$

and has the same form as in (6.1) with

$$B(\hat{r}) = \frac{\hat{A}(\hat{r}) - \Phi(\hat{r})}{2} + \frac{1}{2}\log V(\tau(\hat{r})) \tag{6.74}$$

Asymptotically the last term dominates (it behaves like τ^2, which is exponential in the original r coordinate, while A_S grows logarithmically and Φ a power-law of r), and we find, using eq. (6.61):

$$B(\hat{r}) \sim -\frac{3}{4\ell^2}\left(\frac{\alpha\ell^2}{2R^2}\right)^{\alpha-1}\hat{r}^2\left(\log\hat{r}/\tau_0\right)^{\alpha-1} \tag{6.75}$$

From the general analysis of section 6.1, and in particular from eq. (6.6), the leading behavior of the vector meson Schrödinger potential is that of a (logarithmically corrected) harmonic oscillator, therefore it exhibits an approximately linear mass spectrum.[26] This is a concrete realization of the general mechanism described in [5].

Notice that the meson spectrum is generically controlled by a different energy scale than the one that sets the glueball masses: the two scales are

$$\Lambda_{\text{glueballs}} = \frac{1}{R}, \qquad \Lambda_{\text{mesons}} = \frac{3}{\ell}\left(\frac{\alpha\ell^2}{2R^2}\right)^{(\alpha-1)/2} \propto \frac{1}{R}\left(\frac{\ell}{R}\right)^{\alpha-2}. \tag{6.76}$$

Interestingly, the two scales happen to coincide in the special case $\alpha = 2$, in which the asymptotic glueball spectrum is *also* linear.

As a final remark we comment on the importance of $1/N_c^2$ corrections due to the bulk (closed sector) on the meson spectrum. It seems that at least for questions of the meson spectrum, lattice calculations indicate that such corrections are small. The errors for the pion and ρ-meson masses were estimated at around 4% for $N_c = 3$ in [46] working in the quenched approximation.

[26] One can get rid of the extra log by a slight modification of the tachyon potential.

7. The parameters of the correspondence

QCD with gauge group SU(N_c) has three parameters: the bare coupling constant λ_0, the theta-angle θ and the number of colors N_c. On the other hand, through dimensional transmutation the bare coupling constant is replaced by the dynamically generated strong coupling scale $\Lambda_{\rm QCD}$. In the large N_c limit therefore, apart from θ, this is the single parameter of the theory. It sets the scale for the glueball and meson masses.

7.1 Parameters in the gravitational action

On the gravity side, we have a number of parameters entering the Lagrangian (and the fundamental string action) and a set of integration constants for the vacuum solutions. The parameters that appear in the action are the 5D Planck scale M, the string scale ℓ_s, the AdS radius ℓ (via the overall scale of the potential, $V_0 = 12/\ell^2$). Moreover, the potential as a function has dimensionless parameters. In its weak coupling expansion, they are in one to one correspondence with the coefficients of the β-function, b_n. Among the parameters b_n, as we discussed above, the only scheme independent coefficients are b_0 and b_1. For practical reasons we restrict ourselves to potentials parameterized only by these two. Moreover, the ambiguity in the normalization of λ, amounts to b_0 being a parameter that we eventually fit. b_1/b_0^2 however remains and we take its value from the QCD β-function. The strategy however is clear: although the potential is an a priori arbitrary function, our eventual choice will have very few adjustable parameters.

The Planck scale governs the strength of bulk interactions. In the underlying string theory, it is determined in terms of the string scale. However here, this relation is not known and it will have to be taken as an extra parameter, that can be fixed by matching to interactions, or to the finite temperature free energy.

On the other hand, either of the two dimensionfull parameters ℓ or ℓ_s can be used to set the units. We choose to measure all the dimensionfull quantities in units of ℓ.

Apart from the parameters of the action, there are in general three integration constants that parameterize the solutions to the Einstein-dilaton system.

Now, we discuss them one by one. In the dual gauge theory the β-function is fixed, and this is in one-to-one correspondence with the function X or the superpotential W on the gravity side. Once the potential V is given, there are infinite number of W that solve (2.10), parameterized by a single boundary condition. However in appendix (E) we show that the confining asymptotics of the form,

$$W \to \Phi^{\frac{P}{2}} e^{\frac{2}{3}\Phi}, \tag{7.1}$$

is a unique solution to the equation (2.10).

Therefore the requirement of confinement uniquely fixes the superpotential W and reduces the number of independent integration constants from three to two. The IR asymptotics above indeed evolves into an asymptotic AdS space in the UV as,

$$W \to \left(\frac{3}{4}\right)^{\frac{3}{2}} V_0^{\frac{1}{2}} + \mathcal{O}(\lambda). \tag{7.2}$$

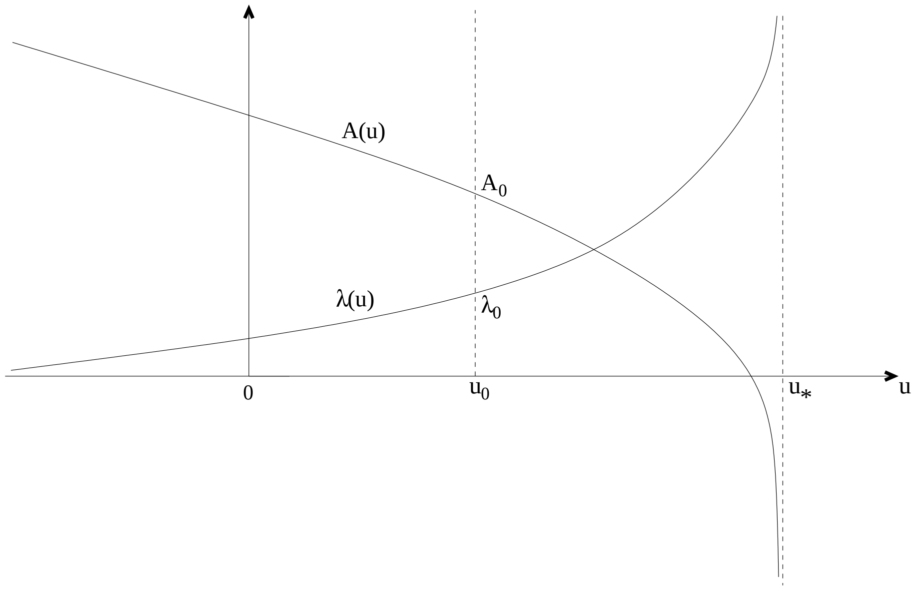

Figure 3: The profile of the scale factor and the dilaton in a typical solution. u_* is the curvature singularity where the scale factor shrinks to zero and the dilaton blows up.

Given the superpotential the equations of motion reduce to two first-order equations (2.9).

7.2 Reparametrization symmetry and integration constants

The remaining two initial conditions of the first order system of motion are related to the "radial reparametrization symmetry" of the equations of motion. Indeed from the Einstein's equations (2.9) one learns that, for any solution $A_*(u)$, $\Phi_*(u)$ there exist other solutions parametrized by two numbers:

$$A(u) = A_*(u - u_0) + A_0, \qquad \Phi(u) = \Phi_*(u - u_0). \tag{7.3}$$

The parameters A_0 and u_0 are in one-to-one correspondence with the two integration constants.

It is useful to describe the symmetries (7.3) graphically. In figure 3 we exhibit a typical solution that obeys our UV and IR criteria. Given the solution in figure 3, one can generate another by shifting $A(u)$ vertically. This corresponds to the first shift symmetry $A \to A + A_0$ in (7.3). The second shift symmetry $u \to u + u_0$, corresponds to generating another solution by shifting both $\lambda(u)$ and $A(u)$ horizontally in figure 3. In practice, the solution is fixed by two initial conditions set at an arbitrary point u_0: $\{A(u_0), \lambda(u_0)\} = \{A_0, \lambda_0\}$.

The next observation is that the integration constant u_0 is just a gauge artifact. This is because the original system is translation invariant in the radial variable. In fact, using this reparametrization symmetry, one can use λ in place of the radial variable u and then the physics is completely specified by the function $A(\lambda)$. Clearly a horizontal shift in figure 3, although changes u_0, leaves $A(\lambda)$ invariant. In other words, the only physical integration constant in the system is the one that parametrizes the solutions of

$$dA/d\lambda = \beta^{-1}(\lambda). \tag{7.4}$$

The general solution is:

$$A(\lambda) = A_0 + \int_{\lambda_0}^{\lambda} \frac{d\lambda}{\beta(\lambda)}, \tag{7.5}$$

and it is invariant under:

$$\lambda_0 \to \lambda_0 + \delta, \qquad A_0 \to A_0 + \int_{\lambda_0}^{\lambda_0+\delta} \frac{d\lambda}{\beta(\lambda)}. \tag{7.6}$$

Therefore, in (7.5) there is a single combination of A_0 and λ_0 that specifies the full solution. This can be taken as the value of A at some fixed λ, e.g. $A_0 = A(\lambda_0)$.[27]

Therefore, all physically distinct solutions only differ by a constant shift in A. Fixing the integration constant $A_0 = A(\lambda_0)$ is equivalent to specifying $\Lambda_{\rm QCD}$ in the gauge theory, because it sets the energy scale through the relation $E = \exp A$. In fact, this is the only way the integration constant A_0 affects any physical quantity: a change in A_0 induces a constant rescaling of all dimensionfull quantities, such as masses, confining string tension, etc. In particular, mass ratios are completely independent of all integration constants, and only depend on the parameters that appear in the gravity Lagrangian.

Consider for example the scalar or tensor fluctuations. The corresponding spectral equations follow from an action of the form (6.1), with the functions B and M given by eqs. (6.26) and (6.29). We can change coordinates from r to $\Phi \equiv \log\lambda$ in (6.1), and derive the corresponding spectral equation for the fluctuations $\zeta(\Phi)$:

$$-e^{-3B-A}\partial_\Phi \left(e^{3B+A}\partial_\Phi W \partial_\Phi \zeta\right) = \frac{e^{-2A}}{\partial_\Phi W} m^2 \zeta \tag{7.7}$$

Under a constant shift $A \to A + \delta A_0$, and B also shifts by a constant. The left hand side is therefore invariant, and the right hand side is rescaled by $e^{-2\delta A_0}$; Thus, the only effect on the spectrum is an overall rescaling of all the mass eigenvalues by $e^{\delta A_0}$.

The same considerations hold for the confining string tension, eq. (3.12): a constant shift in A does not change the position of the minimum of $A_S(r)$, but it only rescales the tension by $e^{2\delta A_0}$. In particular, the ratios m_n^2/T_s are independent of the integration constant.

A change in A_0 has the same effect also on the scale governing the perturbative running of the coupling, that gives rise to dimensional transmutation: if initial conditions are chosen at $\lambda_0 \ll 1$, integration of the β-function equation (7.5) leads to:

$$\frac{1}{\lambda} = \frac{1}{\lambda_0} + b_0 \log\frac{E}{\Lambda_0}, \qquad E = \frac{e^A}{\ell}, \quad \Lambda_0 \equiv \frac{e^{A_0}}{\ell}. \tag{7.8}$$

We can identify the "perturbative" RG-invariant QCD scale as follows. Integrating eq. (7.5) for small λ, λ_0 up to two loops, with $\beta(\lambda) \simeq -b_0\lambda^2 - b_1\lambda^3 + O(\lambda^4)$, we obtain:

$$A(\lambda) - \frac{1}{b_0\lambda} - \frac{b_1}{b_0^2}\log(b_0\lambda) + O(\lambda) = A_0 - \frac{1}{b_0\lambda_0} - \frac{b_1}{b_0^2}\log(b_0\lambda_0) + O(\lambda_0) \simeq \textit{constant}. \tag{7.9}$$

[27]Note that this is not the case for a conformally invariant theory. In that case, one cannot use the coupling as a new coordinate as it is constant.

Therefore, the scale

$$\Lambda_p \equiv \frac{1}{\ell}\frac{\exp\left[A(\lambda_0) - \frac{1}{b_0\lambda_0}\right]}{(b_0\lambda_0)^{b1/b_0^2}} \tag{7.10}$$

is approximately independent of λ_0 as long as it is small. This scale appears in the UV expansion of the coupling in the form:

$$\frac{1}{b_0\lambda} = \log\frac{E}{\Lambda_p} - \frac{b_1}{b_0^2}\log\log\frac{E}{\Lambda_p} + \cdots \tag{7.11}$$

It is the same scale appearing in the UV expansion of the solution in conformal coordinates, (2.14), as one can see by substituting $E \simeq 1/r$ on the l.h.s. of eq. (7.11).

All the different scales we have analyzed above behave in the same way under a change in the integration constants, so the relations between them is a property of the gravity model, not of each particular solution.

In the explicit examples we present in section 8, we fix the energy scale to match the lowest glueball mass, and as we have discussed this fixes unambiguously all other dimensionfull quantities. In particular we obtain a value for Λ_p in eq. (7.10):

$$\Lambda_p = 290\,MeV. \tag{7.12}$$

This value is larger than the usual QCD value ($\sim 200\,MeV$). However one should keep in mind that the definition of the strong coupling scale in perturbation theory is somewhat arbitrary, and moreover we are not including the effect of quarks in the running of the coupling. When comparing with data (lattice or experiment) it is more meaningful to look at unambiguous quantities, e.g. the value of the strong coupling constant α_s at a given energy. For example, we find.[28]

$$\alpha_s(1.2\,GeV) = 0.34 \tag{7.13}$$

which is very close to the experimental value $\alpha_s^{(exp)}(1.2\,GeV) = 0.35 \pm 0.02$

In summary, like in QCD, in the gravity side solution is specified by the β-function plus a single dimensionfull quantity e^{A_0}/ℓ, that parametrizes the different solutions and sets all the relevant mass scales. It can be related to $\Lambda_{\rm QCD}$ of the gauge theory, and it can be understood holographically as the constant of motion that is preserved under the shift symmetry $u \to u + u_0$. This is precisely A_0 in our set-up.

8. Concrete backgrounds

In this section we present explicit backgrounds that exhibit all of the features we require (asymptotic freedom, confinement, discrete spectrum). Then we compute the glueball spectra numerically.

We consider two backgrounds belonging to two distinct classes. The first is a background with an exponentially decaying scale factor, and with an infinite range of the

[28] See section 8 for a more detailed discussion, and in particular for the relation between λ and α_s

conformal coordinate. We focus on the case $\alpha = 2$ in (see equation (6.24)). As shown in section 6.3 this gives an asymptotically linear glueball spectrum. Secondly, we analyze an example of a background with finite range of the conformal coordinate. In both cases we fix the 5D theory by providing a function $X(\lambda)$ that interpolates between the required UV and IR asymptotics. As we discussed, this is equivalent to fixing the exact β-function. The RG-flow trajectory is further specified by the UV initial conditions, which we input for the numerical integration. This fixes the gravity dual completely.

In this paper we only present the glueball spectra. Although straightforward in principle, the meson spectra require considerably more complicated numerics. The main obstacle from the numerical point of view is identifying the correct initial conditions for the non-linear tachyon equation, (which is then used as an input in the computation of the meson spectrum). Therefore we leave the computation of the meson spectrum for future work.

Finally, we compare the glueball spectra with the available lattice data. For the model with infinite range of r and $\alpha = 2$ we can fix the parameters in such a way to produce a very good agreement, at a quantitative level.

8.1 Background I: unbounded conformal coordinate

For an asymptotically free, confining theory, the function $X(\lambda)$ has the following UV asymptotics (see eq. (2.18))

$$X(\lambda) \sim -\frac{b_0}{3}\lambda - \frac{b_1}{3}\lambda^2 + \cdots \qquad \lambda \to 0 \tag{8.1}$$

where b_k are the k-th order coefficients of the perturbative β-function. In the IR we require (see (3.17)):

$$X(\lambda) = -\frac{1}{2} - \frac{a}{\log\lambda} + \cdots \qquad \lambda \to \infty, \tag{8.2}$$

where the parameter a determines the large-r behavior of the scale factor:

$$A \sim -C\, r^{\alpha} \qquad a \equiv \frac{3}{8}\frac{\alpha-1}{\alpha}. \tag{8.3}$$

We seek for a function of λ that interpolates between the two asymptotics (8.1) and (8.2). A simple function that is regular and has this property is,

$$X(\lambda) = -\frac{b_0\lambda}{3+2b_0\lambda} - \frac{(2b_0^2+3b_1)\lambda^2}{9(1+\lambda^2)\left(1+\frac{1}{9a}\left(2b_0^2+3b_1\right)\log(1+\lambda^2)\right)}. \tag{8.4}$$

This expression is motivated by the UV and the IR asymptotics in (8.1) and (8.2) and by the requirement that there are no poles or branch cut singularities in λ. Also, the function $X(\lambda)$ (hence also $\beta(\lambda)$) is strictly negative for $\lambda > 0$, therefore there are no IR fixed points.

Starting from eq. (8.4), we solve for the metric and dilaton using eqs. (2.12):

$$\dot{\lambda} = -\frac{4}{3\ell}X(\lambda)W(\lambda)\lambda e^{A}, \qquad \dot{A} = -\frac{4}{9\ell}W(\lambda)e^{A}. \tag{8.5}$$

The superpotential $W(\lambda)$, is given in terms of X as in (2.22),

$$W = \frac{9}{4}\left(1+\frac{2}{3}b_0\lambda\right)^{2/3}\left[1+\frac{(2b_0^2+3b_1)}{9a}\log(1+\lambda^2)\right]^{2a/3}, \tag{8.6}$$

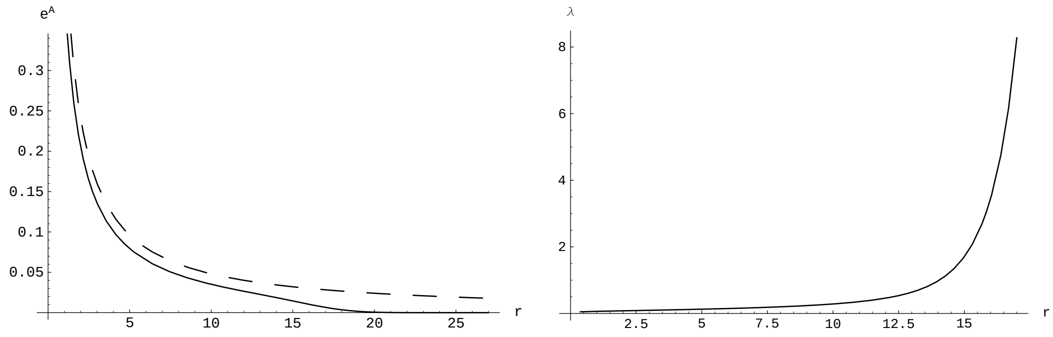

Figure 4: The scale factor and 't Hooft coupling that follow from (8.4), $b_0 = 4.2$, and initial conditions $A_0 = 0$, $\lambda_0 = 0.05$ at $r = 0.36$. The units are such that $\ell = 1$. The dashed line represents the scale factor for pure AdS.

and in writing (8.5) we have explicitly extracted the overall scale ℓ. In the integration of (8.5), we fix the integration constants as:

$$A(r_{\text{in}}) = A_0, \qquad \lambda(r_{\text{in}}) = \lambda_0. \tag{8.7}$$

for $r_{\text{in}}/\ell \ll 1$ and $\lambda_0 \ll 1$, in order to implement the correct UV asymptotics.

The scalar and tensor glueball spectra are completely fixed by the metric and dilaton background. For the pseudoscalar glueballs, we need to specify also the axion kinetic function $Z(\Phi)$ appearing in eq. (6.31). From the discussion sections 5 and 6.2.3, we assume the asymptotic behaviors:

$$Z(\lambda) \to \begin{cases} Z_a & \lambda \to 0 \\ c_a \lambda^4 & \lambda \to \infty \end{cases} . \tag{8.8}$$

We take the function $Z(\lambda)$ to be the simplest one satisfying these asymptotics

$$Z(\lambda) = 1 + c_a \lambda^4 \tag{8.9}$$

where we have fixed the $Z_a = 1$ by an overall rescaling of $Z(\lambda)$, which does not affect the glueball spectrum. c_a is an extra dimensionless parameter.[29]

8.1.1 The glueball spectra in background I

We solve the eq. (6.5) with the Schrödinger potential (6.6) numerically. We compute the spectrum of scalar and tensor glueballs where the function B in (6.6) is given by eqs. (6.26) and (6.29) respectively, whereas the 5D mass-term M in (6.6) is zero.

[29] We could take a more general form that includes the perturbative string theory term $\sim \lambda^2$,

$$Z(\lambda) = 1 + b_a \lambda^2 + c_a \lambda^4,$$

however for the sake of simplicity we set $b_a = 0$ in our fits. A non-zero b_a would imply a different preferred value for c_a, but this does not change the spectrum significatively. However this could have a non-negligible effect on the axion profile, see figure 1.

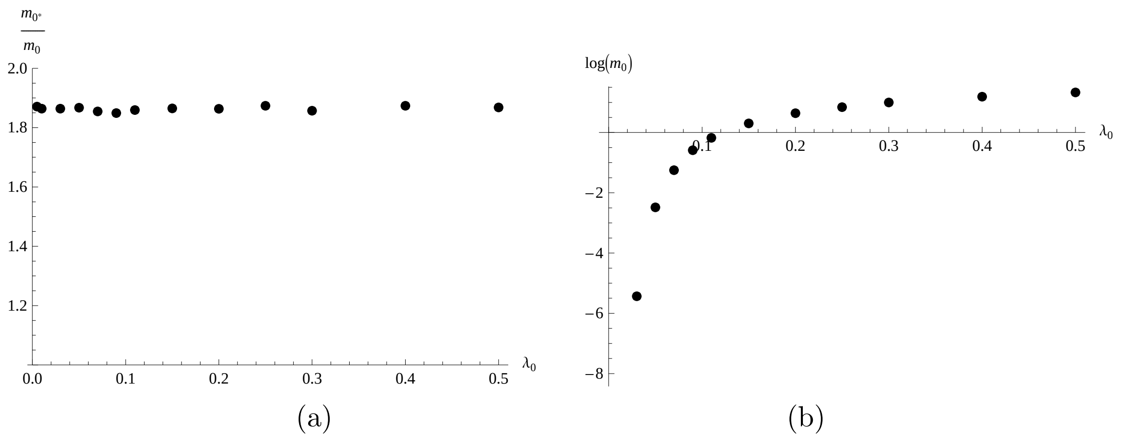

Figure 5: Dependences on initial condition λ_0 of (a) the mass ratios $R_{00} = m_{0*++}/m_{0++}$ (squares) and $R_{20} = m_{2++}/m_{0++}$ (triangles); (b) the absolute scale of the lowest lying scalar glueball (shown in Logarithmic scale).

One has to supply the Schrödinger equation with the boundary condition in the UV, (as $r \to 0$),

$$\psi \to C_0 r^{\frac{5}{2}} + C_1 r^{-\frac{3}{2}} \tag{8.10}$$

Particle states correspond to normalizable solutions. Therefore, normalizability in the UV requires $C_1 = 0$. Normalizability in the IR, on the other hand fixes the discrete values for m in (6.5). In practice, we use the shooting method to determine the spectrum: we scan the values for m and pick the values at which an extra node in the wave function appears. Precisely at this value of m, the wave function becomes normalizable in the IR.

In principle, the spectrum depends on the parameters of the background, b_0 and b_1, the integration constants of the geometry λ_0 and A_0 (eqs. (8.7)) and the boundary condition of (8.10), i.e. C_0. However, not all of these parameters affect the spectrum nontrivially.

- The constant C_0 is clearly immaterial, due to the linearity of the equation for $\psi(r)$. We set $C_0 = 1$ without loss of generality,

- As we discussed in section 7, the only physical integration constant for the background is the choice of A_0 at some value λ_0, and it only affects the overall scale of the masses. This expectation is confirmed by the numerical results, as shown explicitly in figure 5. Thus, the mass ratios will be independent of A_0 and λ_0, as well as of the AdS scale. The overall energy scale can then be fixed by matching e.g. the mass of the lowest state in the spectrum.

- As discussed in [1], b_0 cannot be determined from first principles in our setup, as the overall coefficient in the relation (2.16) between the dilaton and 't Hooft coupling is not known. We keep b_0 as a free parameter. On the other hand, the ratio b_1/b_0^2 is independent of such normalization. In pure YM this ratio is given by 51/121 and this is what we use.

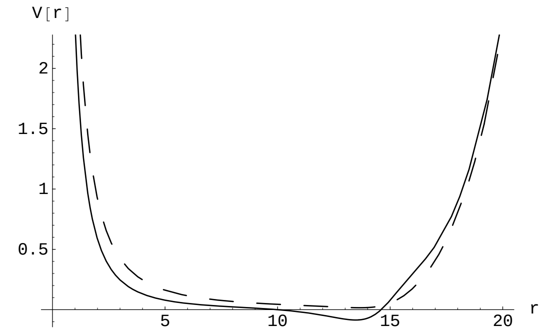

Figure 6: Effective Schrödinger potentials for scalar (solid line) and tensor (dashed line) glueballs. The units are chosen such that $\ell = 1$.

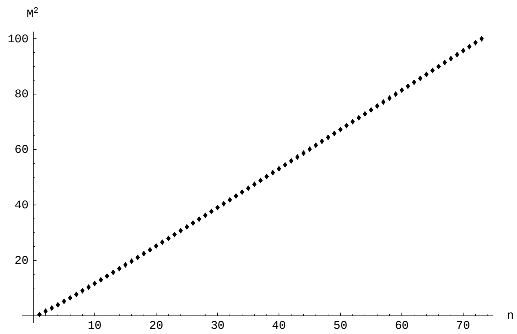

(a)

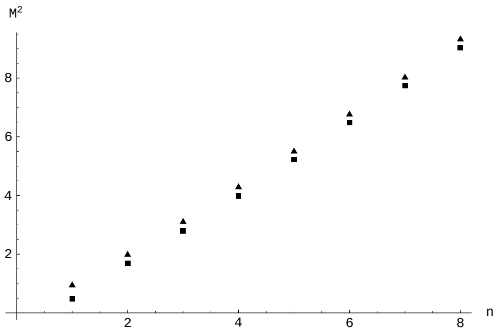

(b)

Figure 7: (a) Linear pattern in the spectrum for the first 40 0^{++} glueball states. M^2 is shown units of $0.007\ell^{-2}$. (b) The first 8 0^{++} (squares) and the 2^{++} (triangles) glueballs. These spectra are obtained in the background I with $b_0 = 4.2$.

- The superpotential completely fixes the scalar and tensor glueball mass ratios; the pseudoscalar glueball masses also depend on the additional parameter c_a that enter the definition of the axion kinetic term, eq. (8.9)

In light of the above, we vary only b_0 for the purpose of fitting the scalar and tensor glueball lattice data, and c_a to fit the pseudoscalar glueball data.

We perform most of the numerical analysis for the background that gives linear spectrum, i.e. $\alpha = 2$ (we discuss the dependence of the spectrum on the parameter α at the end of this section.). To make the numerics easier, we fix $\ell = 1$ and work in dimensionless units. The geometry looks typically like in figure 4, the effective Schrödinger potentials as in figure 6, and the glueball spectrum as in figure 7.

We note that, unlike the simple AdS/QCD setup, the scalar and tensor glueballs are not degenerate, but the tensor glueballs are generically heavier than the scalar ones with the same quantum number n. The tensor-scalar mass difference decreases for larger n, indicating that the slopes governing the asymptotics of the two spectra are the same. This is in accord with our discussion in section 6.

J^{PC}	ref. I $(m/\sqrt{\sigma})$	ref. I (MeV)	ref. II (mr_0)	ref. II (MeV)	$N_c \to \infty(m/\sqrt{\sigma})$
0^{++}	3.347(68)	1475(30)(65)	4.16(11)(4)	1710(50)(80)	3.37(15)
0^{++*}	6.26(16)	2755(70)(120)	6.50(44)(7)	2670(180)(130)	6.43(50)
0^{++**}	7.65(23)	3370(100)(150)	NA	NA	NA
0^{++***}	9.06(49)	3990(210)(180)	NA	NA	NA
2^{++}	4.916(91)	2150(30)(100)	5.83(5)(6)	2390(30)(120)	4.93(30)
2^{++*}	6.48(22)	2880(100)(130)	NA	NA	NA
0^{-+}	5.11(14)	2250(60)(100)	6.25(6)(6)	2560(35)(120)	NA
0^{-+*}	7.66(35)	3370(150)(150)	NA	NA	NA
R_{20}	1.46(5)	1.46(5)	1.40(5)	1.40(5)	1.46(11)
R_{00}	1.87(8)	1.87(8)	1.56(15)	1.56(15)	1.90(17)
R_{A0}	1.52(8)	1.52(8)	1.50(5)	1.50(5)	NA

Table 2: Available lattice data for the scalar and the tensor glueballs. Ref. I denotes [40] and ref. II denotes [38] and [39]. The first error in the ref.I and ref. II correspond to the statistical error from the the continuum extrapolation. The second error in ref.I is due to the uncertainty in the string tension $\sqrt{\sigma}$. (Note that this does not affect the mass ratios). The second error in the ref. II is the estimated uncertainty from the anisotropy. In the last column we present the available large N_c estimates according to [37]. The parenthesis in this column shows the total possible error following by the estimations in [37].

8.1.2 Lattice Data

Available sources for the glueball mass spectra come from computations on the lattice. Our backgrounds naturally give predictions for the $N_c = \infty$ theory. Although there are large-N_c extrapolations (see for example [37]), there exist richer and more precise data for SU(3), especially for the excited glueball states. Therefore, we choose to fix our parameters in order to fit the available data for $N = 3$. We note that the error one makes for using $N = 3$ data instead of $N = \infty$ is within 5 percent [37]. This is well within the error bars of the lattice computations for SU(3) (see [38−40]).

There exist a vast literature on the lattice computations for the glueball spectra. We take as reference, the papers [38, 39] and [40].[30] We listed the available data in table 2. In that table ref. I denotes [40] and ref. II denotes [38] and [39]. Although we listed the lattice results also in the units of MeV, it is more convenient to use the units of r_0 (the "hadronic length scale") or $\sqrt{\sigma}$ (the confining string tension). In order to compare the data according to the two references, one should take $\sigma r_0^2 \approx 1.36$.[31]

In order to avoid the error in the choice of the unit mass scale, we fit our parameters by the mass ratios ratios, that we denote as:

$$R_{00} = \frac{m_{0*++}}{m_{0++}}, \qquad R_{20} = \frac{m_{2++}}{m_{0++}}, \qquad R_{A0} = \frac{m_{0-+}}{m_{0++}}. \tag{8.11}$$

There is a slight mismatch for the values of these ratios in the refs. [38] and [40], (see table I). Thus, in the next section, we shall present our results for fitting our parameters according to both of these references separately.

[30] We thank H. B. Meyer, C. J Morningstar and M. Teper for pointing us to these references.

[31] We thank H.B. Meyer for explaining this to us.

Notice that we could have computed the string tension σ by looking at the minimum value of the string frame scale factor, as explained in section 3. To obtain any numerical information, however, would further require knowledge of the relation between the fundamental string tension and the AdS scale. The latter sets the overall mass unit. Since this relation is not fixed in our model it does not constitute an independent check.

Finally we should mention that the experimental identification of glueballs in high energy experiments has a long and not very successful history. The main problem is to find unambiguous criteria that would distinguish glueballs from others states (mesons, and hybrids) in the experimental data. Recent discussions on the status of the experimental glueballs search both for scalar and pseudoscalar ones can be found in references [41, 42].

8.1.3 Fit for reference I

0^{++} and 2^{++} glueballs. As we discussed above, the numerical integration of (6.5) determines the spectrum in terms of b_0, up to a choice of scale. We showed that the mass ratios are independent of A_0 and λ_0.

We fix $\lambda_0 = 0.05$, then vary b_0 to obtain the ratios $R_{00} = 1.87$ and $R_{20} = 1.46$ (table I). We then fix the overall energy scale to set $m_{0^{++}} = 1475$. As explained in section 7, this is equivalent to fixing $\Lambda_{\rm QCD}$, and completely determines the background solution. We then compare our results with those in the third column of table 2.

The value of b_0 that fits $R_{00} = 1.87$ is $b_0 = 4.2$. Fixing this, we find $R_{20} = 1.40$. The masses for the lowest lying states are found to be:

$$0^{++} \qquad m_1,\, m_2, \ldots = 1475,\, 2753,\, 3561,\, 4253,\, 4860,\, 5416 \cdots \; MeV. \tag{8.12}$$

$$2^{++} \qquad m_1,\, m_2, \ldots = 2055,\, 2991,\, 3739,\, 4396,\, 5530, \ldots \; MeV. \tag{8.13}$$

Notice that the spectrum of excited states is in good agreement with the available data from ref. I. We compare our results with the lattice data and the standard AdS/QCD predictions in figure 8. The glueball spectrum in the standard AdS/QCD model is worked out in appendix F.[32] We note that the glueball spectra in the hard-wall model were first discussed in [44] and [45] with Dirichlet boundary conditions at the wall.

String tension. From the first column of table 2 we can estimate the fundamental string tension T_f in AdS units:

$$T_f \ell^2 = \sigma \ell^2 e^{-2A_s(r_*)} = \frac{m^2_{0^{++}} \ell^2}{(3.347)^2} e^{-2A_s(r_*)} \tag{8.14}$$

The string frame scale factor is shown in figure 9, and numerically we find that at the minimum $e^{2A_s(r_*)} \simeq 2 \times 10^{-4}$. This gives

$$T_f \; \ell^2 = \frac{\ell^2}{2\pi \ell_s^2} \simeq 6.24 \qquad \rightarrow \qquad \frac{\ell}{\ell_s} \simeq 6.26 \tag{8.15}$$

[32]There, we fixed r_0 by the meson data. If one leaves r_0 as a free parameter in the glueball sector, one can obtain better fits in the AdS/QCD set-up. For example, [43] finds good fit with the Pomeron trajectory with Neumann boundary conditions.

JHEP02(2008)019

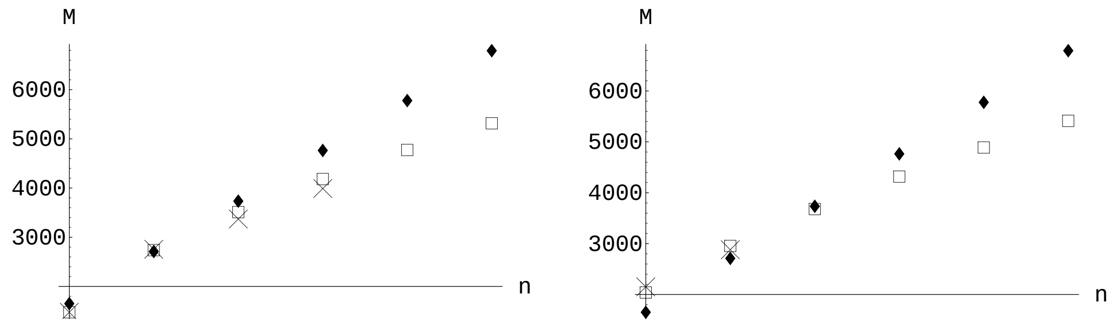

(a) (b)

Figure 8: Comparison of glueball spectra from our model with $b_0 = 4.2$ (boxes), with the lattice QCD data from ref. I (crosses) and the AdS/QCD computation (diamonds), for (a) 0^{++} glueballs; (b) 2^{++} glueballs. The masses are in MeV, and the scale is normalized to match the lowest 0^{++} state from ref. I.

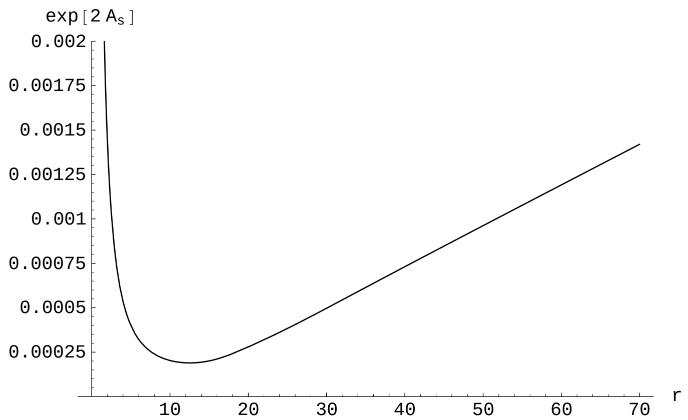

Figure 9: The string frame scale factor in background I with $b_0 = 4.2$. The units on the horizontal axis are such that $\ell = 1$.

The size of the UV geometry is several times the string length. This in particular shows that the dimensionless curvature invariant (in the Einstein frame) near the AdS_5 boundary is

$$\ell_s^2 R \simeq -0.5 \tag{8.16}$$

Running coupling and QCD scale. Using our choice of λ_0 and A_0 we can compute the perturbative QCD scale as defined in eq. (7.10). We obtain

$$\Lambda_p \simeq 290\, MeV, \tag{8.17}$$

which is the correct order of magnitude, but not very close to the generally assumed value of around $200\, MeV$. This can be attributed to the fact that in deriving the latter value, the effect of five flavors of quarks is assumed to contribute to the running, whereas we are dealing with pure Yang-Mills. Moreover one should keep in mind that there is no unambiguous definition of Λ [47]. It is more meaningful to compare with experiment the value of the strong coupling constant α_s at some energy scale. In order to do this, we must first identify the relation between our coupling constant λ and the strong coupling constant α_s. This is fixed once we set the parameter b_0, and can be obtained by comparing the one-loop beta-functions:

$$\frac{\partial\lambda}{\partial\log E} = -b_0\lambda^2 + \cdots\,, \tag{8.18}$$

$$\frac{\partial\alpha_s}{\partial\log E} = -\frac{\beta_0}{2\pi}\alpha_s^2 + \cdots\,, \qquad \beta_0 = \frac{11}{3}N_c. \tag{8.19}$$

From the two expressions we find the relation:

$$\alpha_s = \frac{2\pi b_0}{11N_c/3}\lambda = 2.4\lambda \tag{8.20}$$

where we have set $N_c = 3$ in the last step.[33] Using our numerical solution we can compute the value of α_s at some radius ρ; this can then be translated into an energy scale through the relation $E = E_0 e^{A(r)}$, in which E_0 is fixed by matching the lowest glueball mass (in our case $E_0 = 17630\,MeV$). For example, we find

$$\alpha_s(1.2\,GeV) = 0.34, \tag{8.21}$$

which is within the error of the quoted experimental value [47], $\alpha_s^{(exp)}(1.2\,GeV) = 0.35 \pm 0.01$.[34]

0^{-+} glueballs. Having fixed b_0, we can now vary the parameter c_a to fit the lowest pseudoscalar glueball mass. First, we notice that for large values of c_a (greater than ~ 10), the spectrum depends very weekly on this parameter. This is shown in figure 10

The ref. I value $R_{A0} = 1.52$ is obtained for $c_a = 0.05$. For this value the lowest pseudoscalar glueball masses are found to be:

$$0^{-+} \quad m_1, m_2, \ldots = 2243,\ 3436,\ 4396,\ 4911,\ 5541,\ ,\ldots\ MeV. \tag{8.22}$$

Again, after fitting the lowest state, the first excited state is in good agreement with the lattice data of ref. I. The comparison between our result and the data of ref. I is summarized in table 3. In figure 11 we show the wave-function profiles of the lowest 0^{++}, 0^{-+} and 2^{++} states.

8.1.4 Fit to reference II

0^{++} and 2^{++} glueballs. We use the data from [38] for our fit, since that work includes values for some of the excited states masses. Although older, these data do not differ

[33] In $\mathcal{N} = 4$ SYM the identification is fixed by the D3 brane coupling to the dilaton, $\alpha_s = g_s = \lambda/N_c$

[34] The uncertainty on this value is not reported in [47]; rather, it is an estimate obtained from the corresponding uncertainty in the data $\alpha_s(M_Z) = 0.1202 \pm 0.005$

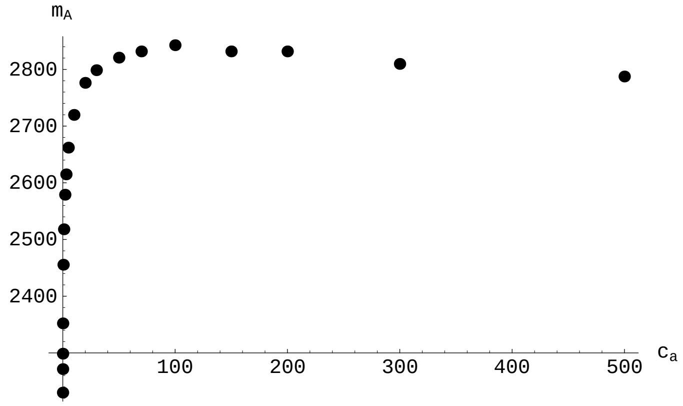

Figure 10: Lowest 0^{-+} glueball mass in MeV as a function of c_a.

J^{PC}	Ref I (MeV)	Our model (MeV)	Mismatch	$N_c \to \infty$ [37]	Mismatch to $N_c \to \infty$
0^{++}	**1475 (4%)**	**1475**	0	**1475**	0
2^{++}	2150 (5%)	2055	4%	2153 (10%)	5%
0^{-+}	**2250 (4%)**	**2243**	0		
0^{++*}	**2755 (4%)**	**2753**	0	2814 (12%)	2%
2^{++*}	2880 (5%)	2991	4%		
0^{-+*}	3370 (4%)	3436	2%		
0^{++**}	3370 (4%)	3561	5%		
0^{++***}	3990 (5%)	4253	6%		

Table 3: Comparison between the glueball spectra in ref. I and in our model. The states we use as input in our fit are marked in boldface. The parenthesis in the lattice data indicate the percent accuracy. The data in [37] are given in terms of mass ratios; here they have been rescaled to match the lowest state mass.

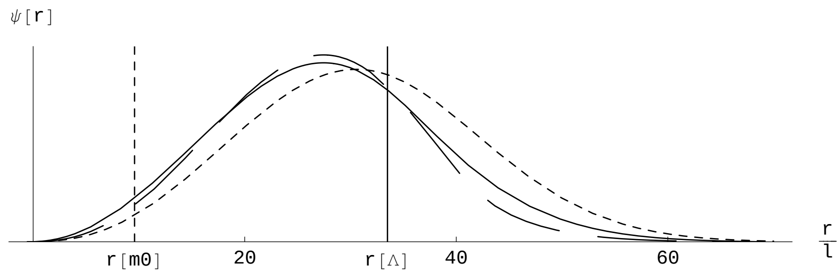

Figure 11: Normalized wave-function profiles for the ground states of the 0^{++} (solid line),0^{-+} (dashed line), and 2^{++} (dotted line) towers, as a function of the radial conformal coordinate. The vertical lines represent the position corresponding to $E = m_{0^{++}}$ and $E = \Lambda_p$.

significantly from the more recent ones reported in [39], where however no excited states masses are given. We fix b_0 to match $R_{00} = 1.54$. The preferred value is now $b_0 = 2.5$.

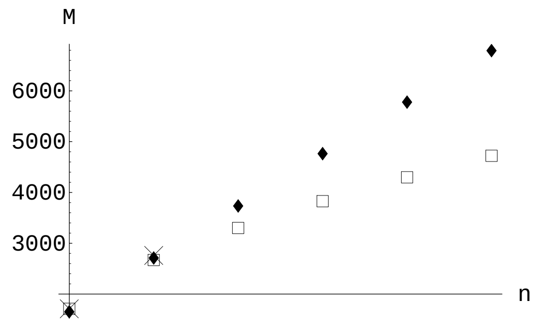

(a)

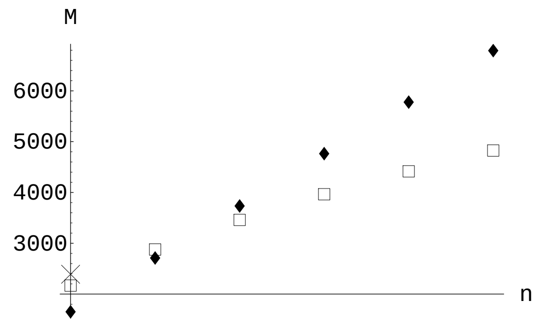

(b)

Figure 12: Comparison of glueball spectra from our model with $b_0 = 2.5$ (boxes), with the lattice QCD data from ref. II (crosses) and the AdS/QCD computation (diamonds), for (a) 0^{++} glueballs; (b) 2^{++} glueballs. The masses are in MeV, and the scale is normalized to match the lowest 0^{++} state from ref. II.

J^{PC}	Ref II (MeV)	Our model (MeV)	Mismatch	$N_c \to \infty$ [37]	Mismatch to $N_c \to \infty$
0^{++}	**1710 (5%)**	**1710**	0	**1710**	0
2^{++}	2390 (5%)	2194	8%	2502 (10%)	10%
0^{-+}	**2560 (5%)**	**2582**	0		
0^{++*}	**2670 (5%)**	**2697**	1%	3262 (12%)	18%
0^{-+*}	3640 (5%)	3434	6%		

Table 4: Comparison between the glueball spectra in ref. II (taken from [38]) and in our model. The states we use as input in our fit are marked in boldface. The parenthesis in the lattice data indicate the percent accuracy. The data in [37] are given in terms of mass ratios; here they have been rescaled to match the lowest state mass.

Then, we set the energy units so that $m_{0^{++}} = 1730$. The lowest lying states have masses:

$$0^{++}: \quad m_1, m_2, \ldots = 1730,\ 2697,\ 3321,\ 3853,\ 4319,\ 4747,\ 5139, \ldots\ MeV. \tag{8.23}$$

$$2^{++}: \quad m_1,\ m_2, \ldots = 2194,\ 2897,\ 3485,\ 3987,\ 4440,\ 4851, 5229,\ \ldots\ MeV. \tag{8.24}$$

Running coupling and QCD scale. Proceeding like in the previous section, we obtain:

$$\Lambda_p = 356\, MeV, \qquad \alpha_s(1.2\, GeV) = 0.38 \tag{8.25}$$

These values are farther from the observational expectations compared to the result of the fit to ref. I.

0^{-+} glueballs. We now vary the parameter c_a to fit the lowest pseudoscalar glueball mass.

The ref. II value $R_{A0} = 1.50$ is obtained for $c = 0.023$. For this value the first pseudoscalar glueball masses are found to be:

$$0^{-+} \quad m_1,\ m_2, \ldots = 2597,\ 3434,\ 3965,\ 4407,\ 4851,\ 5246,\ \ldots\ MeV. \tag{8.26}$$

The comparison between our result and the data of ref. II is summarized in table 4.

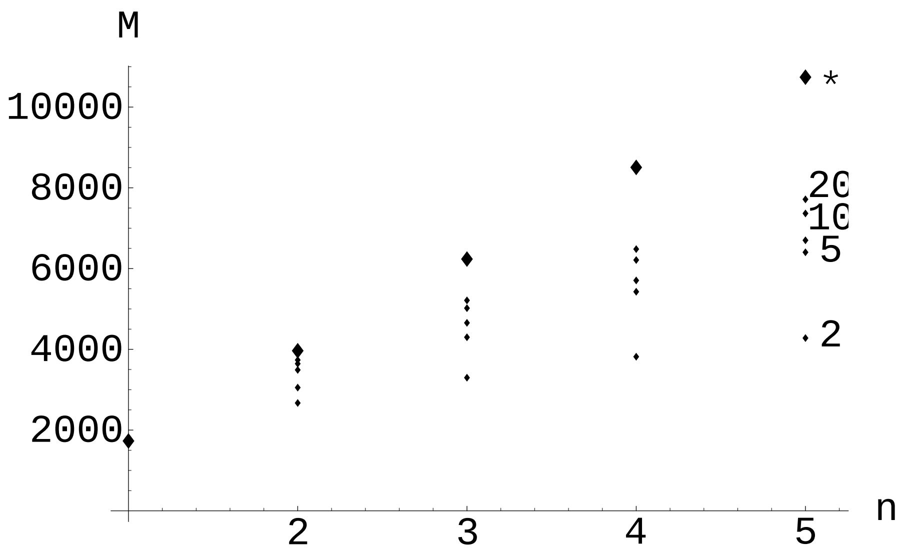

Figure 13: The 0^{++} spectra for varying values of α that are shown at the right end of the plot. The symbol * denotes the AdS/QCD result.

8.1.5 Dependence of the spectrum on the spectral parameter α

Up to now we have set the spectral parameter $\alpha = 2$, as it corresponds to linear confinement, $m_n^2 \propto n$ for large n. However, unlike in the case of mesons, there is no direct lattice or experimental evidence for such a behavior for the glueballs. In particular, the lattice simulations are only available up to $n = 4$ (for 0^{++} only). Therefore, it is interesting to examine the dependence of the spectrum on α. We recall that the effective Schrödinger potential in the IR behaves as,

$$V(r) \sim r^{2(\alpha-1)}, \qquad as\ \ r \to \infty. \tag{8.27}$$

Hence, one expects that the mass spectrum will move upwards as one increases α. One also expects that the hard-wall approximation of AdS/QCD would correspond to $\alpha \to \infty$.

We carried out the necessary numerical analysis for the 0^{++} glueballs, for fixed values of λ_0, b_0 and A_0 and varying α. We fix $b_0 = 4.2$, as in the fit for ref. I, so that the mass ratio of R_{00} is 1.87 for $\alpha = 2$. We normalize the spectra so that the lowest scalar glueball has the same mass for all α we consider. Our results are depicted in figure 13 where we also included the AdS/QCD result for comparison.[35] One indeed finds that as α increases the spectrum of our background approaches to that of standard AdS/QCD, and the agreement with ref. I becomes worse for larger α. However, if we allow to change b_0 we can fit the data equally well for $\alpha \neq 2$ but not too large, so there is no conclusive evidence that $\alpha = 2$ is preferred.

8.2 Background II: singularity at finite r

In this section we compute the spectrum in a 5D background with different IR asymptotics, namely the one in which the IR singularity is at finite r. We assume a power-law

[35]To compare with AdS/QCD we fixed the value of r_0 of [2] such that the first glueball lies at 1475 MeV.

δ	R_{00}	R_{20}
1.01	1.50	1.20
1.05	1.48	1.19
1.1	1.48	1.19
1.5	1.41	1.16
2	1.37	1.13
3	1.27	1.09
4	1.27	1.08
5	1.24	1.07
7	1.20	1.05
10	1.16	1.04

(a) $b_0 = 4.2$

b_0	R_{00}	R_{20}
0.5	1.47	1.17
0.75	1.42	1.15
1	1.39	1.14
2	1.38	1.14
3	1.37	1.13
5	1.37	1.13
10	1.37	1.13
25	1.40	1.10
40	1.41	1.07
100	1.47	1.05

(b) $\delta = 2$

$R_{00}^{(II)} = 1.87,\ R_{20}^{(II)} = 1.46$

Table 5: Lowest glueball mass ratios for a) $b_0 = 4.2.$, $l_0 = 0.05$, for varying δ; b) $\delta = 2.$, $l_0 = 0.05$, for varying b_0

IR singularity,

$$A(r) \sim \delta \log(r_0 - r), \quad r \to r_0. \tag{8.28}$$

For the phase space variable, we take the same UV asymptotics (8.1), whereas in the IR, according to eqs. (A.65), one has:

$$X(\lambda) = -\frac{3}{4}Q + \cdots \qquad Q = \frac{2}{3}\sqrt{1+\delta^{-1}} \tag{8.29}$$

As interpolating function we choose:

$$X(\lambda) = -\frac{b_0\lambda}{3+2b_0\lambda} - \frac{(2b_0^2+3b_1^2)\lambda^2}{9+\frac{2}{\eta}\left(2b_0^2+3b_1^2\right)\lambda^2}, \qquad \eta \equiv \sqrt{1+\delta^{-1}} - 1 \tag{8.30}$$

To compute the spectrum we use the same procedure we employed in the previous example. We first integrate numerically the equations for the metric and dilaton, then we use a shooting method to find the mass eigenstates. We use b_0 and δ as fitting parameters.

8.2.1 The glueball spectra in background II

First, we obtain the spectrum for the same value of b_0 that gives the best fit to the data from ref. I, namely $b_0 = 4.2$, and we vary the parameter δ.[36] Varying δ between $\delta = 1.01$ and $\delta = 10$ we obtain the results in table 5 a). To explore the dependence on b_0 we fix $\delta = 2$ and vary b_0 (see table 5 b). For a wide range of b_0 R_{00} and R_{20} are significantly smaller than the lattice values.

[36]We always use $\delta > 1$ because of the reasons discussed in section 6.6.1

0^{++} and 2^{++} glueballs: fit for reference I. To fit the data in ref. I we use the following procedure: for different values of δ, we fix b_0 to obtain the mass ratio $R_{00} = 1.87$ as close as possible. Then we compare our finding for R_{20} with the lattice value. Since the dependence on b_0 for a given δ does not follow a clear pattern, it is very hard to fit exactly any particular value of R_{00}. It turns out that we were not able, with this ansatz for $X(\lambda)$, to obtain an R_{00} larger than 1.65, for which $R_{20} = 1.3$.

0^{++} and 2^{++} glueballs: fit for reference II. Contrary to the case of ref. I above, one can fit the value $R_{00} = 1.56$ in ref. II (table 2), by choosing $b_0 = 0.96$ and $\delta = 1.01$. However, we cannot find a set of parameters which also gives a good result for R_{20}. For the aforementioned values of b_0 and δ, one obtains $R_{20} = 1.25$.

8.3 Estimating the effect of the UV running

In this subsection we investigate how the logarithmic running of the coupling in the UV affects the IR properties, such as the glueball mass spectrum. To address this issue, we compare the spectrum of background I ($\alpha = 2$, $b_0 = 4.2$) with another background obtained by keeping the same IR properties, but with a conformal fixed point in the UV. In the latter background, the geometry is asymptotically AdS_5 up to power-law corrections, and the 't Hooft coupling flows to a non-zero value λ_*, which can be chosen to be small. Such a geometry has the following asymptotics for the superpotential and β-function in the UV (i.e. for $\lambda \sim \lambda_*$):

$$W_{\rm conf} = W_0 + W_1(\lambda - \lambda_*)^2 + \cdots, \qquad W_0 = \frac{9}{4\ell} \tag{8.31}$$

$$\beta_{\rm conf}(\lambda) \sim -\tilde{b}_0 \lambda_* (\lambda_* - \lambda) \qquad \tilde{b}_0 > 0, \lambda_* \ll 1 \tag{8.32}$$

In the IR, we take the new background to have the same large λ asymptotics as background I, as in (8.2) and (8.3) with $\alpha = 2$. Moreover, we fix the initial conditions and the parameter λ_* such that the strong-coupling scale of the two backgrounds are the same. As a definition of the strong coupling scale we take the slope of the scalar glueball mass spectrum: $m_n^2 = \Lambda^2 n$ for large n.

As a simple example of an asymptotically conformal background with the desired IR properties we can take:

$$e^A(r) = \frac{\ell}{r} e^{-(r/R)^2}, \qquad \Phi(r) = \Phi_0 + \frac{3}{2}\frac{r^2}{R^2}\sqrt{1 + 3\frac{R^2}{r^2}} + \frac{9}{4}\log \frac{2\frac{r}{R} + 2\sqrt{\frac{r^2}{R^2} + \frac{3}{2}}}{\sqrt{6}}. \tag{8.33}$$

One can easily check that the above solves Einstein's for an appropriate choice of superpotential, that is detailed in appendix G. This is an example of an explicit "soft wall" background, in which both the metric and the dilaton are known exactly, and that can be derived as a consistent solution of Einstein's equations.

We use the same shooting method as before to compute the mass eigenvalues. We can fix $\Phi_0 \equiv \Phi(0)$ and R in (8.33) to match the slope of the glueball masses found in the asymptotically free background.

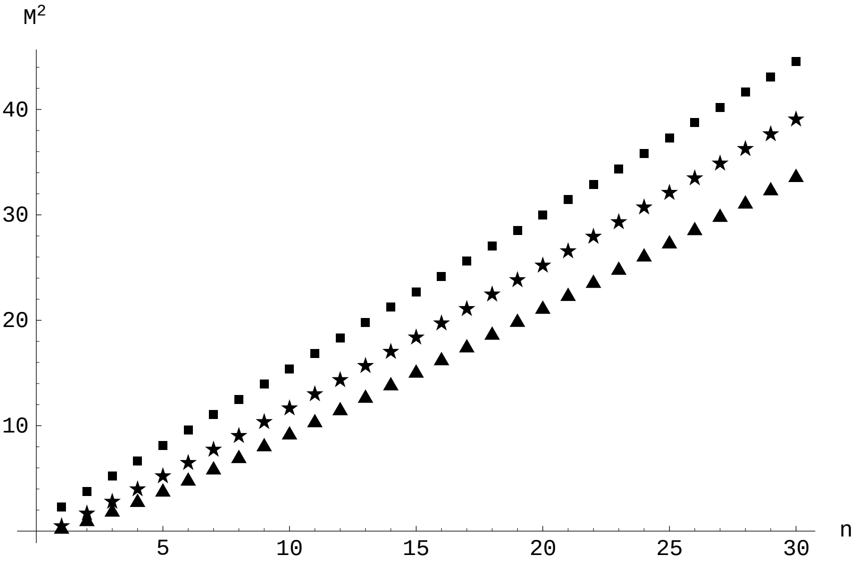

Figure 14: The comparison of the scalar glueball masses for the asymptotically free and the two conformal backgrounds: the stars correspond to the asymptotically free background (8.4) with $b_0 = 4.2$ and $\lambda_0 = 0.05$; the squares correspond the results obtained in the background (8.33) with $R = 11.4\ell$; the triangles denote the spectrum in the background given the superpotential (8.31) with $b0 = 4.2$, $\lambda_0 = 0.071$ and $\lambda_* = 0.01$. These values are chosen so that the slopes coincide asymptotically for large n.

As an alternative background, we start with the exact superpotential:

$$W_{\rm conf} = W_0 \left(1 + \frac{4}{9} b_0^2 (\lambda - \lambda_*)^2)^{1/3}\right) \left(9a + (2b_0^2 + 3b_1) \log\left[1 + (\lambda - \lambda_*^2)\right]\right)^{2a/3} . \qquad (8.34)$$

This amounts to a small modification of the superpotential (8.6), but it behaves asymptotically as (8.31) in the UV.

The results are shown in figure 14.

8.4 Discussion

Here we summarize the results of our numerical analysis. From the qualitative point of view, our general setup can reproduce the known features of the scalar and tensor glueball spectra. For example, as in the lattice studies, the 0^{++} states are lighter than the 2^{++} states, contrary to the AdS/QCD models of [2, 3], in which the two towers are exactly degenerate. The pattern $m_n^{(0)} < m_n^{(2)}$ seems to be a generic feature of the dual backgrounds in which the dilaton is taken to be non-trivial. We see numerically that this behavior is realized in all the backgrounds we considered, and it was also observed in [15]. Moreover, we always observe $R_{00} > R_{20}$, which is common to all lattice results.

The "linear" model with $\alpha = 2$ seems to reproduce the pattern of excited spin-0 glueballs found in the lattice study [40] which to our knowledge is the only work that computes the masses of such states. From the quantitative point of view, we can make the following comments. We remind the reader that our fits refer to mass ratios, as we can always choose arbitrarily the absolute energy scale.

- For the infinite range background (background I) one can fit both sets of the available lattice data, Ref I. and Ref II, by fixing the parameter b_0. To check agreement with the lattice, one should look at the last column of table 2, as our setup is supposed to describe 4D YM at large N_c. Notice that the large N_c mass ratios R_{00} and R_{20} are very close to the ones of ref. I. Moreover, the uncertainties in R_{00} and R_{20} for large N_c are larger than the ones reported for the glueball masses in both refs. I and II. Our best fit for ref. I is well within the large N_c error-bars.

- The value of the spectral parameter α affects the results. We fix it to $\alpha = 2$ in order to obtain a linear Regge trajectory. We note however that it is possible to fit the lattice data for a different set of values for b_0 and $\alpha \neq 2$. In this case the large n asymptotics in the spectrum will not be linear.

- As a general conclusion for the finite range background (background II), we can say that we could not find a range of parameters that yield good fits for both the scalar *and* tensor glueball masses. In particular, if one adjusts the parameters in order to fit the scalar ratio R_{00}, then the tensor glueball masses turn out to be significantly lower than the lattice results, and outside the large N_c error bars.

- We analyzed the dependence of the spectrum on the logarithmic running of the coupling in the UV, by comparing our results with a background where one has the same IR but a conformal fixed point in the UV. This background has power law running for the coupling. One finds that for a fixed slope of the glueball spectrum, the overall scale of the masses do change. However it is possible to fit the lattice data by a choice of different parameters. Therefore, one can obtain in principle the same spectrum (at least for small n) in a theory where the UV is a conformal fixed point.

- A final word on fitting the lattice data: our strategy is to fit R_{00} by fixing the parameter b_0 in our backgrounds and then obtain a prediction for the ratio R_{20}. As we mentioned, this prediction falls into the error bars in the references I and II that account for the uncertainty in the large N_c limit (see table(2)). Furthermore our predictions for the higher excited states also turn out within those error bars, if we assume the same large N_c uncertainty as for the lowest states[37] This is despite the fact that our method of fitting the data is somewhat crude. A better method would be to apply a global fit both for R_{00} and R_{20}. One expects from this method to produce better results for the higher excited states as well.

Note added: while this paper was being completed we became aware of work along similar directions, which appeared in [48].

[37] There is no large N_c extrapolation available for the third and fourth excited 0^{++} states.

Acknowledgments

It is a pleasure to thank B. Bringoltz, R. Casero, L. Giusti, D. K. Hong, K. Intriligator, M. Luscher, J. Mas, H.B. Meyer, C. Morningstar, V. Niarchos, C. Nunez, H. Panagopoulos, I. Papadimitriou, S. Pal, A. Paredes, G. Policastro, F. Sannino, C. Skenderis, M. Shifman, E. Shuryak, S. J. Sin, J. Sonnenschein, M. Teper, J. Troost, A. Vainshtein, G. Veneziano, A. Vladikas for useful discussions and correspondence. We would also like to thank A. Schwimmer for reminding one of us the dictum of St John the Chrysostom.

UG and FN are supported by European Commission Marie Curie Postdoctoral Fellowships, under contract number MEIF-CT-2006-039962 and MEIF-CT-2006-039369. This work was also partially supported by INTAS grant, 03-51-6346, RTN contracts MRTN-CT-2004-005104 and MRTN-CT-2004-503369, CNRS PICS # 2530, 3059 and 3747, and by a European Union Excellence Grant, MEXT-CT-2003-509661.

A. Characterization of confining backgrounds

We consider the Einstein frame metric in the conformal coordinates,

$$ds^2 = e^{2A(r)}\left(dr^2 + \eta_{ij}dx^i dx^j\right), \qquad 0 < r < r_0, \tag{A.1}$$

where $r = 0$ is the AdS boundary. The corresponding string frame metric is

$$ds^2 = e^{2A_s(r)}\left(dr^2 + \eta_{ij}dx^i dx^j\right), \qquad A_S(r) = A(r) + \frac{2}{3}\Phi(r). \tag{A.2}$$

Given the behavior of the scale factor close to the singularity, the asymptotic behavior of the dilaton is uniquely fixed by the first of eqs. (2.11),

$$\dot{\Phi}^2(r) = -\frac{9}{4}\left(\ddot{A}(r) - \dot{A}^2(r)\right). \tag{A.3}$$

Knowledge of $A(r)$ and $\Phi(r)$ uniquely determines the asymptotics of the phase space variable X, therefore those of the β-function from eqs. (2.18). Asymptotics of the superpotential W can be determined from eqs. (2.18), or from the second eq. in (2.12). X, β and W can then be expressed as functions of Φ by inverting asymptotically the relation between Φ and r.[38]

Therefore, we can parametrize different backgrounds by the asymptotics of the scale factor alone, since this completely determines the asymptotics of all other quantities. The singularity can be at a finite or an infinite value in the conformal coordinate. We discuss these two cases separately. For all cases analyzed below, we give the IR asymptotics of the following quantities, found by the following equations:

- Einstein frame scale factor $A(r)$,
- Dilaton and 't Hooft coupling $\Phi = \log\lambda$.

[38]This can be done in backgrounds where the NEC is satisfied, see section 2.

- String frame scale factor:

$$A_S = A + \frac{2}{3}\Phi \tag{A.4}$$

- Einstein frame and string frame curvatures:[39]

$$R \sim e^{-2A}\dot{A}^2, \quad R_S \sim e^{-2A_S}\dot{A}_S^2 \tag{A.5}$$

- Phase space variable and β-function,

$$X(\Phi) = \frac{\dot{\Phi}}{3\dot{A}}, \quad \beta(\lambda) = 3\lambda X(\lambda) \tag{A.6}$$

- Superpotential

$$W(\lambda) \sim \exp\left[-\frac{4}{3}\int \frac{d\lambda}{\lambda} X(\lambda)\right] \tag{A.7}$$

- Dilaton potential (in Einstein and string frame actions):

$$V(\Phi) = -\frac{4}{3}\left(\frac{dW}{d\Phi}\right)^2 + \frac{64}{27}W^2, \quad V_S(\Phi) = e^{-4\Phi/3}V(\Phi) \tag{A.8}$$

- Metric and dilaton asymptotics in the domain-wall coordinate u:

$$u = \int dr e^A(r) \tag{A.9}$$

A.1 Unbounded conformal coordinate

If the space-time extends over an infinite range of the r coordinate, the Einstein frame scale factor $e^A(r)$ necessarily vanishes as $r \to \infty$, as a consequence of eq. (2.24). Therefore, $A(r) \to -\infty$ as $r \to \infty$. We analyze two possible types of behavior for $A(r)$, logarithmic and power law (the latter was also discussed in section 3). In both cases the singularity is at a finite value u_0 in "domain wall" coordinates.

A.1.1 Logarithmic divergence

Consider backgrounds such that, for large r:

$$A(r) \sim -\gamma \log r + \cdots \qquad \gamma \geq 1. \tag{A.10}$$

The constraint $\gamma \geq 1$ comes from the Null Energy Condition discussed in section 2. $\gamma = 1$ corresponds to AdS asymptotics in the IR, which does not lead to confinement. For any $\gamma > 1$, there is no confinement either, as we show below. We have, asymptotically:

$$\dot{A} \sim -\frac{\gamma}{r}, \quad \ddot{A} \sim \frac{\gamma}{r^2}. \tag{A.11}$$

[39] In the Einstein frame there are two independent curvature invariants, $(\partial_r\Phi)^2$ and the Ricci scalar. They both behave asymptotically as $e^{-2A}\dot{A}^2$, and will be denoted collectively by R. The same holds for the string frame.

From (A.3) we obtain:

$$\dot{\Phi}^2 \sim \frac{9}{4}\frac{\gamma^2-\gamma}{r^2}. \tag{A.12}$$

Eq. (A.12) integrates to:

$$\Phi \sim \frac{3}{2}\sqrt{\gamma^2-\gamma}\log r. \tag{A.13}$$

From eq. (A.2), the string frame scale factor behaves asymptotically as:

$$A_S(r) \sim -\gamma\left(1-\sqrt{1-\gamma^{-1}}\right)\log r, \tag{A.14}$$

Since the overall coefficient is negative ($\gamma \geq 1$), $A_S(r) \to -\infty$ as $r \to \infty$. Therefore the string tension vanishes and there is no area law in this case. These are the asymptotics of the relevant quantities:

$$\text{as} \quad r \to \infty :$$

$$A \sim -\gamma \log r, \qquad \gamma > 1; \qquad Q \equiv \frac{2}{3}\sqrt{1-\frac{1}{\gamma}} < \frac{2}{3} \tag{A.15}$$

$$\text{color confinement:} \quad \text{NO} \tag{A.16}$$

$$\Phi \sim \frac{3}{2}\sqrt{\gamma^2-\gamma}\log r = \frac{9}{4}\gamma Q \log r, \tag{A.17}$$

$$A_S \sim -\gamma\left(1-\frac{3}{2}Q\right)\log r, \tag{A.18}$$

$$R \sim r^{2(\gamma-1)} \to \infty, \tag{A.19}$$

$$R_S \sim r^{2(\gamma-1)-3\gamma Q} \to \begin{cases} 0 & 1<\gamma<\frac{1}{2}(1+\sqrt{5}) \\ \infty & \gamma > \frac{1}{2}(1+\sqrt{5}) \end{cases} \tag{A.20}$$

$$X(\lambda) \sim -\frac{1}{2}\frac{3Q}{2}, \qquad W(\lambda) \sim \lambda^Q \tag{A.21}$$

$$V \sim \lambda^{2Q}, \qquad V_S = \lambda^{-\frac{4}{3}}V \sim \lambda^{2Q-\frac{4}{3}} \tag{A.22}$$

$$u \sim u_0 - O\left(\frac{1}{r^{\gamma-1}}\right) \tag{A.23}$$

$$A(u) \sim -\frac{\gamma}{\gamma-1}\log(u_0-u). \tag{A.24}$$

A.1.2 Power-law divergence

Next we consider the following large r behavior:

$$A(r) \sim -Cr^\alpha + \cdots, \qquad C>0, \alpha>0, \tag{A.25}$$

where the precise nature of the subleading terms is immaterial. This case was discussed in section (3). It leads to confinement if and only if $\alpha \geq 1$. We have:

$$\dot{A} \sim -C\alpha r^{\alpha-1}, \quad \ddot{A} \sim -C\alpha(\alpha-1)r^{\alpha-2} \tag{A.26}$$

Notice that $\ddot{A}/\dot{A} \sim r^{-1}$, therefore eq. (A.3) is solved, asymptotically, by:

$$\Phi = -\frac{3}{2}A + \frac{3}{4}\log|\dot{A}| + \Phi_0 + O\left(\frac{1}{r}\right) \tag{A.27}$$

where we have kept the first subleading term, which is universal and independent of the subleading terms in (A.25). The string frame metric, from eq. (A.2), is:

$$A_S \sim \frac{(\alpha-1)}{2}\log r + \frac{2}{3}\Phi_0 + O\left(\frac{1}{r}\right) \tag{A.28}$$

Notice that the leading terms cancel. (A.28). Therefore:

$$A_S \to \begin{cases} -\infty, & 0<\alpha<1 \\ const, & \alpha = 1 \\ +\infty, & \alpha > 1 \end{cases} \tag{A.29}$$

and we have confinement if and only if $\alpha \geq 1$. In the borderline case $\alpha = 1$, A_S asymptotes to a finite constant as $r \to \infty$. The string frame metric is asymptotically Minkowski, and the dilaton is linear in r, up to subleading corrections. The string of minimal world-sheet area stretches all the way to $r = \infty$, but the confining string tension is nevertheless finite.

We list below various relevant quantities:

$$\text{as} \quad r \to \infty :$$

$$A \sim -Cr^{\alpha}, \qquad \alpha > 0, C > 0; \qquad P \equiv \frac{\alpha-1}{\alpha} < 1 \tag{A.30}$$

$$\text{color confinement: if } \alpha \geq 1 \tag{A.31}$$

$$\Phi \sim \frac{3}{2}Cr^{\alpha} + \frac{3}{4}(\alpha-1)\log r, \tag{A.32}$$

$$A_S \sim \frac{(\alpha-1)}{2}\log r, \tag{A.33}$$

$$R \sim e^{2Cr^{\alpha}} r^{2(\alpha-1)} \to \infty, \tag{A.34}$$

$$R_S \sim \frac{1}{r^{a+1}} \to 0 \tag{A.35}$$

$$X(\lambda) \sim -\frac{1}{2}\left(1 + \frac{3P}{2}\frac{1}{\log\lambda}\right), \qquad W(\lambda) \sim (\log\lambda)^{\frac{P}{2}}\lambda^{\frac{2}{3}} \tag{A.36}$$

$$V \sim (\log\lambda)^P \lambda^{\frac{4}{3}}, \qquad V_S = \lambda^{-\frac{4}{3}} V \sim (\log\lambda)^P \tag{A.37}$$

The domain wall coordinate u terminates at a finite value u_0, as the integral in eq. (A.9) converges as $r \to \infty$. The metric and dilaton in this frame are, close to the singularity:

$$u \to u_0, \qquad \log(u_0 - u) \sim -Cr^{\alpha} \tag{A.38}$$

$$A(u) \sim \log(u_0 - u) + P\log\left[-\log(u_0-u)\right] + \cdots, \tag{A.39}$$

$$\Phi(u) \sim -\frac{3}{2}\log(u_0-u) - \frac{3}{4}P\log\left[-\log(u_0-u)\right] \tag{A.40}$$

A.2 Finite range of the conformal coordinate

Now suppose that the singularity is at a finite value of the conformal coordinate, $r = r_0$. By monotonicity of $A(r)$, the scale factor at the singularity either vanishes, or stays finite.

A.2.1 Finite $A(r_0)$

If $A(r_0)$ is finite, the singularity must be caused by non-analyticity in A. The dilaton may stay finite at r_0, or asymptote to $+\infty$ (we are assuming strong coupling in the IR, so we exclude the case $\Phi(r_0) = -\infty$). In any case, the string frame scale factor, $A + 2\Phi/3$, is either finite at r_0 or asymptotes to $+\infty$, therefore it must have a minimum for some r_* in the range $(0, r_0]$. The value at the minimum must be finite (otherwise there would be a singularity at $r_* < r_0$), leading to a confining string with non-zero tension.

According to the identification (2.15), the fact that the Einstein frame scale factor is nowhere vanishing means that the dual 4D theory is defined only above a certain energy $E_{\min} \sim e^{A_{\min}}$. We will discard this case for a different reason: there is no screening of the magnetic color charge.

A.2.2 Power-law divergence

Next, we consider the case when the Einstein metric scale factor vanishes at some $r = r_0$ as a power-law:

$$A(r) \sim -\frac{C}{(r_0 - r)^{\tilde{\alpha}}}, \qquad \tilde{\alpha} > 0, C > 0. \tag{A.41}$$

Below we show that the string has a finite tension for all acceptable values of $\tilde{\alpha}$ and C. The argument we present holds for any generic subleading behavior. One can easily check that the solution of (A.3) close to r_0 is given by

$$\Phi(r) \sim -\frac{3}{2}A(r) + \frac{3}{4}\log|\dot{A}(r)| + \Phi_0. \tag{A.42}$$

This ansatz solves (A.3) up to a term proportional to $(\ddot{A}/\dot{A})^2 \sim (r_0 - r)^{-2}$, which for $\alpha > 0$ is subleading w.r.t the term $\dot{A}^2 \sim (r_0 - r)^{2\tilde{\alpha}+2}$ in eq. (A.3) . The string frame metric asymptotes as:

$$A_S \sim \frac{1}{2}\log \dot{A} \sim -\frac{(\tilde{\alpha}+1)}{2}\log(r_0 - r). \tag{A.43}$$

The leading terms cancel, and the first subleading term is universal. Eq. (A.43) shows that $A_s \to +\infty$ as $r \to r_0$ for any positive $\tilde{\alpha}$, and we always obtain a confining string.

We list below various relevant quantities:

$$\text{as} \quad r \to r_0 :$$

$$A \sim -\frac{C}{(r_0 - r)^{\tilde{\alpha}}}, \qquad \tilde{\alpha} > 0, C > 0; \qquad P \equiv \frac{\tilde{\alpha}+1}{\tilde{\alpha}} > 1 \tag{A.44}$$

$$\text{color confinement} = \text{YES} \tag{A.45}$$

$$\Phi \sim \frac{3}{2}\frac{C}{(r_0 - r)^{\tilde{\alpha}}} - \frac{3}{4}(\tilde{\alpha}+1)\log(r_0 - r), \tag{A.46}$$

$$A_S \sim -\frac{(\tilde{\alpha}+1)}{2}\log(r_0 - r), \tag{A.47}$$

$$R \sim \frac{1}{(r_0 - r)^{2(\tilde{\alpha}+1)}} e^{\frac{2C}{(r_0-r)^{\tilde{\alpha}}}} \to \infty, \tag{A.48}$$

$$R_S \sim (r_0 - r)^{\tilde{\alpha}-1} \to \begin{cases} \infty & 0 \leq \tilde{\alpha} < 1 \\ const & \tilde{\alpha} = 1 \\ 0 & \tilde{\alpha} > 1 \end{cases} \tag{A.49}$$

$$X(\lambda) \sim -\frac{1}{2}\left(1 + \frac{3P}{2}\frac{1}{\log\lambda}\right), \qquad W(\lambda) \sim (\log\lambda)^{\frac{P}{2}}\lambda^{\frac{2}{3}} \tag{A.50}$$

$$V \sim (\log\lambda)^P \lambda^{\frac{4}{3}}, \qquad V_S = \lambda^{-\frac{4}{3}} V \sim (\log\lambda)^P, \tag{A.51}$$

$$u \sim u_0 - e^{-C/(r_0-r)^{\tilde{\alpha}}},$$

$$A(u) \sim \log(u_0 - u) + P\log\left[-\log(u_0 - u)\right] + \cdots, \tag{A.52}$$

$$\Phi(u) \sim -\frac{3}{2}\log(u_0 - u) - \frac{3}{4}P\log\left[-\log(u_0 - u)\right]. \tag{A.53}$$

A.2.3 Logarithmic divergence

In this case we have, asymptotically:

$$A \sim \delta\log(r_0 - r), \qquad \delta > 0, \tag{A.54}$$

and

$$\dot{A} \sim -\frac{\delta}{(r_0 - r)}, \quad \ddot{A} \sim -\frac{\delta}{(r_0 - r)^2}. \tag{A.55}$$

From (A.3) we obtain:

$$\dot{\Phi}^2 \sim \frac{9}{4}\frac{\delta^2 + \delta}{(r_0 - r)^2}, \tag{A.56}$$

Eq. (A.56) integrates to:

$$\Phi \sim -\frac{3}{2}\sqrt{\delta^2 + \delta}\log(r_0 - r). \tag{A.57}$$

where we chose the branch ($\Phi > 0$). The string frame scale factor behaves asymptotically as:

$$A_S(r) \sim \delta\left(1 - \sqrt{1 + \delta^{-1}}\right)\log(r_0 - r). \tag{A.58}$$

For large r it asymptotes to $+\infty$, as the overall coefficient is negative for positive δ. Thus, the fundamental string confines.

In this case we have:

$$\text{as} \quad r \to r_0 :$$

$$A \sim \delta\log(r_0 - r), \qquad \delta > 0; \quad Q \equiv \frac{2}{3}\sqrt{1 + \frac{1}{\delta}} > \frac{2}{3} \tag{A.59}$$

$$\text{color confinement} = \text{YES} \tag{A.60}$$

$$\Phi \sim \frac{3}{2}\sqrt{\delta^2 + \delta}\log r = \frac{9}{4}\delta Q\log r, \tag{A.61}$$

$$A_S \sim -\delta\left(1 - \frac{3}{2}Q\right)\log r = -\frac{1}{1 + 3Q/2}\log(r_0 - r), \tag{A.62}$$

$$R \sim \frac{1}{(r_0 - r)^{2(\delta+1)}} \to \infty, \tag{A.63}$$

$$R_S \sim (r_0 - r)^{-\frac{3Q}{3Q/2+1}} \to \infty \tag{A.64}$$

$$X(\lambda) \sim -\frac{1}{2}\frac{3Q}{2}, \quad W(\lambda) \sim \lambda^Q \tag{A.65}$$

$$V \sim \lambda^{2Q}, \qquad V_S = \lambda^{-\frac{4}{3}} V \sim \lambda^{2Q-\frac{4}{3}} \tag{A.66}$$

$$u \sim u_0 - O\left((r_0 - r)^{\delta+1}\right) \tag{A.67}$$

$$A(u) \sim \frac{\delta}{\delta+1} \log(u_0 - u) \tag{A.68}$$

B. Magnetic charge screening: the finite range

Here we want to determine the potential between two magnetic charges at large separation, for the type of backgrounds with $r_0 < +\infty$. The case $r_0 = +\infty$ was treated in section (3.4).

B.1 $A(r_0)$ finite

If the Einstein frame scale factor does not vanish at the IR singularity, the D-string frame scale factor cannot vanish either, and there is no difference between the calculation of the 't Hooft loop and that of the Wilson loop on the same background. As explained in appendix (3), section A.2.1, in this case the electric string confines. Therefore the magnetic string confines too. These kinds of background fail to satisfy an important test for a candidate holographic dual of QCD. The same consideration applies to all theories where the 5th dimension terminates at a regular IR boundary.

B.2 $A(r_0) \to -\infty$

We treat the case of power-law decay of the scale factor e^A. The exponential case can be discussed along the same lines. We take

$$A \sim \delta \log(r_0 - r), \qquad \delta > 0. \tag{B.1}$$

From eqs. (A.54) and (A.57) we see that the D-string scale factor is asymptotically (as $r \sim r_0$)

$$A_D = A + \frac{\Phi}{6} \sim \delta\left(1 - \frac{1}{4}\sqrt{1+\delta^{-1}}\right) \log(r_0 - r). \tag{B.2}$$

For $\delta < 1/15$, $A_D \to +\infty$, the scale factor diverges at the singularity and the magnetic string confines. For $\delta > 1/15$ the scale factor vanishes as a power-law:

$$e^{2A_D} \sim (r_0 - r)^\gamma, \qquad \gamma = 2\delta\left(1 - \frac{1}{4}\sqrt{1+\delta^{-1}}\right) > 0. \tag{B.3}$$

In this case the magnetic string tension vanishes. To investigate the potential between two monopoles at large L, it is sufficient to translate our setup into the notation of [12] and use their results: defining $s = r_0 - r$, we are in the situation described in [12], with $f(s) = g(s) \sim s^\gamma$ as $s \to 0$. In their notation, this is the case $f(0) = 0$ and $k =< j + 1$ (since $k = j = \gamma$). From their general analysis it follows that, for small s_F (the turning point of the world-sheet),

$$L(s_F) \sim s_F^k \tag{B.4}$$

i.e. $L(s_F)$ vanishes as s_F approaches the singularity. The same is true in the UV: $L(s_F)$ always vanishes close to an asymptotic AdS region. Therefore, it must be that L has a maximum value $L_{\max}$ for some $r_{\max} < r_0$, and there is no smooth solution of the geodesic equation for $L > L_{\max}$. As we argued earlier in the case of infinite r_0, the magnetic charges are free for $L > L_{\max}$.

The behavior of $L(r_F)$ in the case with exponential fall-off close to r_0 cannot be deduced directly from the results of [12], but it can be addressed by adapting the discussion in section 3.4, and the result is the same, i.e. $L(r_F)$ cannot diverge.

C. Fundamental string world-sheet embeddings in the presence of a non-trivial dilaton

The relevant world-sheet action is

$$S = \frac{1}{4\pi\ell_s^2}\int d^2\xi\ \sqrt{g}g^{\alpha\beta}G_{\mu\nu}(X)\partial_\alpha X^\mu\partial_\beta X^\nu + \frac{1}{4\pi}\int d^2\xi\sqrt{g}R^{(2)}\Phi(X)\,, \tag{C.1}$$

Instead of solving the equations we will do a simpler test. We will show that the contribution of the dilaton coupling to the full energy of the string is negligible in the limit where the distance between the endpoints of the string becomes large.

We evaluate the action in the vicinity of the point $r = r_*$ at which the scale factor of the target space metric has a minimum. We use the conformal coordinate system:

$$ds^2 = e^{2A_s(r)}\left(dx^2 + dr^2\right), \tag{C.2}$$

where A_s is the string frame scale factor, $A_s = A + \frac{2}{3}\Phi$. We assume that the contribution of the second term in (C.1) is small with respect to the first term and we confirm our assumption, a posteriori. Then the leading term in the solution to the equation of motion that follows from (C.1) is,

$$g_{ab} = \hat{g}_{ab} = G_{\mu\nu}\partial_a X^\mu\partial_b X^\nu. \tag{C.3}$$

We fix the diffeomorphism invariance on the world-sheet by choosing $\tau = X^0$, $\sigma = Y$. Here, Y is the direction in the Minkowski space on which the quark pair lies. Using (C.2) and (C.3), it is straightforward to compute the Ricci scalar on the world-sheet. One finds,

$$\sqrt{g}R = \frac{-2}{(1+B(r)^2)^{\frac{3}{2}}}\left((1+B^2)B^2A_s'' + BB'A_s'\right), \tag{C.4}$$

where we defined $B(r) = (dy(r)/dr)^{-1}$ and the primes denote derivatives w.r.t. r. Notice that $B = 0$ at the world-sheet turning point. The second term in (C.1) becomes,

$$S_{(2)} = T\int\frac{dy}{(1+B^2)^{\frac{3}{2}}}\left((1+B^2)B^2A_s'' + BB'A_s'\right)\Phi(r). \tag{C.5}$$

We assume that the scale factor A_s has a minimum at a point r_*. When the world-sheet turning point reaches r_0, A' and B in (C.5) both vanish and A'' and Φ are some positive constants and the quark pair distance $L = \int dy$ diverges. Then it is clear from above that,

$$S_{(2)} \to const,$$

therefore it is bounded in L, whereas the Polyakov term in (C.1) diverges linearly in L (under the aforementioned assumptions). Hence we can ignore the dilaton coupling in (C.1) consistently. However, one has to be careful about the situations in which the integrand in (C.5) asymptotes to a constant. In these cases, $S_{(2)} \propto L$ and one cannot ignore the dilaton corrections to the induced metric.

The picture we assume is as follows: the string world-sheet is smooth with a single turning point at r_t. The geometry of the string is determined by a single boundary condition that we can take as the length between the end-points of the string on the boundary, L. As L is made larger the turning point r_t approaches the minimum of A_s that we call r_*. In particular we are assuming that there is a single minimum for A_s. As L approaches infinity, the greater part of the world-sheet falls into the minimum r_*. This picture is valid for all of the backgrounds that we analyzed in this paper. Thus, indeed the only term that has a potential divergence is the first term in (C.1).

D. Singularities of the tachyon

Here we analyse the properties of eq. (6.63) in the case with the following asymptotics

$$A(r) \sim -\left(\frac{r}{R}\right)^{\alpha}, \quad A_S(r) \sim \frac{\alpha-1}{2}\log r/R, \qquad \Phi(r) \sim \frac{3}{2}\left(\frac{r}{R}\right)^{\alpha}, \quad \alpha \geq 1 \tag{D.1}$$

First, assume $\tau(r)$ is nonsingular for any finite r. We want to analyse the behavior near $r=\infty$. Asymptotically, (6.63) becomes:

$$\ddot{\tau} - \frac{3\alpha}{2R}\left(\frac{r}{R}\right)^{\alpha-1}\dot{\tau} + \frac{3}{\ell^2}\left(\frac{r}{R}\right)^{\alpha-1}\tau - \frac{3\alpha}{2R}(\dot{\tau})^3 + \frac{3}{\ell^2}\tau(\dot{\tau})^2 = 0. \tag{D.2}$$

We are interested in solutions that diverge as $r \to \infty$. First, suppose that $\tau \to \infty$, but $\dot{\tau}$ stays finite. In this case, the third term in eq (D.2) would be much larger than all others, and the equation would not be solved asymptotically. Then we conclude that as $\tau \to \infty$, $\dot{\tau} \to \infty$ as well. Then the last two terms dominate eq. (D.2), and the solution behaves as:

$$\tau(r) \sim \tau_0 \exp\left[\frac{2}{\alpha}\frac{R}{\ell^2}r\right] \qquad r \to \infty. \tag{D.3}$$

where τ_0 is an integration constant.

Now we want to check if it is possible for the tachyon to diverge at some finite value r_*, where the metric and the dilaton are non-singular. Then, close to r_*:

$$A_S = A_0 + (r-r_*)A_1 + \frac{A_2}{2}(r-r_*)^2 + \cdots \tag{D.4}$$

$$\Phi = \Phi_0 + \Phi_1(r-r_*) + \frac{\Phi_2}{2}(r-r_*)^2 + \cdots \tag{D.5}$$

and we can approximate eq. (6.63) by:

$$\ddot{\tau} + (3A_1 - \Phi_1)\,\dot{\tau} + e^{2A_0}\mu^2\tau + e^{-2A_0}\left[4A_1 - \Phi_1\right](\dot{\tau})^3 + \mu^2\tau(\dot{\tau})^2 = 0. \tag{D.6}$$

If $\tau \to \infty$ at r_*, then the ratios $\dot{\tau}/\tau$, $\ddot{\tau}/\dot{\tau}$ and $\ddot{\tau}/\dot{\tau}$ all diverge at r_*, implying that the terms in eq. (D.6) proportional to $\ddot{\tau}$ and $(\dot{\tau})^3$ diverge faster than all other terms. Therefore close to r_* we can further approximate eq. (D.6) by:

$$\ddot{\tau} + e^{-2A_0}\left[4A_1 - \Phi_1\right](\dot{\tau})^3 = 0. \tag{D.7}$$

This equation is solved by:

$$\tau \simeq \tau_* + c\sqrt{r - r_*}, \qquad c = \frac{1}{2}\frac{e^{2A_0}}{4A_1 - \Phi_1}, \tag{D.8}$$

which is not consistent with the assumption that τ diverges at r_*. Notice however that the approximation we made in writing eq. (D.7) still holds if we make the weaker assumption that $\dot{\tau}$, and not necessarily τ, diverges at r_*. Then, eq. (D.8) correctly describes the asymptotics near r_*. This is, in fact, the generic behavior for arbitrary boundary conditions, the point r_* being determined by initial conditions.

There is one situation when the above argument breaks down, i.e. when there exists a point r_{**} at which $4A_1 - \Phi_1 = 0$. In this case the term in (D.6) proportional to $(\dot{\tau})^3$ acquires an extra $(r - r_{**})$ factor, and it is possible to solve the equation asymptotically with the last two terms:

$$(r - r_{**})e^{-2A_0}\left[4A_2 - \Phi_2\right](\dot{\tau})^3 + \mu^2\tau(\dot{\tau})^2 \simeq 0 \quad \Rightarrow \quad \tau \sim (r - r_{**})^{1+h}, \quad h = \frac{e^{2A_0}\mu^2}{4A_2 - \Phi_2}. \tag{D.9}$$

If $1 + h < 0$, this is consistent with $\tau(r)$ diverging at r_{**}.

E. The superpotential versus the potential

In this appendix we analyze the (important) details of passing from the potential to the superpotential. The first order non-linear differential equation that relates the two is

$$V(\lambda) = -\frac{4}{3}\lambda^2\left(\frac{dW}{d\lambda}\right)^2 + \frac{64}{27}W^2, \tag{E.1}$$

For a given choice of $V(\lambda)$ there is in principle a one-parameter family of solutions to (E.1). This extra parameter that corresponds to the initial condition of the first order differential equation is compensating from the fact that the equations of motion, written in terms of the superpotential are first order and therefore have one less initial condition.

According to our previous discussion, the different solutions to (E.1) correspond to different β-functions, and hence to different 4D gauge theories. However, here we show that the requirement of color confinement in the IR singles out a unique superpotential among these.

As described in detail in [1] asymptotic freedom implies that for small λ:

$$V = \sum_{n=0}^{\infty} V_n\,\lambda^n = V_0 + V_1\lambda + O(\lambda^2). \tag{E.2}$$

A straightforward calculation shows that the one-parameter family of solutions to the non-linear equation (E.1) has the structure

$$W_C = \frac{C}{\lambda^{\frac{4}{3}}} + \frac{1}{C}\sum_{n=0}^{\infty} C_n\, \lambda^{\frac{4}{3}+n} + \frac{1}{C^3}\sum_{n=0}^{\infty} D_n\, \lambda^{5+n} + \frac{1}{C^5}\sum_{n=0}^{\infty} E_n\, \lambda^{\frac{23}{3}+n} + \cdots \tag{E.3}$$

where $C \neq 0$ is the one free parameter, while all other coefficients are uniquely fixed by the expansion of the potential:

$$C_0 = \frac{27}{256}V_0\,, \qquad C_1 = \frac{27}{352}V_1\,, \quad C_2 = \frac{27}{448}V_2\,, \; C_3 = \frac{27}{544}V_3 \tag{E.4}$$

$$C_4 = \frac{27}{640}V_4\,, \qquad C_5 = \frac{27}{736}V_5\,, \quad C_6 = \frac{27}{832}V_6\,, \; C_7 = \frac{27}{928}V_7\,, \qquad C_8 = \frac{27}{1024}V_8 \tag{E.5}$$

$$D_0 = \frac{3}{19}C_0C_1\,, \quad D_1 = \frac{33C_1^2+48C_0C_2}{176}\,, \qquad D_2 = \frac{27C_1C_2+18C_0C_3}{50} \tag{E.6}$$

$$D_3 = \frac{42C_2^2+75C_1C_3+48C_0C_4}{112}\,, \qquad D_4 = \frac{57C_2C_3+48C_1C_4+30C_0C_5}{62} \tag{E.7}$$

$$E_0 = \frac{11}{171}C_0^2C_1\,, \qquad E_1 = \frac{3421C_0C_1^2+2128C_0^2C_2}{16720} \tag{E.8}$$

There exists however a second branch of solutions again parametrized by a single integration constant $\tilde{C}$, disconnected from the family $W_C(\lambda)$:

$$W_{\tilde{C}}(\lambda) = W_0 + W_1\lambda + \mathcal{O}(\lambda^2) + \tilde{C}\lambda^{\frac{16}{9}}e^{-\frac{1}{b_0\lambda}} + \cdots\,, \quad W_0 = \sqrt{\frac{27}{64}V_0},\; W_1 = \sqrt{\frac{27}{64V_0}}\frac{V_1}{2}, \tag{E.9}$$

where the dots denote terms that vanish faster than $\exp(-4/b_0\lambda)$. (E.3) together with (E.9) provide the general solution of (E.1). All the solutions of the continuous family are singular for $\lambda \to 0$, and the corresponding metric is not asymptotically AdS_5. AdS asymptotics require that $W \to const$ in the UV and therefore single out the $W_{\tilde{C}}$ branch. It is the one that leads to the correct β-function, at least perturbatively. However one wonders how the value of $\tilde{C}$ is fixed among the solutions of this branch. For this purpose we turn to the analysis of the IR asymptotics below. Therefore, requiring AdS asymptotics reduces the number of initial conditions of the original system by one.

We now investigate the same problem, namely the solution of equation (E.1) but in the IR region. We have argued that confinement requires that the IR asymptotics of the superpotential must be of the form,

$$V \to A\Phi^P e^{2Q\Phi}, \qquad \Phi \to \infty. \tag{E.10}$$

with $1 \leq Q < 4/3$. Solving the equation for the superpotential we find the one-parameter family of solutions

$$W_C = \left(\frac{3}{4}\right)^{\frac{3}{2}}\sqrt{A}\left\{Ce^{\frac{4}{3}\Phi} + \frac{1}{C}(4-3Q)^{-1}e^{(2Q-\frac{4}{3})\Phi}\Phi^P\right\} + \cdots\,, \tag{E.11}$$

that is parametrized by one integration constant C. In addition there is the "singular" solution,

$$W_* = \sqrt{\frac{27A}{4(16-9Q^2)}}\; e^{Q\Phi}\Phi^{\frac{P}{2}} + \cdots\,. \tag{E.12}$$

Consider now the IR asymptotics of the potential that we expect to give confinement in the case where the range of the radial coordinate is infinite.

$$V = A\, e^{\frac{4}{3}\Phi}\ \Phi^P \tag{E.13}$$

From (E.11) and (E.12) it is the singular solution $W \sim e^{\frac{2}{3}\Phi}\ \Phi^{P/2}$ that we need, rather than the continuous family.

Now, one can show by scanning the space of solutions with all possible asymptotic behaviors in the IR, that the W_* above leads in the UV to $W_{\tilde{C}}$ with $\tilde{C} = 0$. This is done by solving (E.1) numerically.

In view of this phenomenon, the practical strategy for choosing the correct potential is to first choose the appropriate superpotential (or the function X) and then use the differential equation (E.1) to compute the relevant potential.

F. Standard AdS/QCD glueball spectrum

In this appendix we consider the standard AdS/QCD model [2] where the background geometry is AdS_5 with an IR cut-off at $r = r_0$. The dilaton is constant. The glueball spectra in this model were first computed by employing Dirichlet boundary conditions in the papers [44] and [45]. However, here we shall allow for more general boundary conditions.

In this geometry, both the scalar and spin-two glueballs spectra are determined by the following equation:

$$\ddot{\xi} - \frac{3}{r}\dot{\xi} + m^2\xi = 0, \tag{F.1}$$

The corresponding effective Schrödinger potential is,

$$V_s = \frac{15}{4}\frac{1}{r^2}, \qquad r < r_0 \tag{F.2}$$

and there is an infinite wall at $r = r_0$.

The solution to (F.1) that is normalizable in the UV is,

$$\xi = r^2 J_2(kr) \approx r^4 \quad as \quad r \to 0. \tag{F.3}$$

The important difference between our backgrounds and AdS/QCD is that in AdS/QCD the normalizability condition in the IR does not restrict the spectrum. Indeed all the solutions of (F.1) with the UV asymptotics (F.3), are normalizable in the IR. What discretizes the spectrum is the boundary condition at $r = r_0$. In general this can be a mixed boundary condition that may be written as,

$$\dot{\xi}(r_0) - C_i\ \xi(r_0) = 0 \tag{F.4}$$

Here C_i are real numbers and one can have different C_i for different particle species i. Therefore, the free parameters to fit the data are r_0, C_{0++} and C_{2++}. In the standard AdS/QCD model, the value of r_0 is determined by fitting the pion mass which yields $r_0 = 1/322\ MeV^{-1}$.

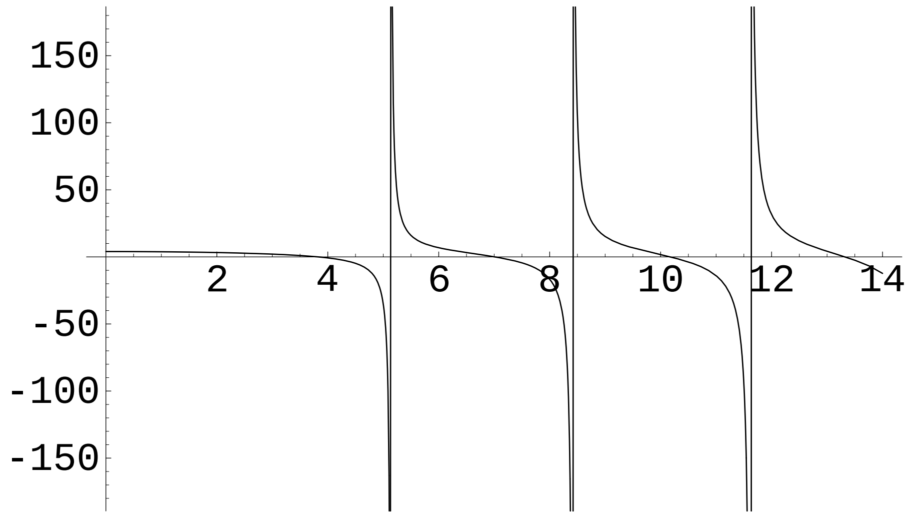

Figure 15: Plot of $\dot{\xi}/\xi$ as a function of mr_0. The spectrum is determined by the points that correspond to the intersection of this plot and the horizontal line $\dot{\xi}/\xi = const$.

We want to determine C_{0++} and C_{2++} to obtain a best fit to the lattice data. To obtain a best fit to the first 0^{++} glueball (1730 MeV), one has to avoid the first solution that is shown in figure 15. We note that $\lim_{m\to 0}\dot{\xi}/\xi(mr_0) = 2$. Hence one needs $C_{0++} > 2$. A quick glance at the figure 15 shows that the best fit (highest possible mass) for the first 0^{++} mass is obtained by setting $C_{0++} = 2 + \epsilon$ in the limit $\epsilon \to 0^+$.

Then one determines the 0^{++} masses as,

$$m_1,\, m_2, \ldots = 1651,\ 2710,\ 3734,\ 4764\, 5778,\ 6792 \cdots\ MeV. \tag{F.5}$$

However now the best fit for the 2^{++} masses is given by the same IR boundary condition in the IR, i.e. $C_{2++} = C_{0++}$.[40] This gives the same mass spectrum for the spin-2 glueballs as in (F.5).

G. A simple analytic solution with AdS and confining asymptotics

We present here a simple analytic solution for the metric and the dilaton that interpolates between AdS_5 and a constant dilaton near the UV boundary and an Gaussian confining behavior and strong coupling in the IR. It is given by

$$e^A(r) = \frac{\ell}{r}e^{-(r/R)^2}, \qquad \Phi(r) = \Phi_0 + \frac{3}{2}\frac{r^2}{R^2}\sqrt{1+3\frac{R^2}{r^2}} + \frac{9}{4}\log\frac{2\frac{r}{R} + 2\sqrt{\frac{r^2}{R^2}+\frac{3}{2}}}{\sqrt{6}}. \tag{G.1}$$

There are two dimensionless parameters that characterize this solution. The first is the asymptotic value of dilaton Φ_0 in the UV parametrizing the UV gauge coupling. To mimic

[40] There is of course the possibility of choosing C_{0++} bigger than $C_{2++} > 2$. However then the first scalar glueball masses becomes smaller than 1651 Mev and the discrepancy with the lattice data increases.

YM, it should be taken large and negative. The other is the ratio R/ℓ, that characterizes the confinement scale R.

The associated superpotential can be given in implicit form (as a function of r):

$$W(r) = \frac{9}{4\ell} e^{r^2/R^2} \left(1 - 2r^2/R^2\right) \tag{G.2}$$

Derivatives with respect to Φ can be computed using the chain rule, $W' = \dot{W}/\dot{\Phi}$ etc. Note that this solution may look similar but is very different from the so called soft-wall AdS/QCD model. Although the dilaton has the same behavior, the metric here in the IR is very different from AdS. On the other hand the metric in the soft-wall AdS/QCD model is AdS everywhere.

References

[1] U. Gursoy and E. Kiritsis, *Exploring improved holographic theories for QCD: part I*, arXiv:0707.1324.

[2] J. Erlich, E. Katz, D.T. Son and M.A. Stephanov, *QCD and a holographic model of hadrons*, *Phys. Rev. Lett.* **95** (2005) 261602 [hep-ph/0501128].

[3] L. Da Rold and A. Pomarol, *Chiral symmetry breaking from five dimensional spaces*, *Nucl. Phys.* **B 721** (2005) 79 [hep-ph/0501218].

[4] S.J. Rey and J.T. Yee, *Macroscopic strings as heavy quarks in large N gauge theory and anti-de Sitter supergravity*, *Eur. Phys. J.* **C 22** (2001) 379 [hep-th/9803001];
J.M. Maldacena, *Wilson loops in large N field theories*, *Phys. Rev. Lett.* **80** (1998) 4859 [hep-th/9803002].

[5] R. Casero, E. Kiritsis and A. Paredes, *Chiral symmetry breaking as open string tachyon condensation*, *Nucl. Phys.* **B 787** (2007) 98 [hep-th/0702155].

[6] K. Skenderis and P.K. Townsend, *Gravitational stability and renormalization-group flow*, *Phys. Lett.* **B 468** (1999) 46 [hep-th/9909070];
O. DeWolfe, D.Z. Freedman, S.S. Gubser and A. Karch, *Modeling the fifth dimension with scalars and gravity*, *Phys. Rev.* **D 62** (2000) 046008 [hep-th/9909134];
D.Z. Freedman, C. Nunez, M. Schnabl and K. Skenderis, *Fake supergravity and domain wall stability*, *Phys. Rev.* **D 69** (2004) 104027 [hep-th/0312055];
K. Skenderis and P.K. Townsend, *Hidden supersymmetry of domain walls and cosmologies*, *Phys. Rev. Lett.* **96** (2006) 191301 [hep-th/0602260]; *Hamilton-Jacobi for domain walls and cosmologies*, *Phys. Rev.* **D 74** (2006) 125008 [hep-th/0609056].

[7] K. Skenderis, *Lecture notes on holographic renormalization*, *Class. and Quant. Grav.* **19** (2002) 5849 [hep-th/0209067].

[8] R. Rattazzi and A. Zaffaroni, *Comments on the holographic picture of the Randall-Sundrum model*, *JHEP* **04** (2001) 021 [hep-th/0012248].

[9] L. Girardello, M. Petrini, M. Porrati and A. Zaffaroni, *Novel local CFT and exact results on perturbations of $N = 4$ super Yang-Mills from AdS dynamics*, *JHEP* **12** (1998) 022 [hep-th/9810126];
D.Z. Freedman, S.S. Gubser, K. Pilch and N.P. Warner, *Renormalization group flows from holography supersymmetry and a c-theorem*, *Adv. Theor. Math. Phys.* **3** (1999) 363 [hep-th/9904017].

[10] F. Bigazzi, R. Casero, A.L. Cotrone, E. Kiritsis and A. Paredes, *Non-critical holography and four-dimensional CFT's with fundamentals*, *JHEP* **10** (2005) 012 [hep-th/0505140].

[11] E. Kiritsis and F. Nitti, *On massless* $4D$ *gravitons from* $5D$ *asymptotically AdS space-times*, *Nucl. Phys.* **B 772** (2007) 67 [hep-th/0611344].

[12] Y. Kinar, E. Schreiber and J. Sonnenschein, $Q\bar{Q}$ *potential from strings in curved spacetime: classical results*, *Nucl. Phys.* **B 566** (2000) 103 [hep-th/9811192].

[13] E. Witten, *Anti-de Sitter space, thermal phase transition, and confinement in gauge theories*, *Adv. Theor. Math. Phys.* **2** (1998) 505 [hep-th/9803131].

[14] Y. Kinar, E. Schreiber, J. Sonnenschein and N. Weiss, *Quantum fluctuations of Wilson loops from string models*, *Nucl. Phys.* **B 583** (2000) 76 [hep-th/9911123].

[15] C. Csáki and M. Reece, *Toward a systematic holographic QCD: a braneless approach*, *JHEP* **05** (2007) 062 [hep-ph/0608266].

[16] H. Boschi-Filho, N.R.F. Braga and C.N. Ferreira, *Static strings in Randall-Sundrum scenarios and the quark anti-quark potential*, *Phys. Rev.* **D 73** (2006) 106006 [*Erratum ibid.* **D 74** (2006) 089903] [hep-th/0512295].

[17] C. Kennedy and A. Wilkins, *Ramond-Ramond couplings on brane-antibrane systems*, *Phys. Lett.* **B 464** (1999) 206 [hep-th/9905195].

[18] P. Kraus and F. Larsen, *Boundary string field theory of the* $D\bar{D}$ *system*, *Phys. Rev.* **D 63** (2001) 106004 [hep-th/0012198].

[19] T. Takayanagi, S. Terashima and T. Uesugi, *Brane-antibrane action from boundary string field theory*, *JHEP* **03** (2001) 019 [hep-th/0012210].

[20] B. Holdom, *Massless QCD has vacuum energy?*, arXiv:0708.1057.

[21] E. Witten, *Instantons, the quark model and the* $1/N$ *expansion*, *Nucl. Phys.* **B 149** (1979) 285.

[22] E. Witten, *Current algebra theorems for the* U(1) *Goldstone boson*, *Nucl. Phys.* **B 156** (1979) 269;
G. Veneziano, U(1) *without instantons*, *Nucl. Phys.* **B 159** (1979) 213.

[23] E. Witten, θ*-dependence in the large N limit of four-dimensional gauge theories*, *Phys. Rev. Lett.* **81** (1998) 2862 [hep-th/9807109].

[24] R.J. Crewther, P.Di Vecchia, G. Veneziano and E. Witten, *Chiral estimate of the electric dipole moment of the neutron in quantum chromodynamics*, *Phys. Lett.* **B 88** (1979) 123 [*Erratum ibid.* **B 91** (1980) 487];
M.A. Shifman, A.I. Vainshtein and V.I. Zakharov, *Can confinement ensure natural CP invariance of strong interactions?*, *Nucl. Phys.* **B 166** (1980) 493.

[25] L. Giusti, G.C. Rossi, M. Testa and G. Veneziano, *The* $\mathrm{U}_A(1)$ *problem on the lattice with Ginsparg-Wilson fermions*, *Nucl. Phys.* **B 628** (2002) 234 [hep-lat/0108009];
M. Lüscher, *Topological effects in QCD and the problem of short-distance singularities*, *Phys. Lett.* **B 593** (2004) 296 [hep-th/0404034].

[26] N. Seiberg and E. Witten, *Electric-magnetic duality, monopole condensation and confinement in* $N=2$ *supersymmetric Yang-Mills theory*, *Nucl. Phys.* **B 426** (1994) 19 [*Erratum ibid.* **B 430** (1994) 485] [hep-th/9407087].

[27] L. Del Debbio, H. Panagopoulos and E. Vicari, *Theta dependence of* SU(N) *gauge theories*, *JHEP* **08** (2002) 044 [hep-th/0204125];
L. Del Debbio, L. Giusti and C. Pica, *Topological susceptibility in the* SU(3) *gauge theory*, *Phys. Rev. Lett.* **94** (2005) 032003 [hep-th/0407052];
L. Del Debbio, G.M. Manca, H. Panagopoulos, A. Skouroupathis and E. Vicari, *θ-dependence of the spectrum of* SU(N) *gauge theories*, *JHEP* **06** (2006) 005 [hep-th/0603041];
L. Giusti, S. Petrarca and B. Taglienti, *θ-dependence of the vacuum energy in the* SU(3) *gauge theory from the lattice*, *Phys. Rev.* **D 76** (2007) 094510 [arXiv:0705.2352].

[28] R.C. Brower, *AdS/CFT duality and the glueball spectrum*, *Int. J. Mod. Phys.* **A 16S1C** (2001) 1005;
E. Caceres, *A brief review of glueball masses from gauge/gravity duality*, *J. Phys. Conf. Ser.* **24** (2005) 111.

[29] A. Karch, E. Katz, D.T. Son and M.A. Stephanov, *Linear confinement and AdS/QCD*, *Phys. Rev.* **D 74** (2006) 015005 [hep-ph/0602229].

[30] H. Forkel, M. Beyer and T. Frederico, *Linear square-mass trajectories of radially and orbitally excited hadrons in holographic QCD*, *JHEP* **07** (2007) 077 [arXiv:0705.1857].

[31] H.R. Grigoryan and A.V. Radyushkin, *Structure of vector mesons in holographic model with linear confinement*, *Phys. Rev.* **D 76** (2007) 095007 [arXiv:0706.1543].

[32] A.B. Kaidalov and Y.A. Simonov, *Glueball masses and pomeron trajectory in nonperturbative QCD approach*, *Phys. Lett.* **B 477** (2000) 163 [hep-ph/9912434].

[33] S. Weinberg and E. Witten, *Limits on massless particles*, *Phys. Lett.* **B 96** (1980) 59.

[34] S. Narison, *Masses, decays and mixings of gluonia in QCD*, *Nucl. Phys.* **B 509** (1998) 312 [hep-ph/9612457].

[35] E. Schreiber, *Excited mesons and quantization of string endpoints*, hep-th/0403226.

[36] P. Brax and A.C. Davis, *On brane cosmology and naked singularities*, *Phys. Lett.* **B 513** (2001) 156 [hep-th/0105269].

[37] B. Lucini and M. Teper, SU(N) *gauge theories in four dimensions: exploring the approach to* $N = \infty$, *JHEP* **06** (2001) 050 [hep-lat/0103027].

[38] C.J. Morningstar and M.J. Peardon, *The glueball spectrum from an anisotropic lattice study*, *Phys. Rev.* **D 60** (1999) 034509 [hep-lat/9901004].

[39] Y. Chen et al., *Glueball spectrum and matrix elements on anisotropic lattices*, *Phys. Rev.* **D 73** (2006) 014516 [hep-lat/0510074].

[40] H.B. Meyer, *Glueball Regge trajectories*, hep-lat/0508002.

[41] M.S. Chanowitz, *Hunting the scalar glueball: prospects for BES III*, *Int. J. Mod. Phys.* **A 21** (2006) 5535 [hep-ph/0609217].

[42] A. Masoni, C. Cicalo and G.L. Usai, *The case of the pseudoscalar glueball*, *J. Phys.* **G 32** (2006) R293.

[43] H. Boschi-Filho, N.R.F. Braga and H.L. Carrion, *Glueball Regge trajectories from gauge/string duality and the pomeron*, *Phys. Rev.* **D 73** (2006) 047901 [hep-th/0507063].

[44] H. Boschi-Filho and N.R.F. Braga, *QCD / string holographic mapping and glueball mass spectrum*, *Eur. Phys. J.* **C 32** (2004) 529 [hep-th/0209080].

[45] H. Boschi-Filho and N.R.F. Braga, *Gauge/string duality and scalar glueball mass ratios*, *JHEP* **05** (2003) 009 [hep-th/0212207].

[46] G. Bali and F. Bursa, *Meson masses at large-N_c*, arXiv:0708.3427.

[47] Particle Data Group collaboration, W.M. Yao et al., *Review of particle physics*, *J. Phys.* **G 33** (2006) 1.

[48] A.L. Cotrone, *On the YM and QCD spectra from five dimensional strings*, arXiv:0707.1483.